5. Heat Flow Structure in the Investigation Area

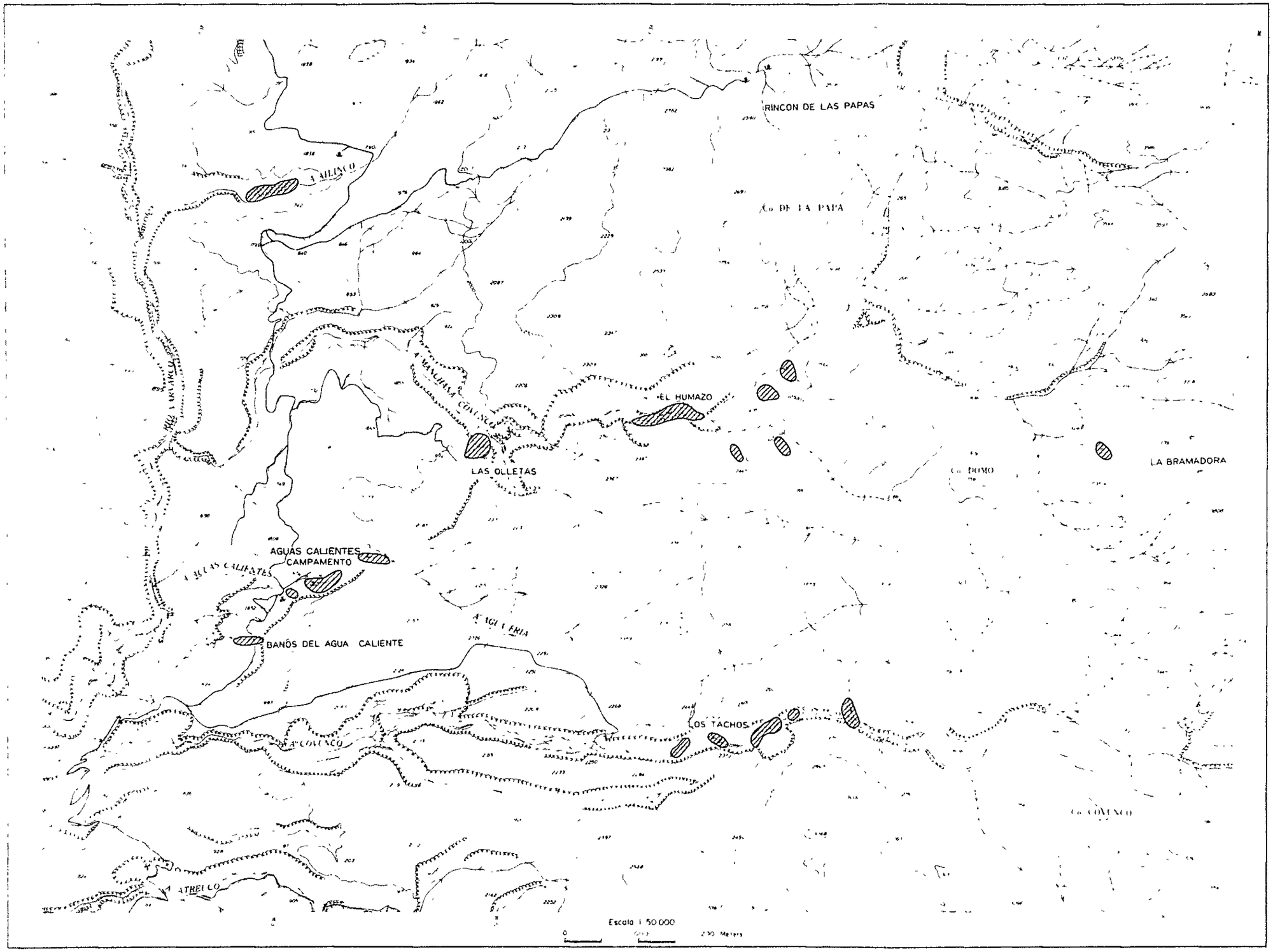

Fig.5-1 Location map of alteration zones

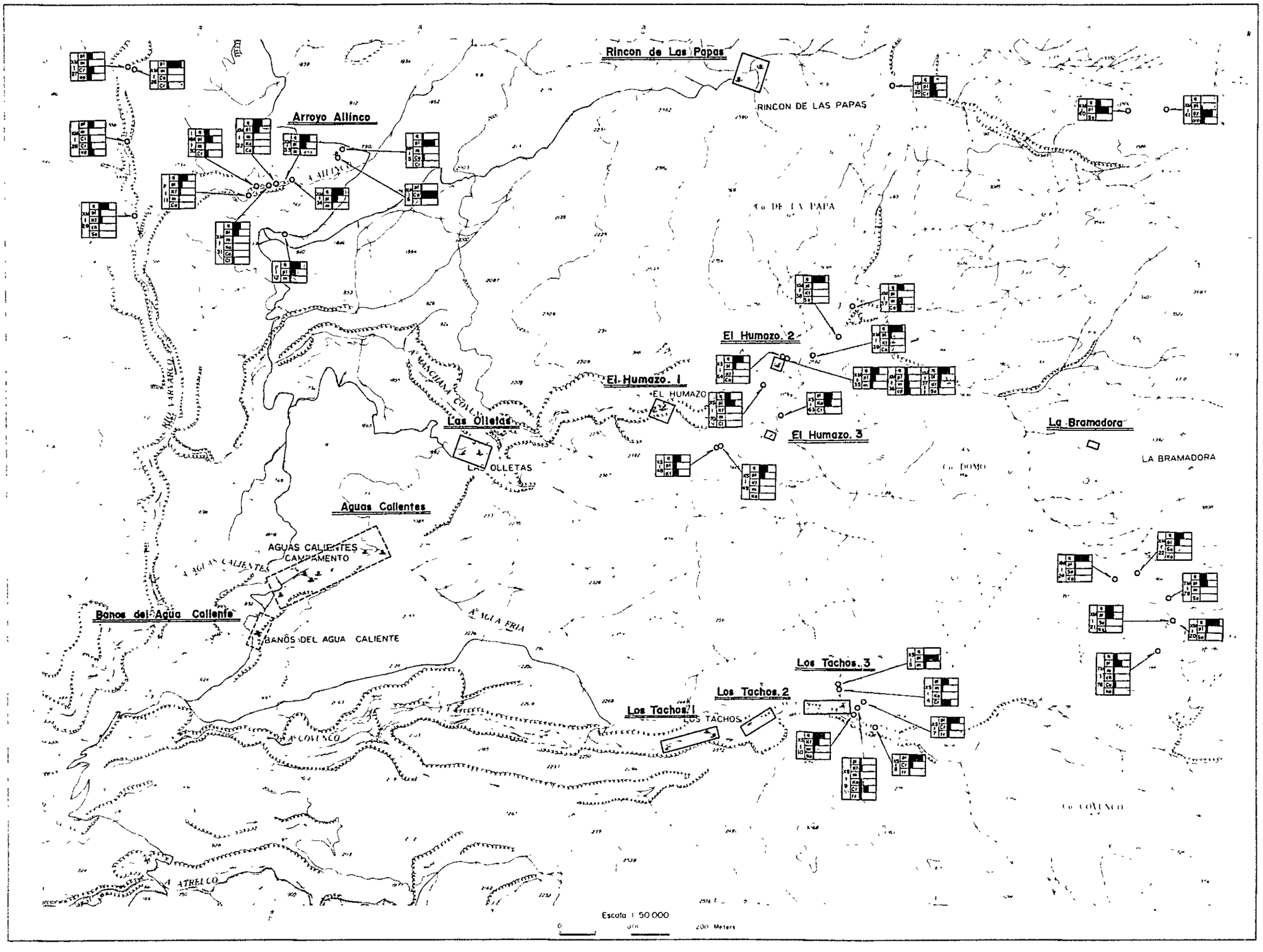

Fig.5-2 Sketched areas of alteration zone and regional distributions of alteration minerals

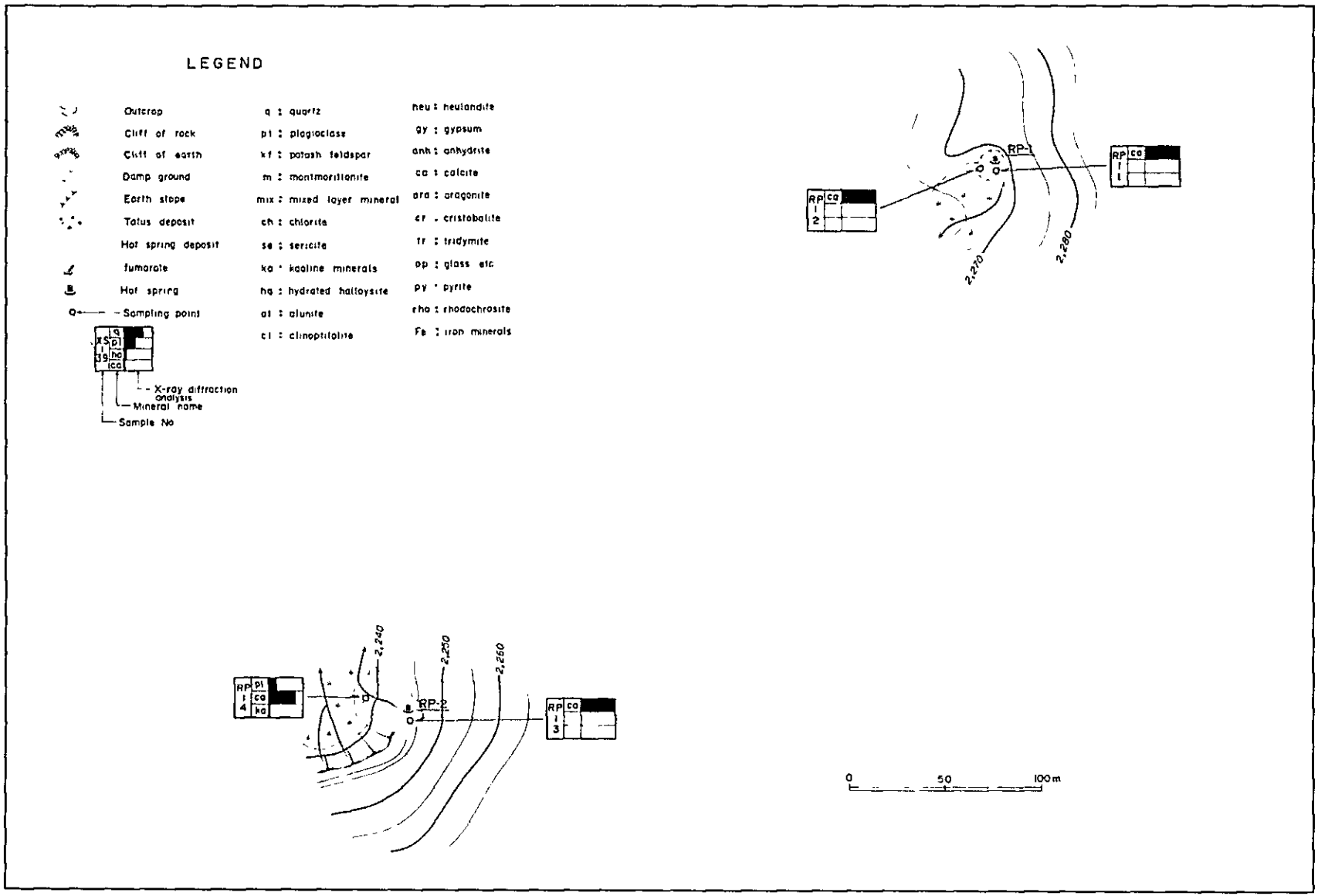

Fig.5-3 Sketch of alteration zone and diagrams of alteration minerals
(1) Rincon de Las Papas

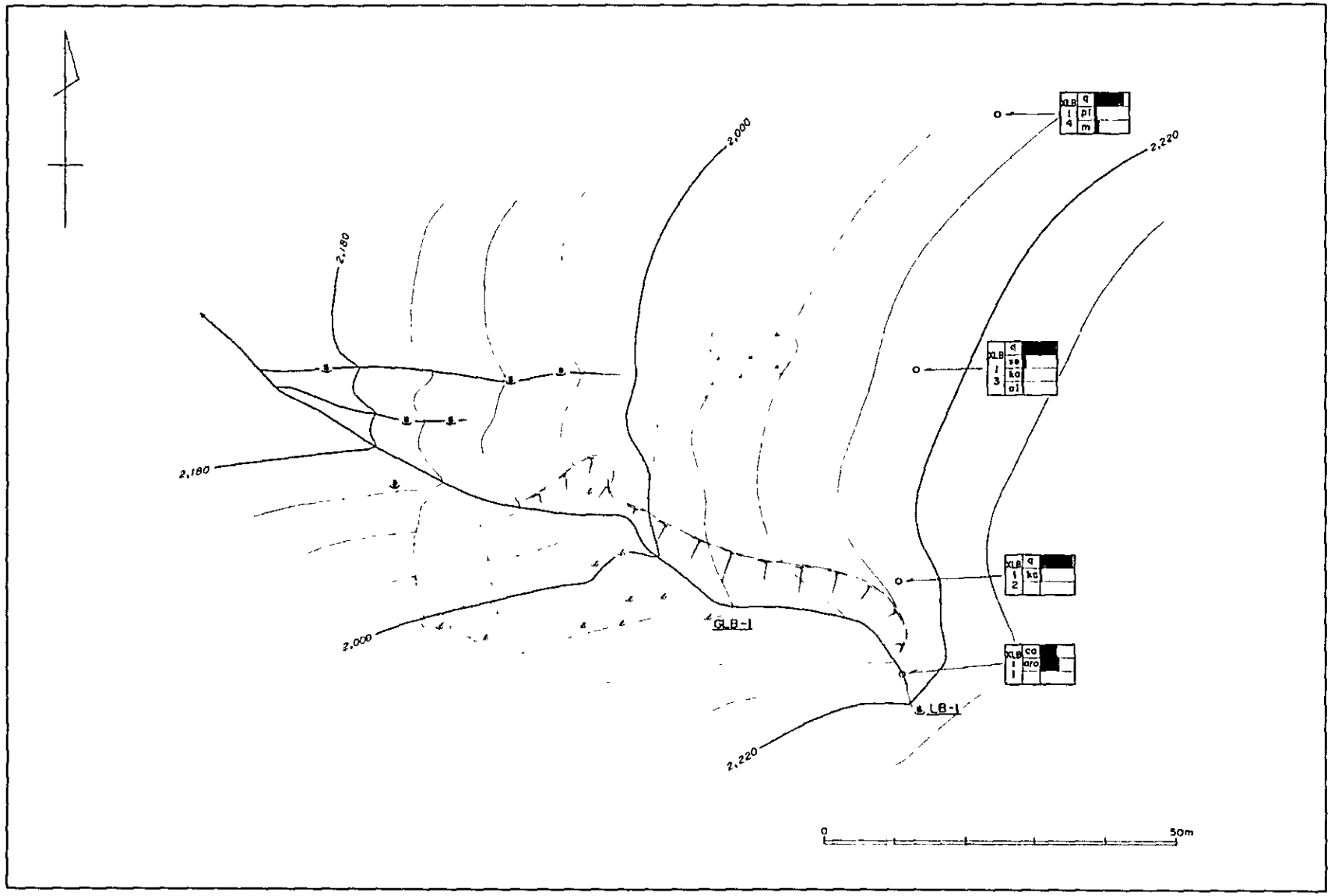

Fig.5-4 Sketch of alteration zone and diagrams of alteration minerals
(2) La Bramadora

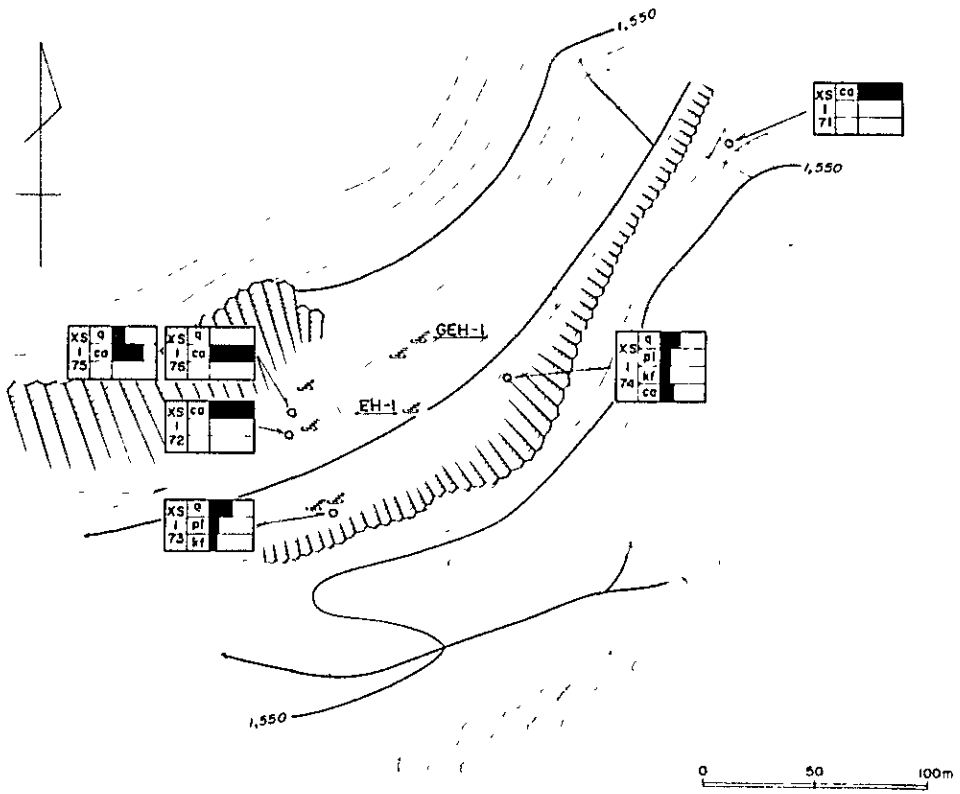

Fig.5-5 Sketch of alteration zone and diagrams of alteration minerals
(3) El Humazo - 1

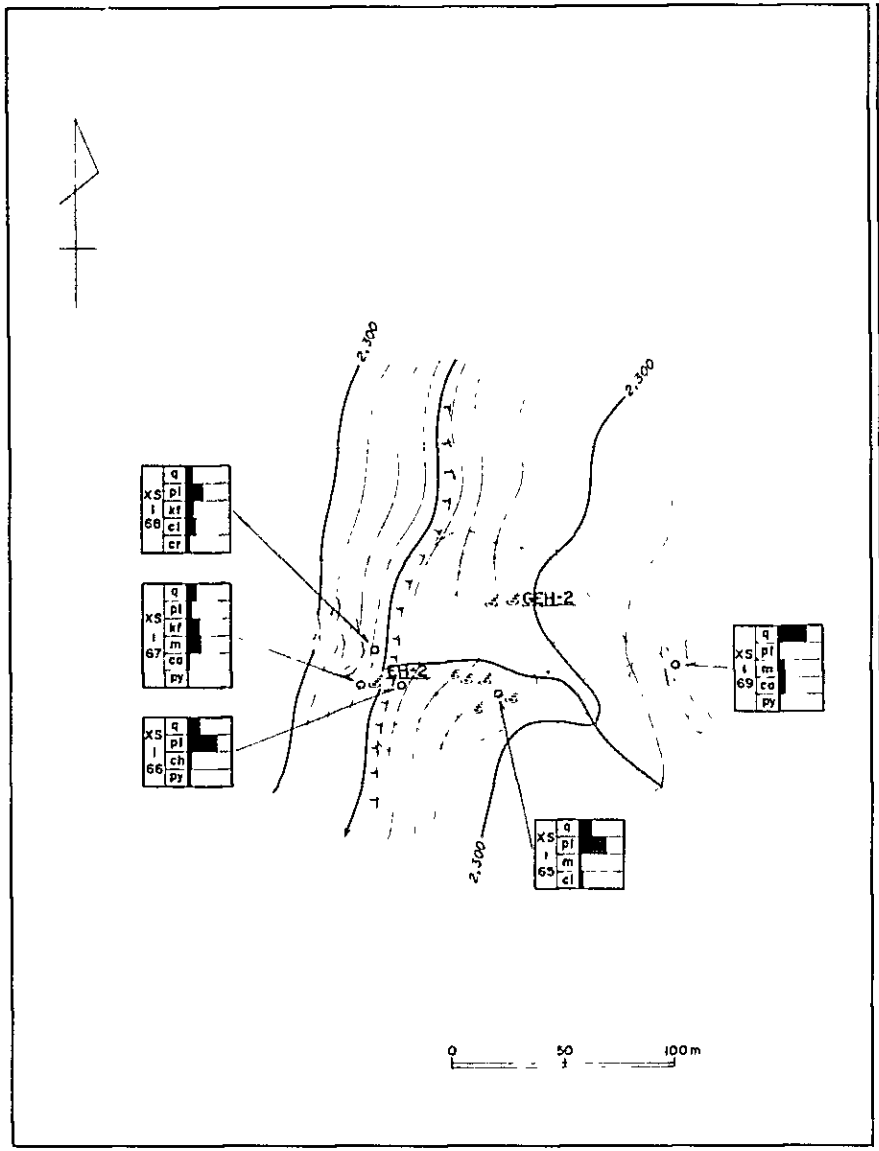

Fig.5-6 Sketch of alteration zone and diagrams of alteration minerals (4) El Humazo - 2

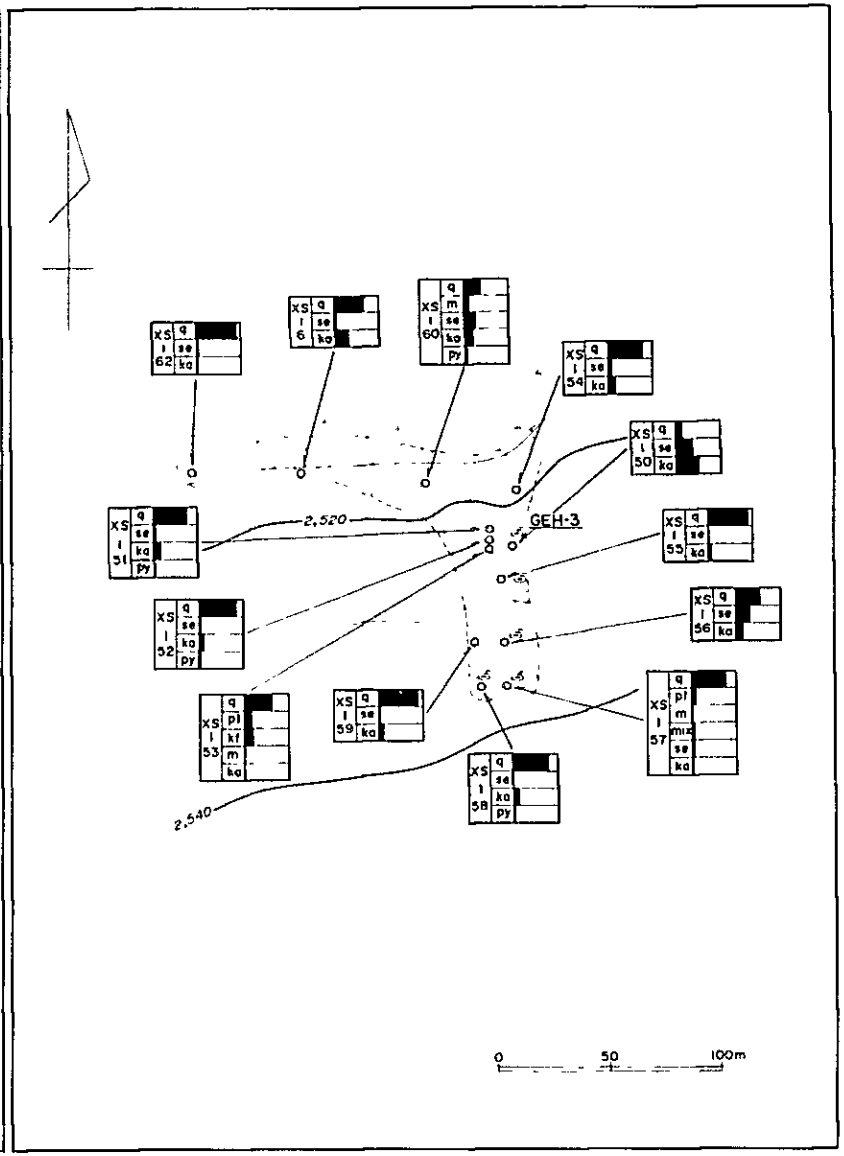

Fig.5-7 Sketch of alteration zone and diagrams of alteration minerals (5) El Humazo - 3

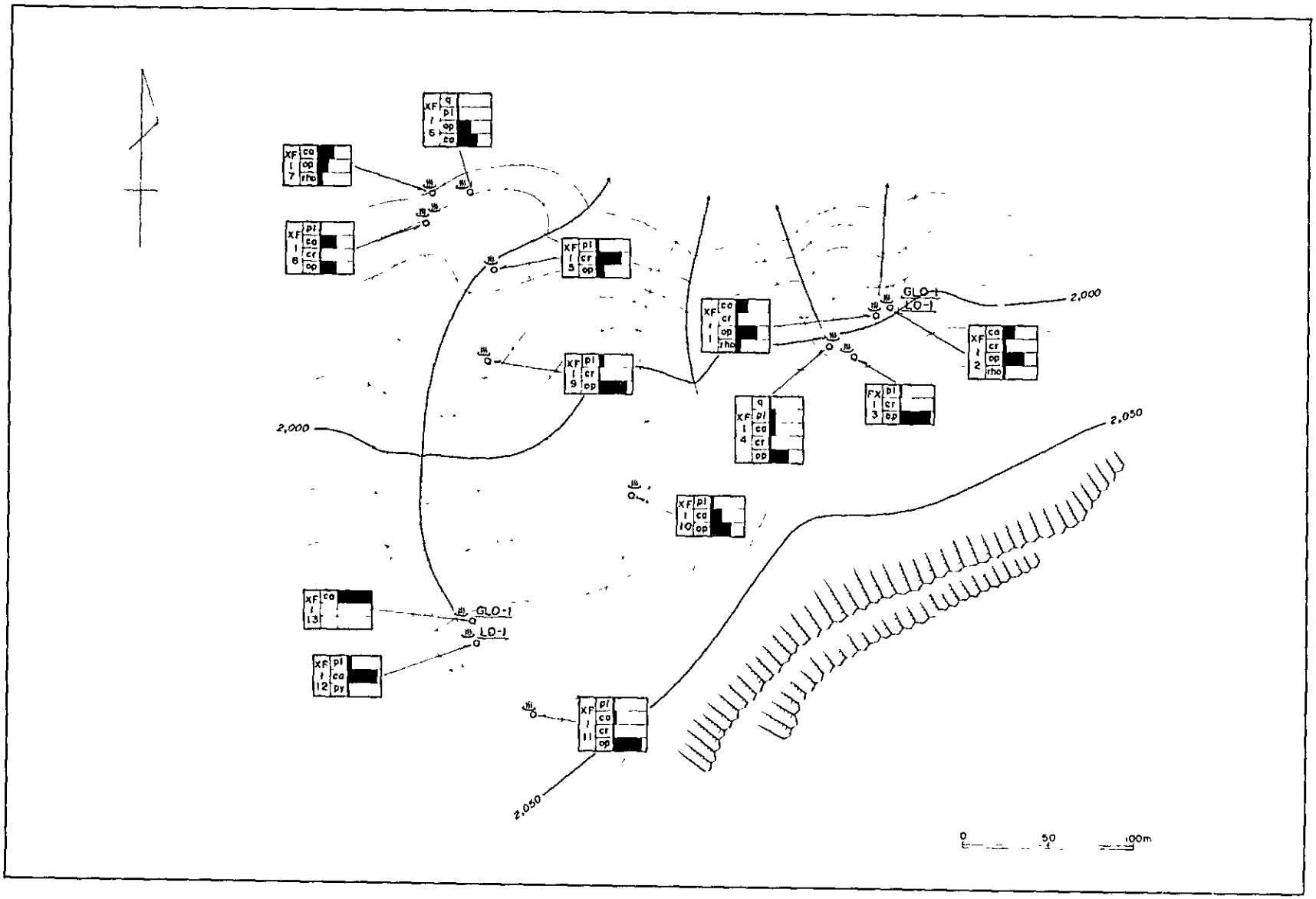

Fig.5-8 Sketch of alteration zone and diagrams of alteration minerals
(6) Las Olletas

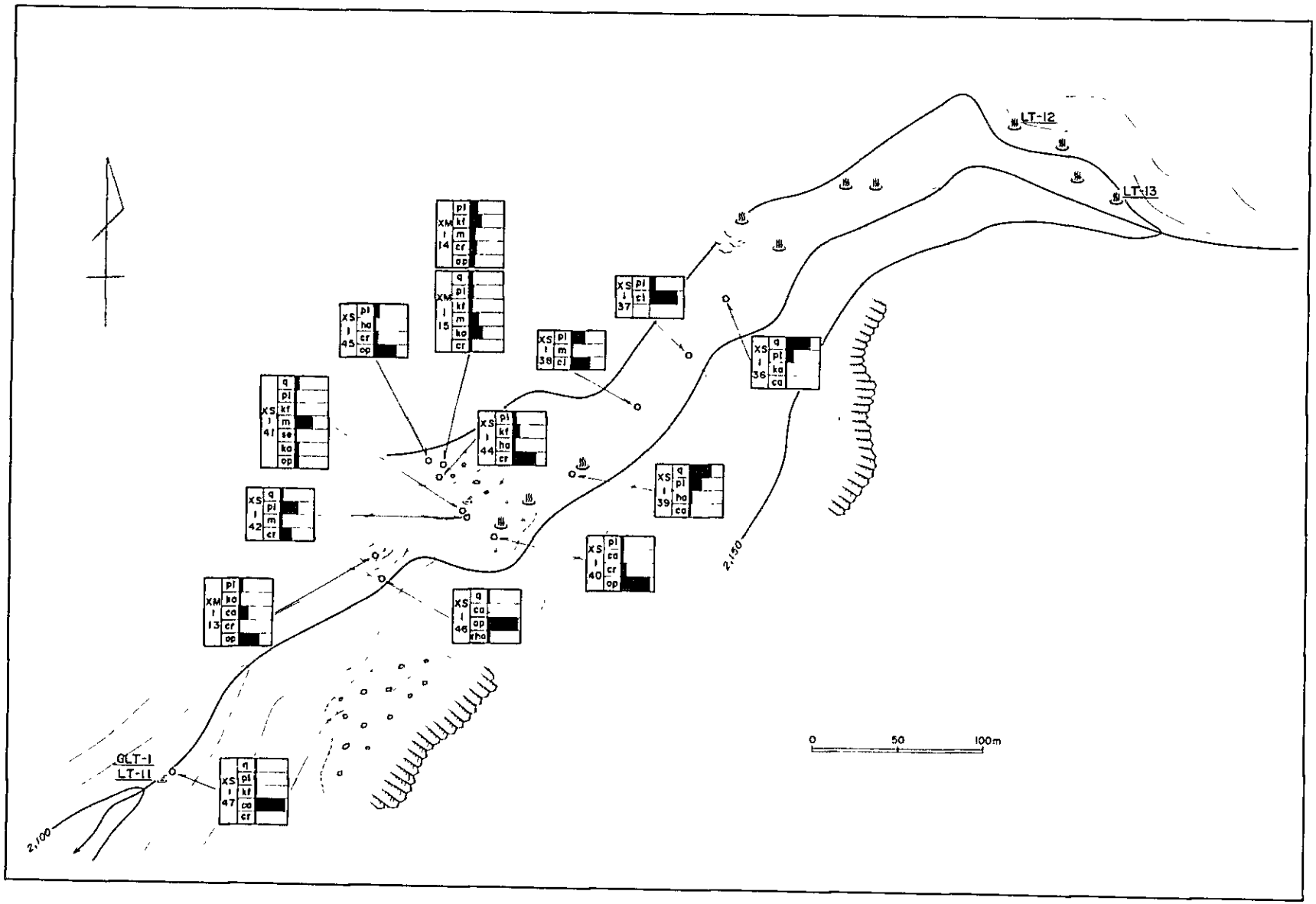

Fig.5-9 Sketch of alteration zone and diagrams of alteration minerals
(7) Los Tachos - 1

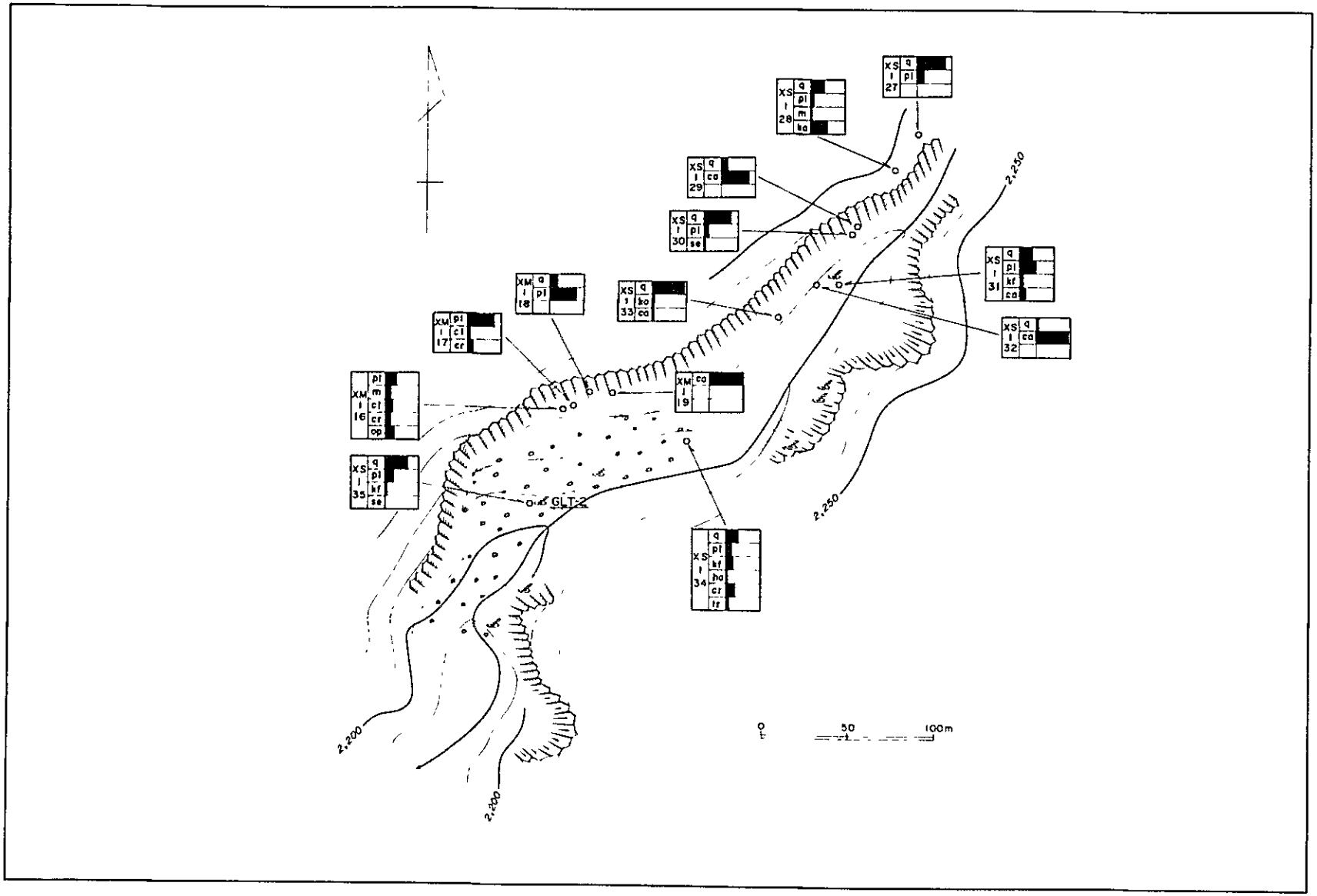

Fig.5-10 Sketch of alteration zone and diagrams of alteration minerals
(8) Los Tachos - 2

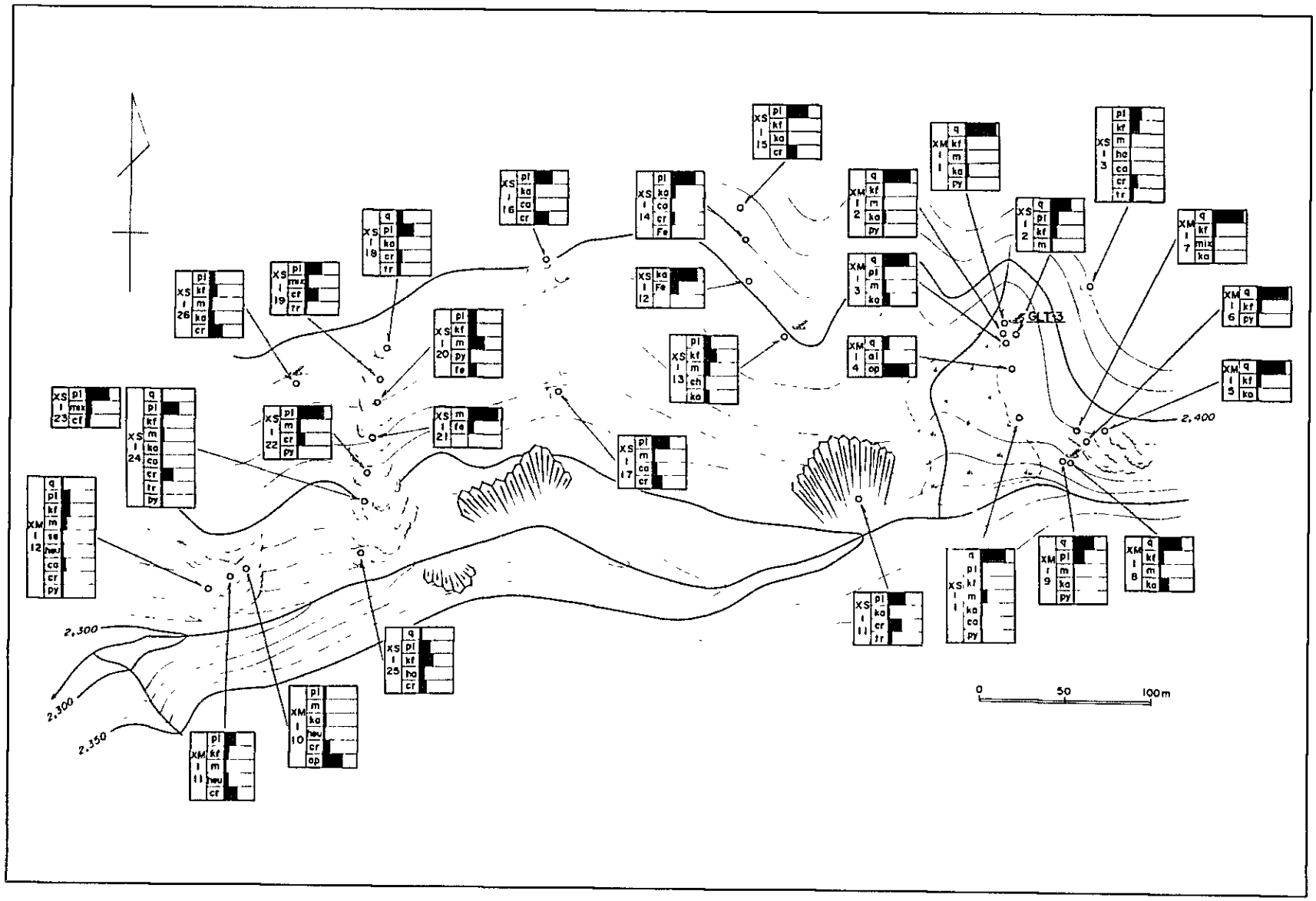

Fig.5-11 Sketch of alteration zone and diagrams of alteration minerals
(9) Los Tachos - 3

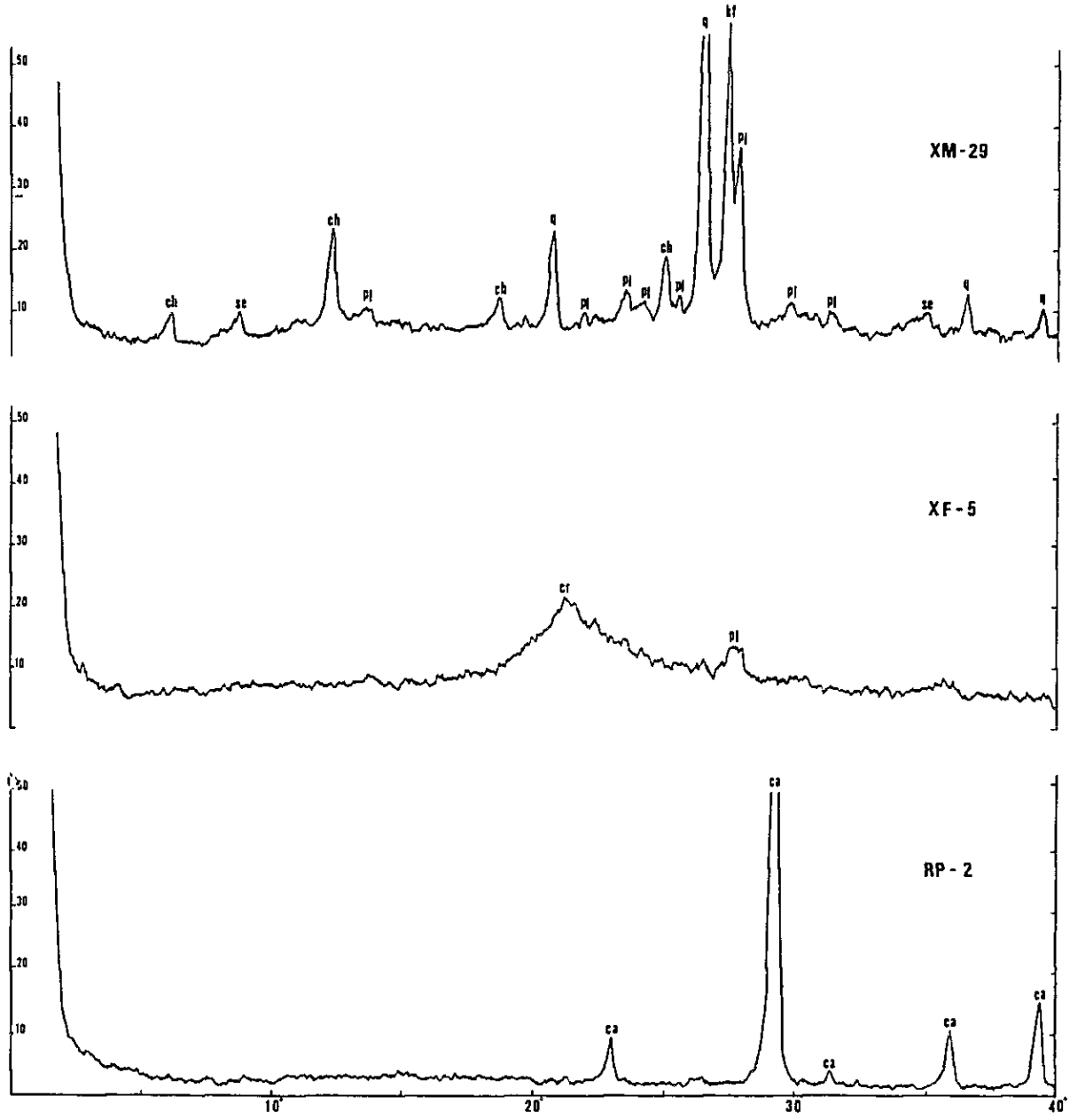

LEGEND

m:	montmorillonite	q:	quartz
ch:	chlorite	kf:	potash feldspar
se:	sericite	pl:	plagioclase
k:	kaolinite	ca:	calcite
ka:	hydrated halloysite	cr:	cristobalite

Fig. 5-12 (1) Typical charts of X-ray diffraction analysis

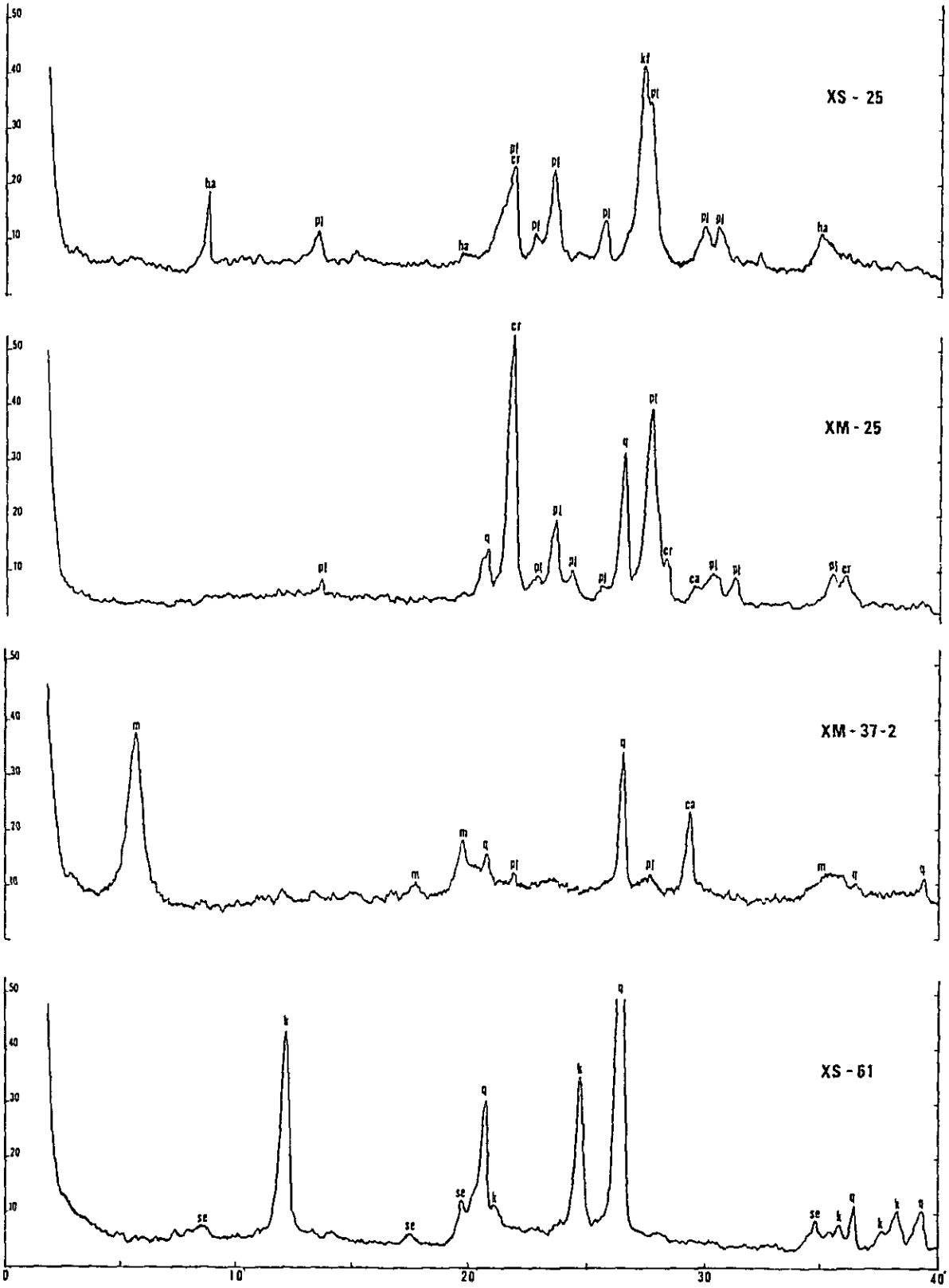

LEGEND

m:	montmorillonite	q:	quartz
ch:	chlorite	kf:	potash feldspar
se:	sericite	pl:	plagioclase
k:	kaolinite	ca:	calcite
ha:	hydrated halloysite	cr:	cristobalite

Fig. 5-12 (2) Typical charts of X-ray diffraction analysis

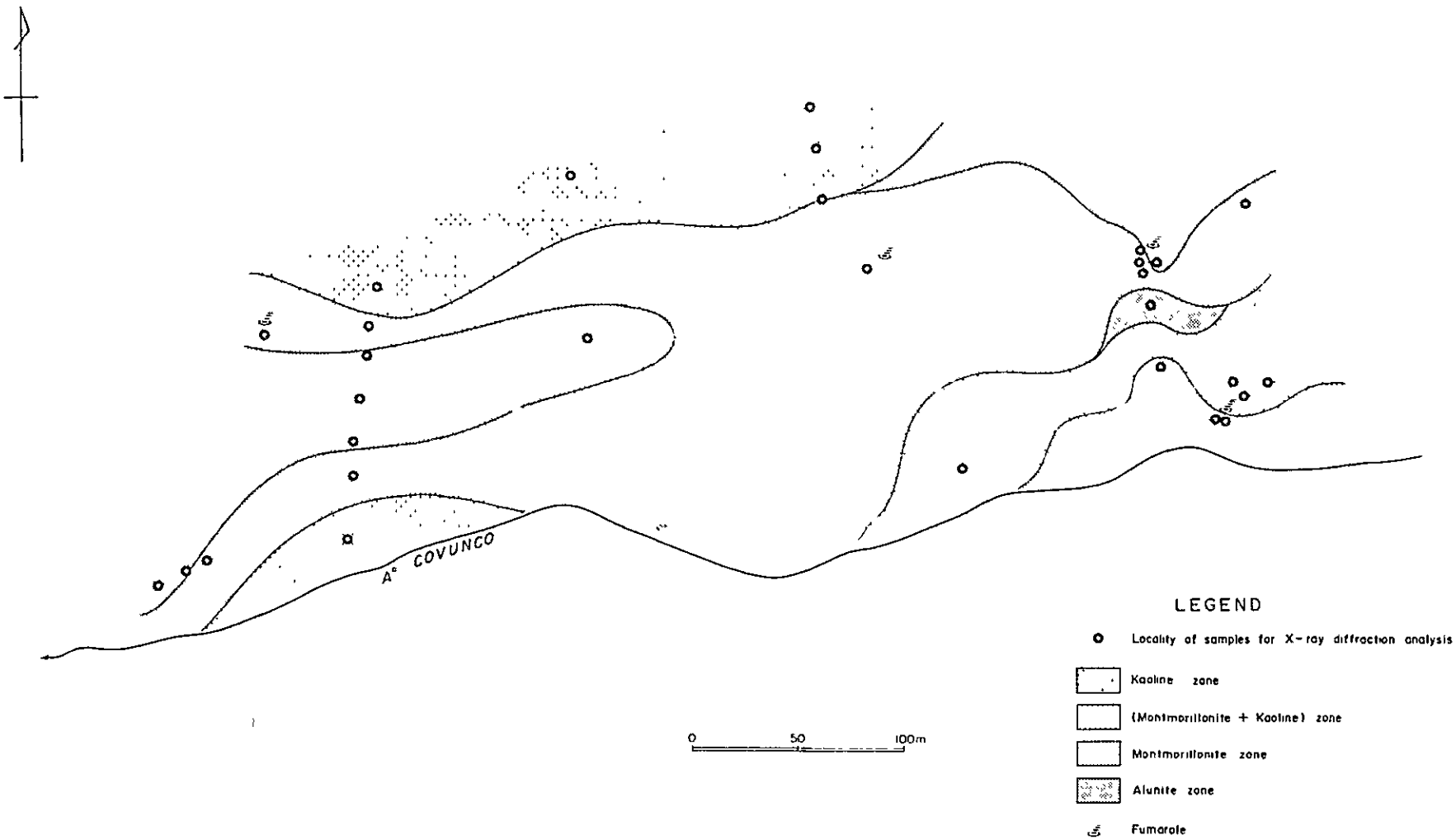

Fig.5-13 Alteration zoning map of Los Tachos - 3

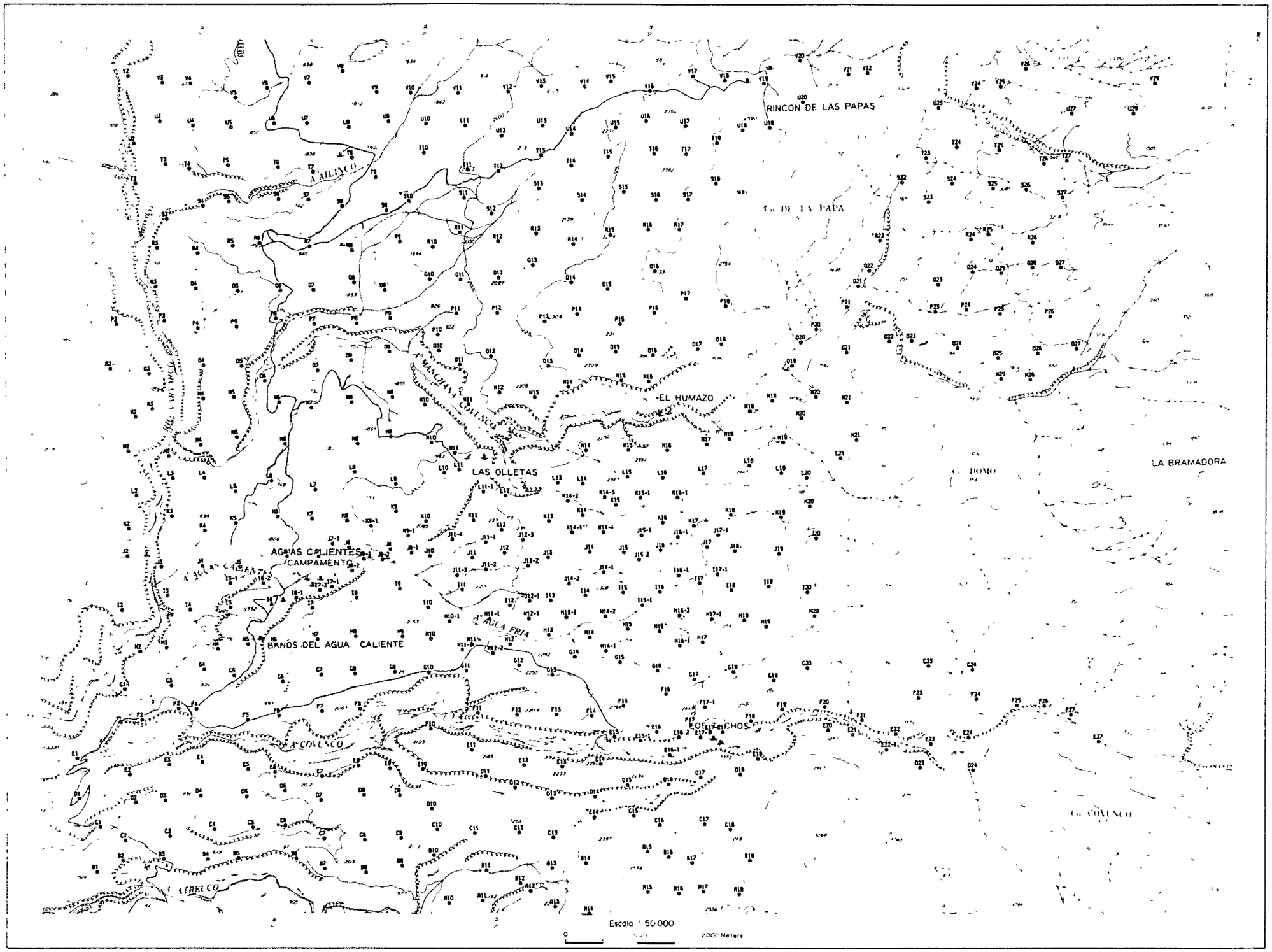

Fig.5-14 Location map of test holes at 1 meter depth

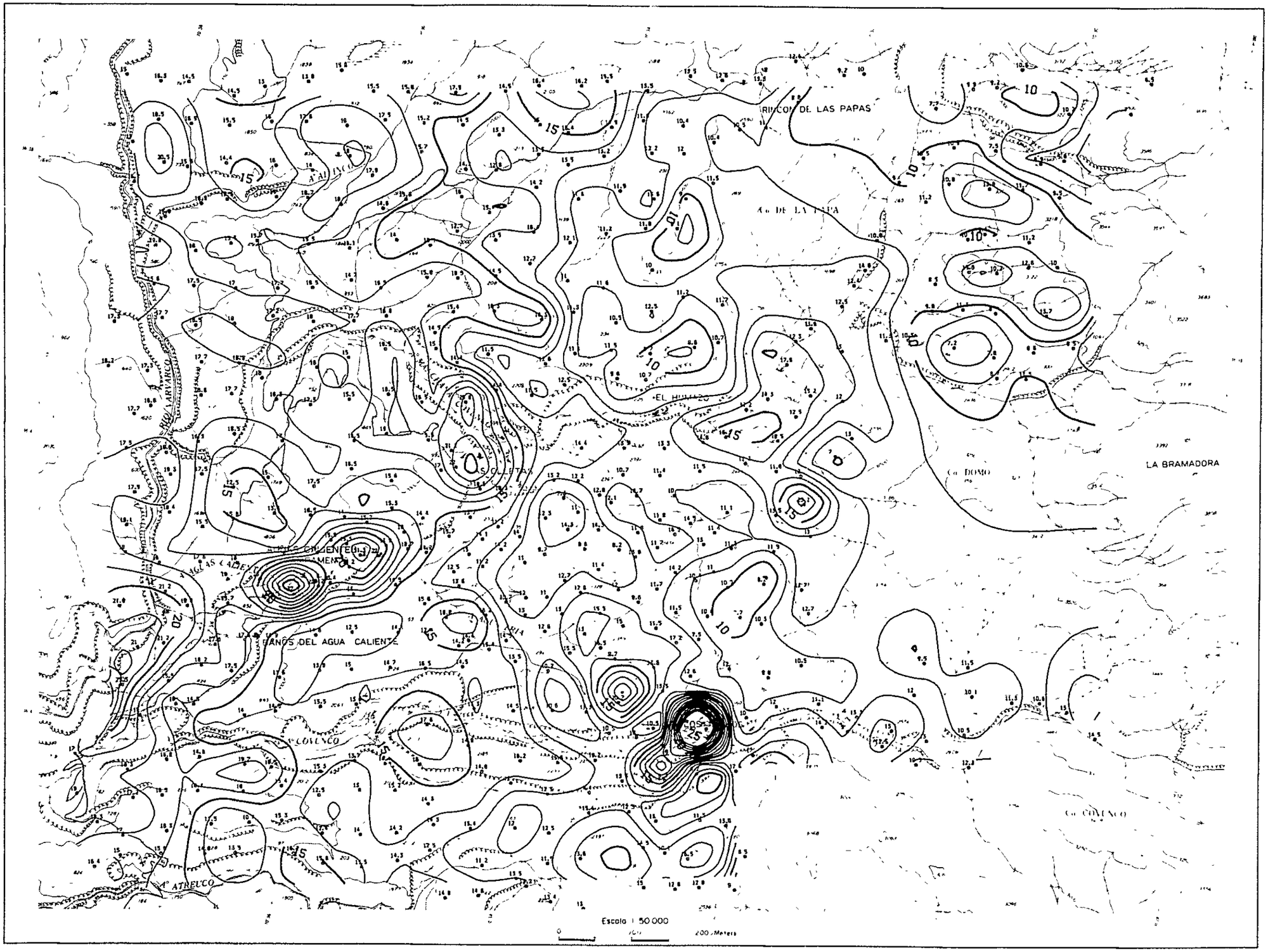

Fig.5-15 Distribution map of ground temperature at 1 meter depth

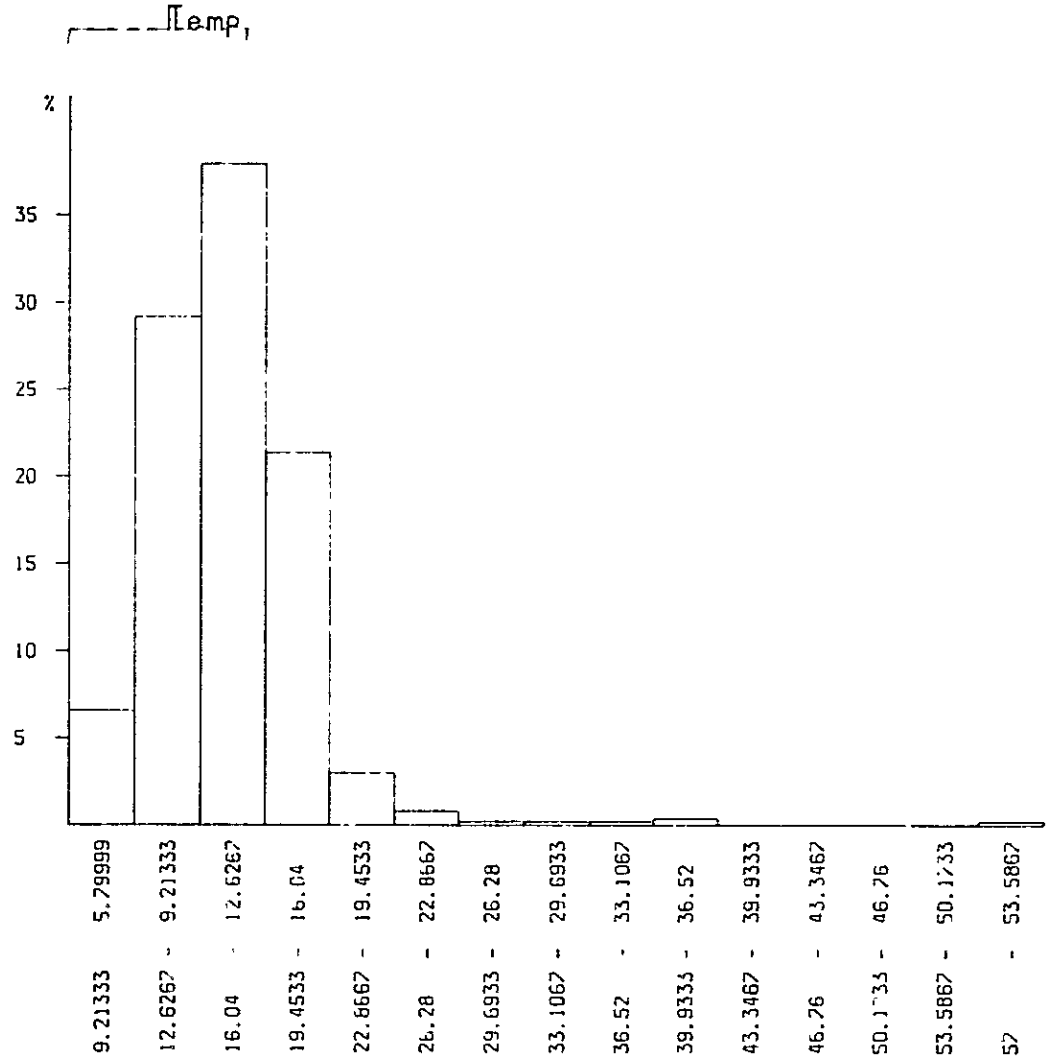

Fig.5-16 Frequency distribution of ground temperature at 1 meter depth

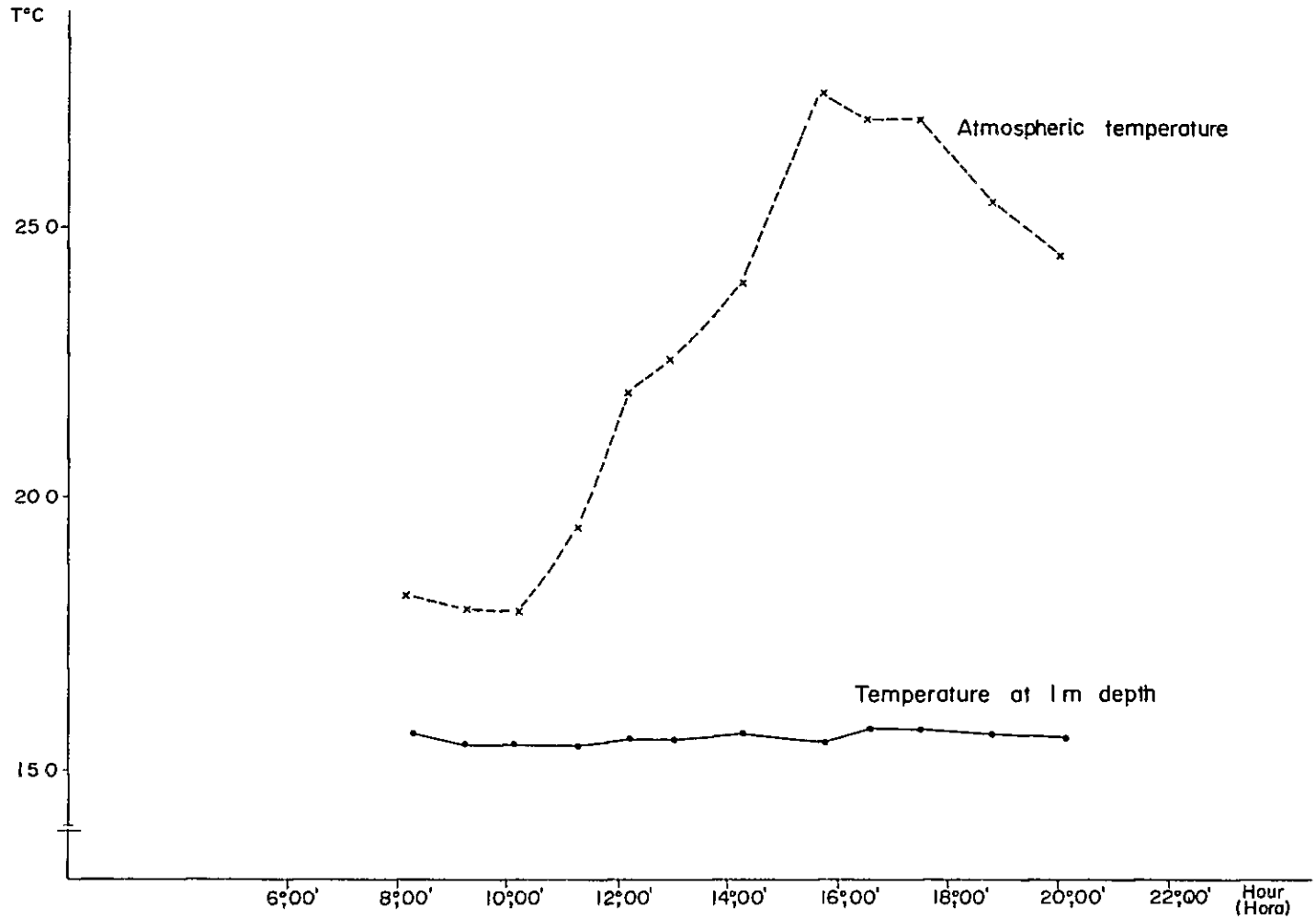

Fig.5-17 Diurnal variation of atmospheric and ground temperatures

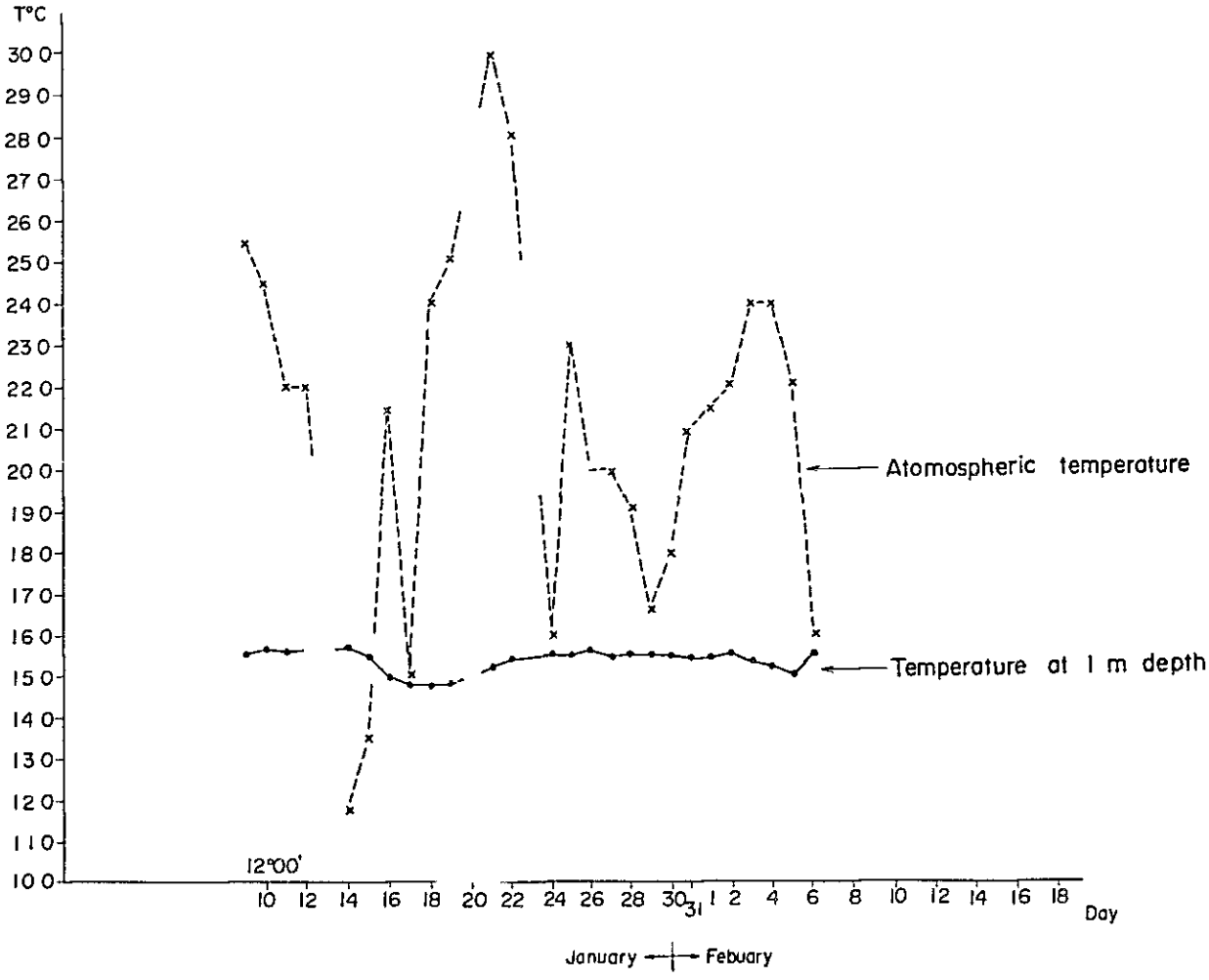

Fig.5-18 Observational results of variation of atmospheric and ground temperatures during period of 1 meter depth survey

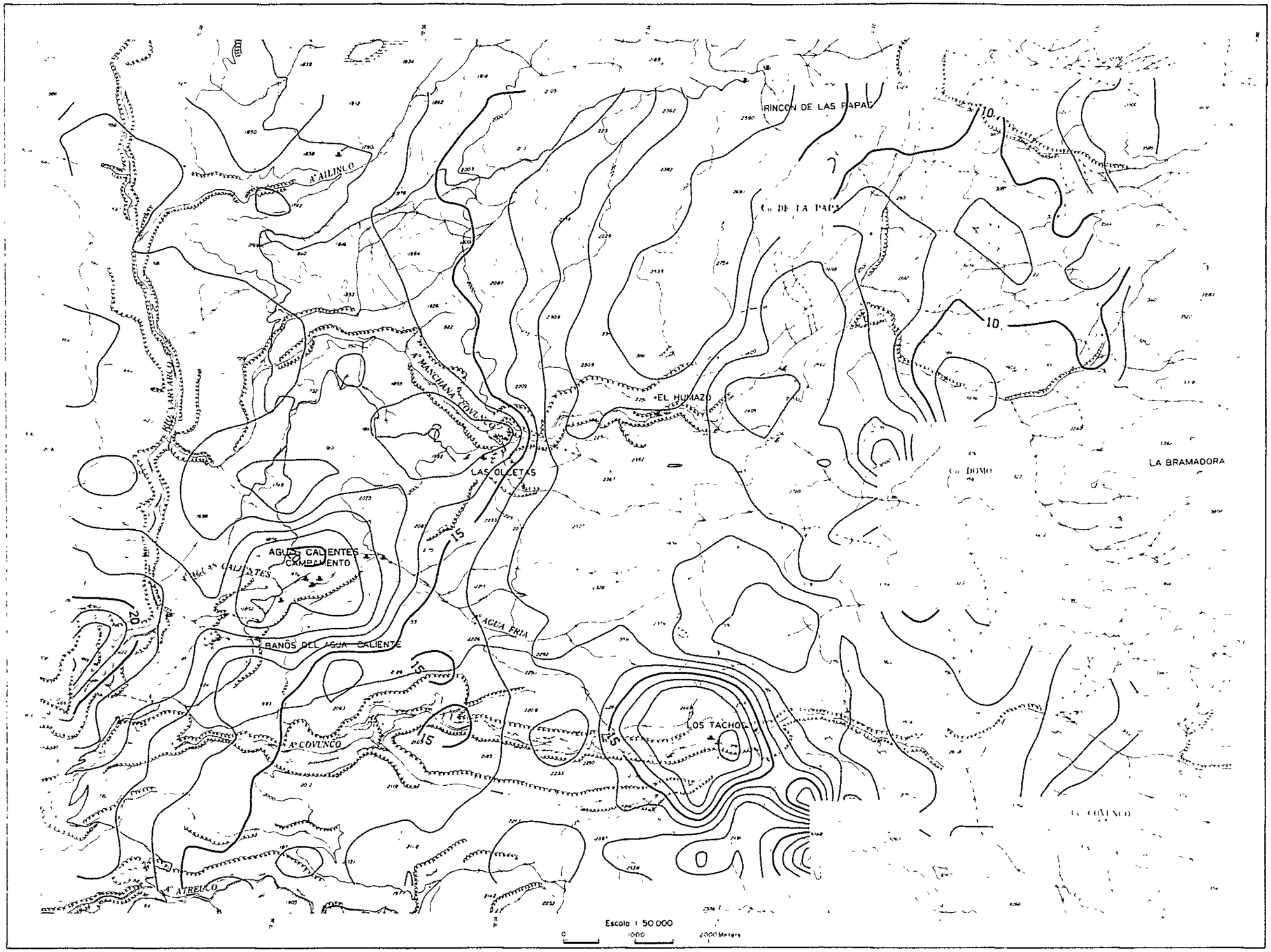

Fig.5-19 Distribution map of ground temperature at 1 meter depth by running average method

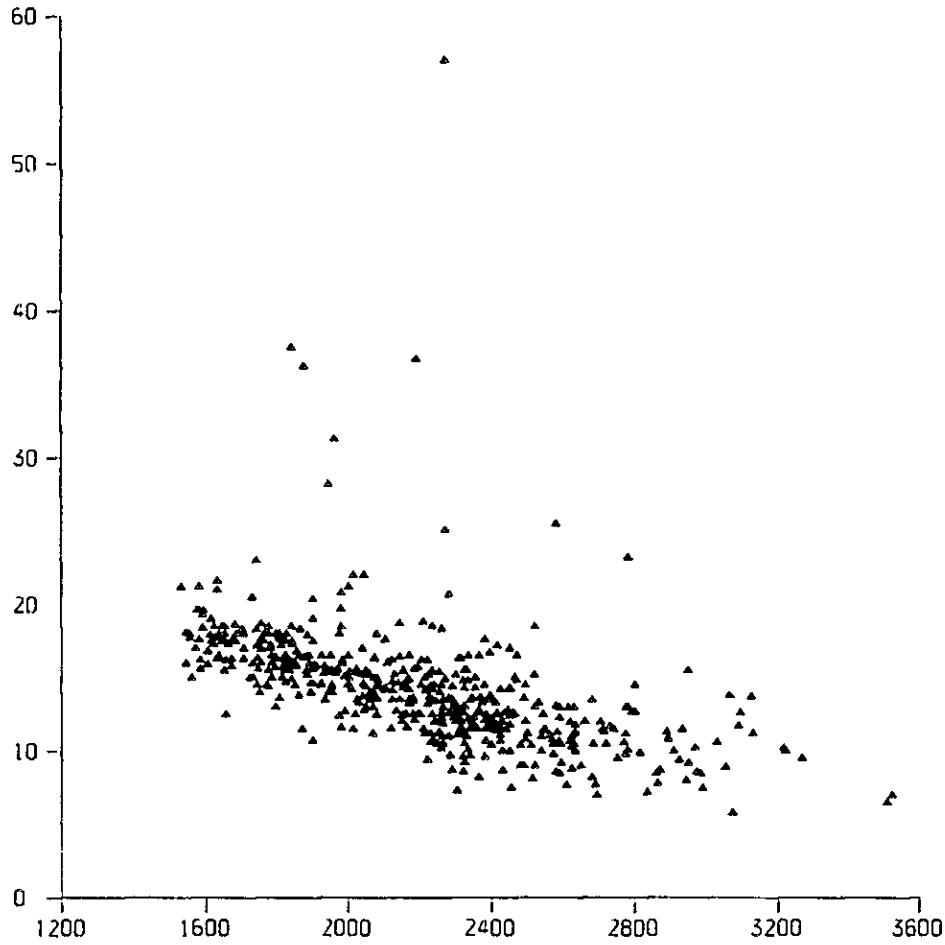

Fig.5-20 Relation between altitude and ground temperature at 1 meter depth

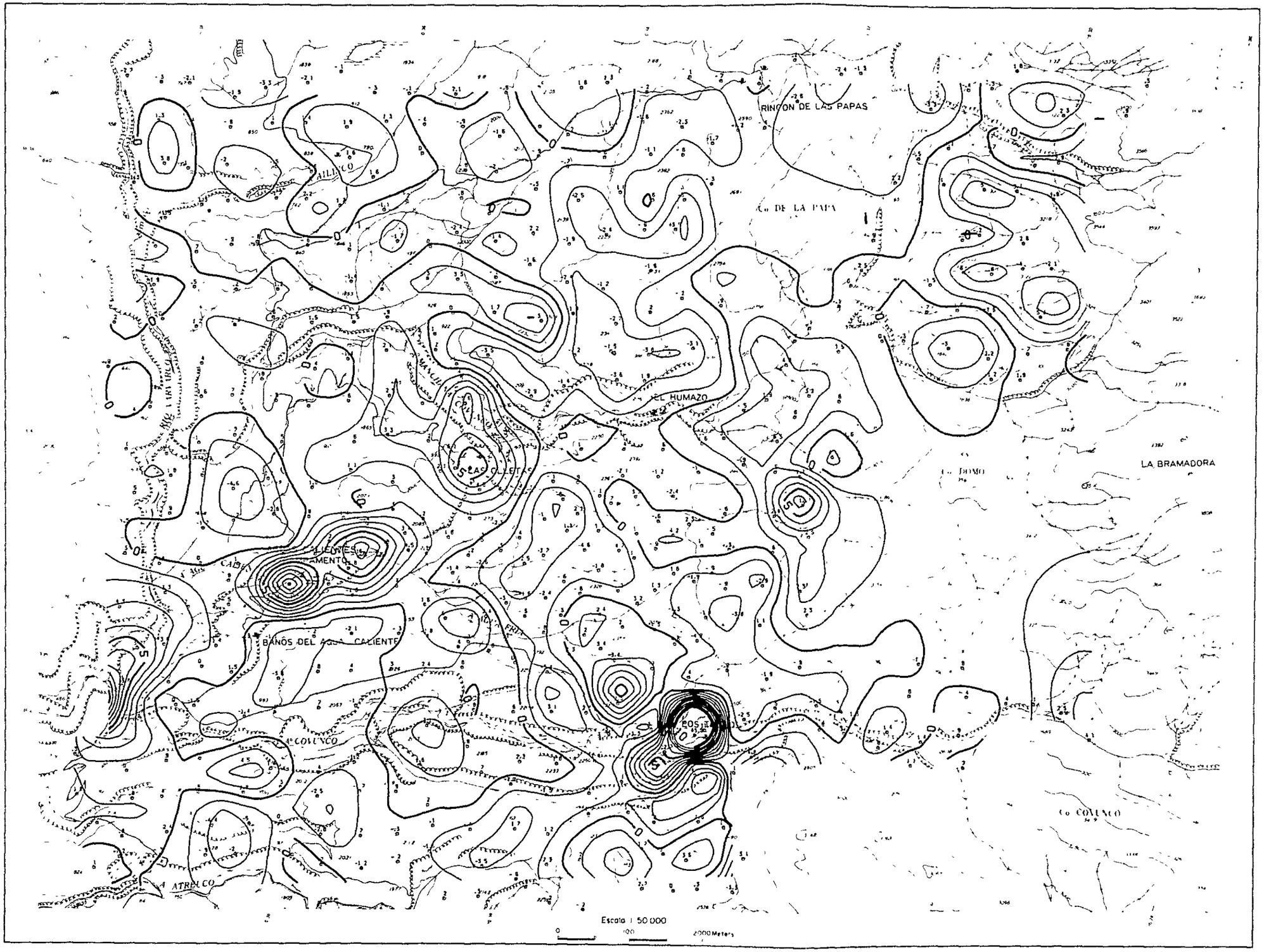

Fig.5-21 Distribution map of residual ground temperature at 1 meter depth (calculated by linear equation)

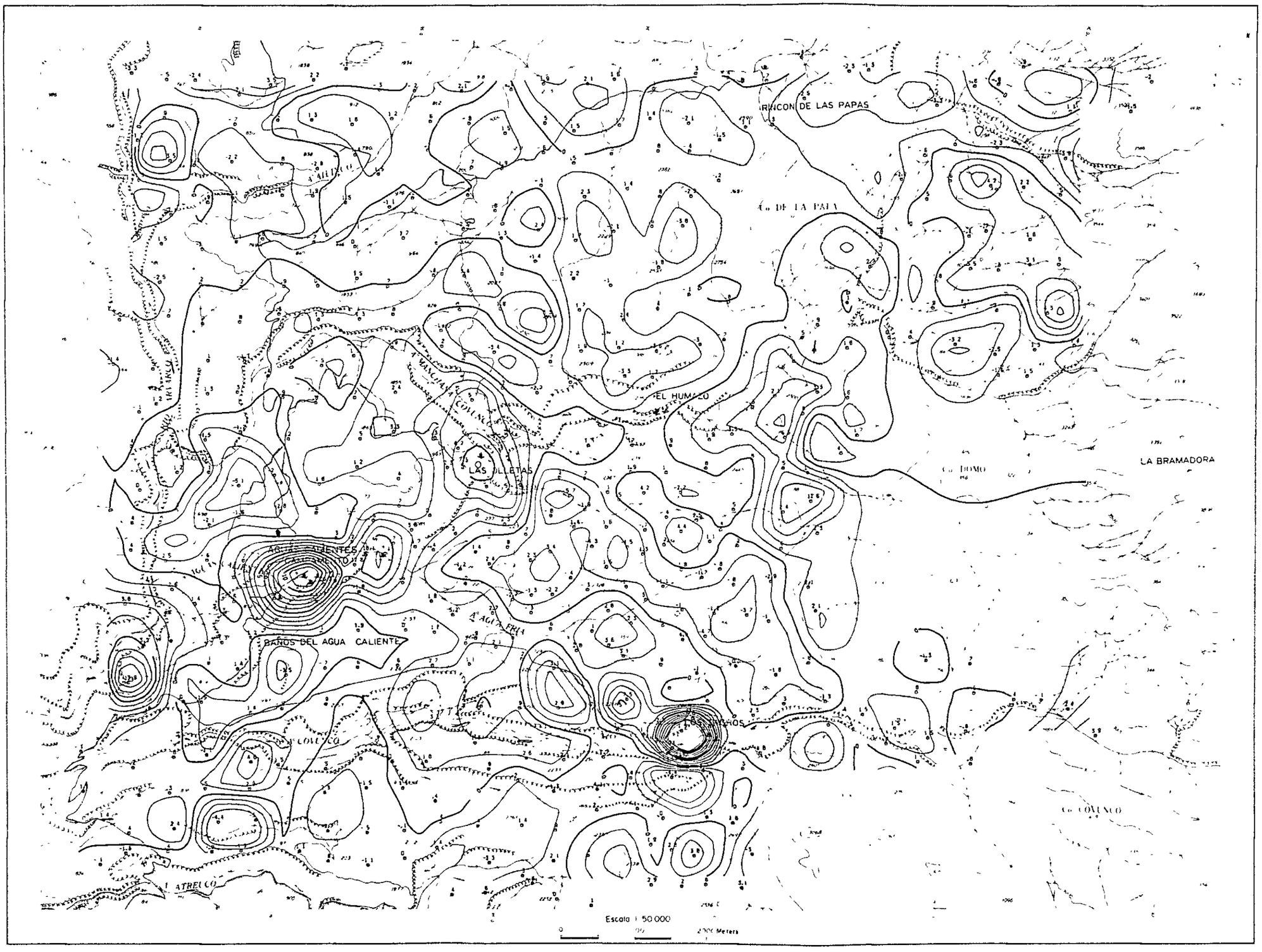

Fig.5-22 Distribution map of residual ground temperature at 1 meter depth (calculated by quadratic equation)

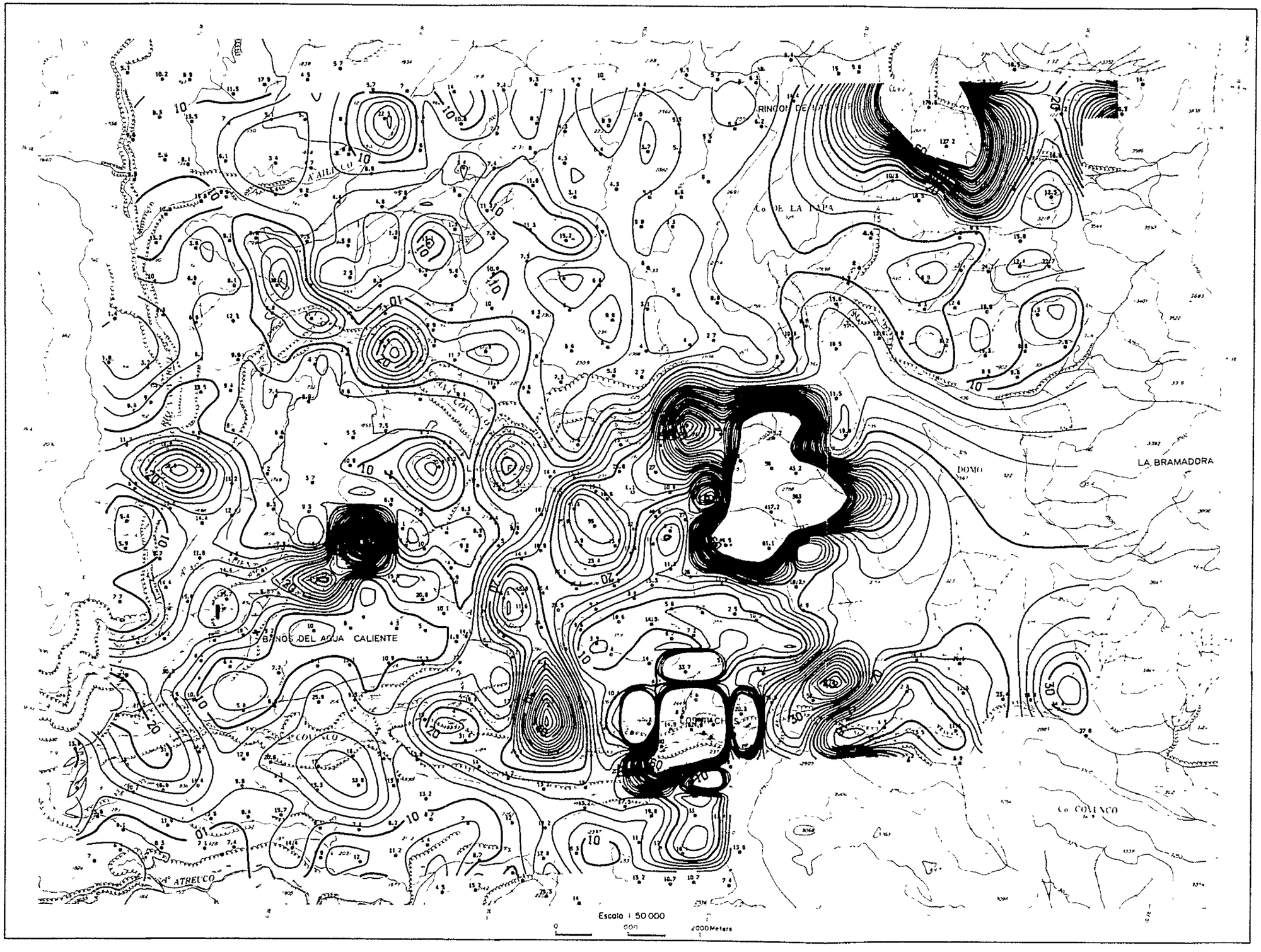

Fig.5-23 Distribution map of Hg - concentration in soil

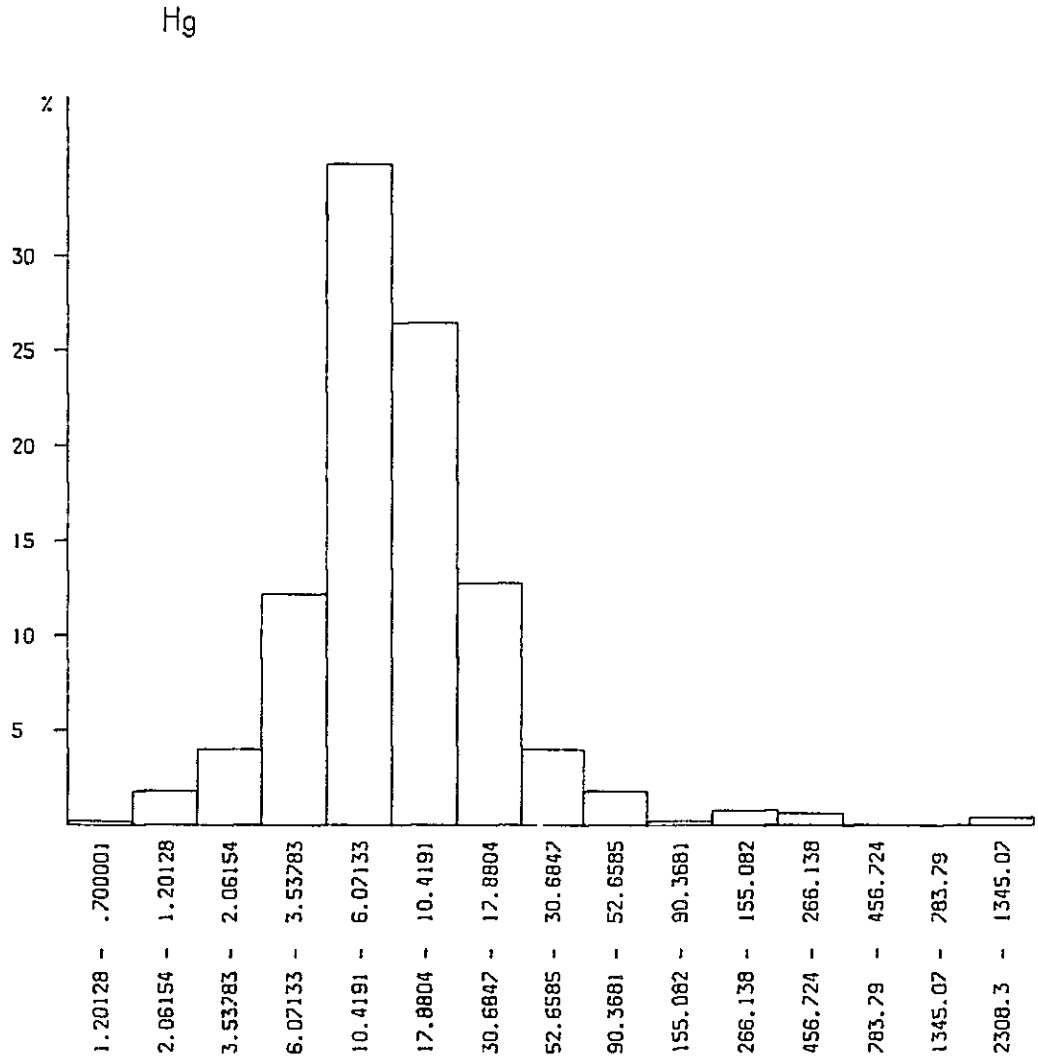

Fig.5-24 Frequency distribution of Hg - concentration in soil

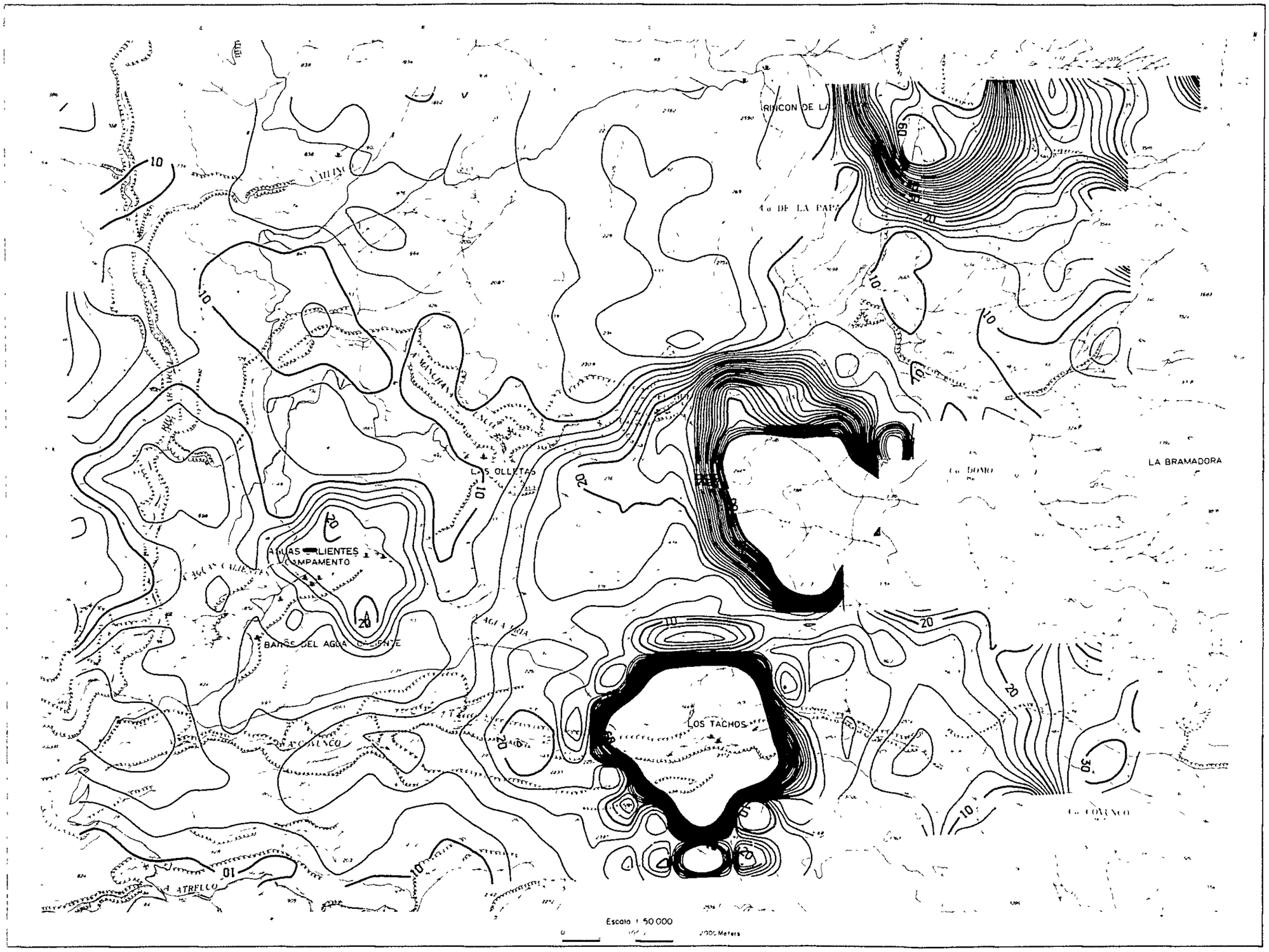

Fig.5-25 Distribution map of Hg - concentration in soil by running average method

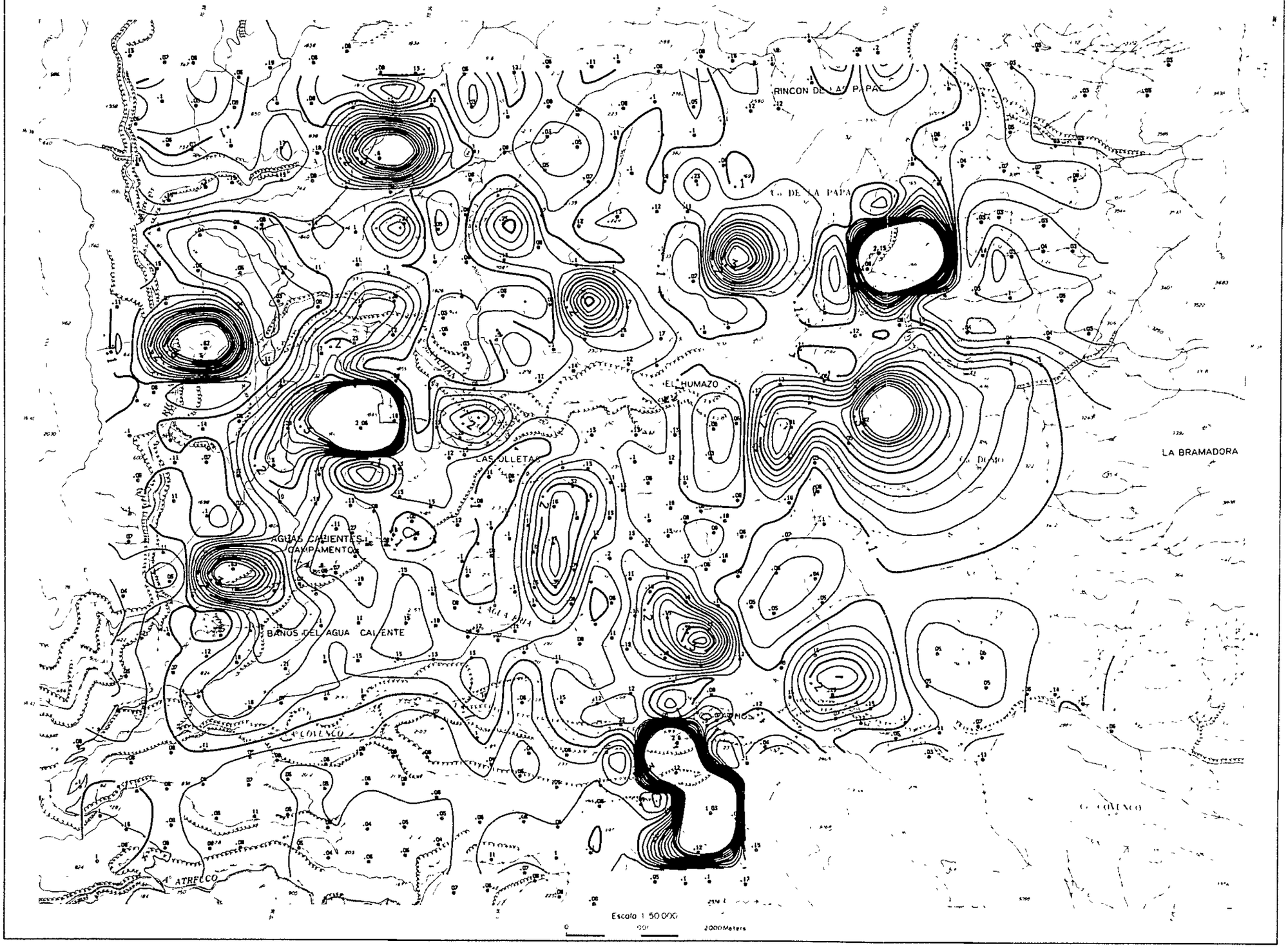

Fig.5-26 Distribution map of CO_2 - concentration in soil-air

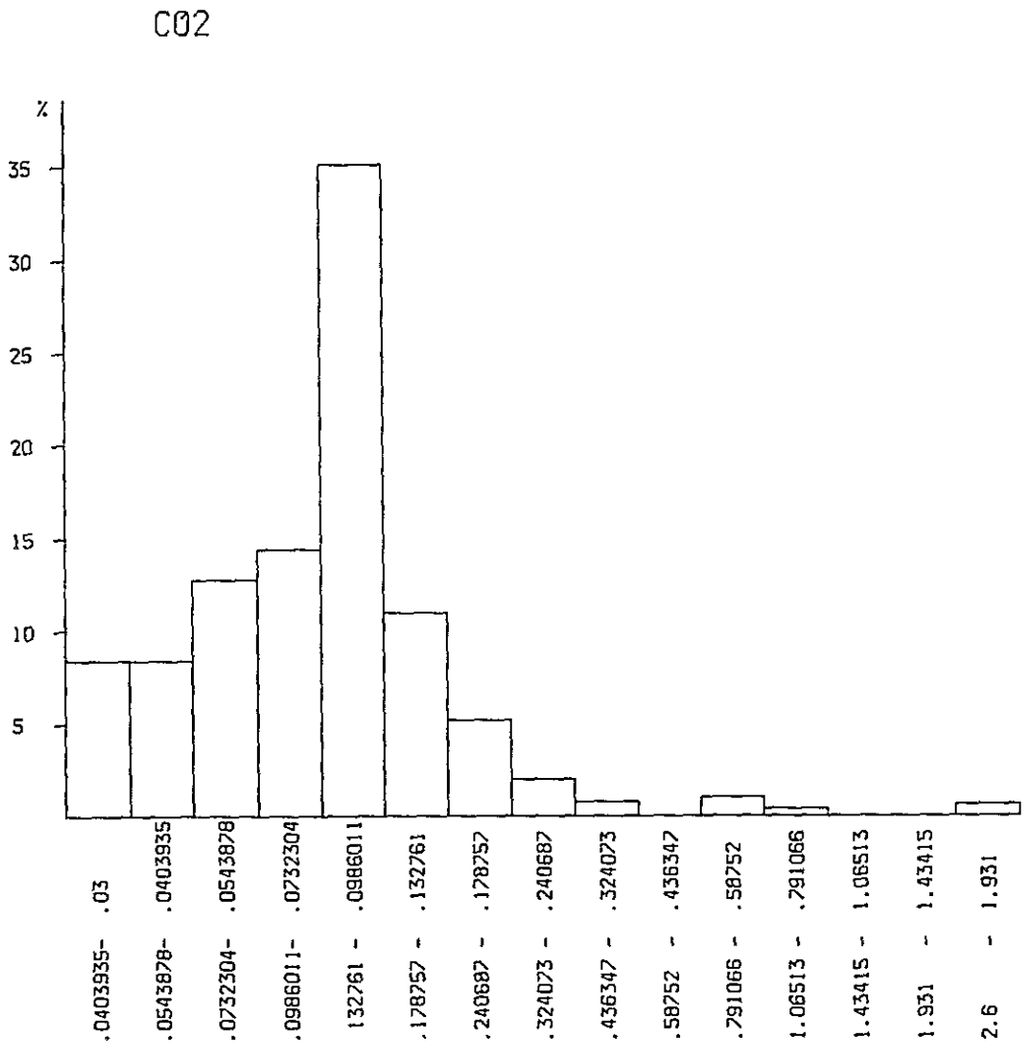

Fig.5-27 Frequency distribution of CO_2 - concentration in soil-air

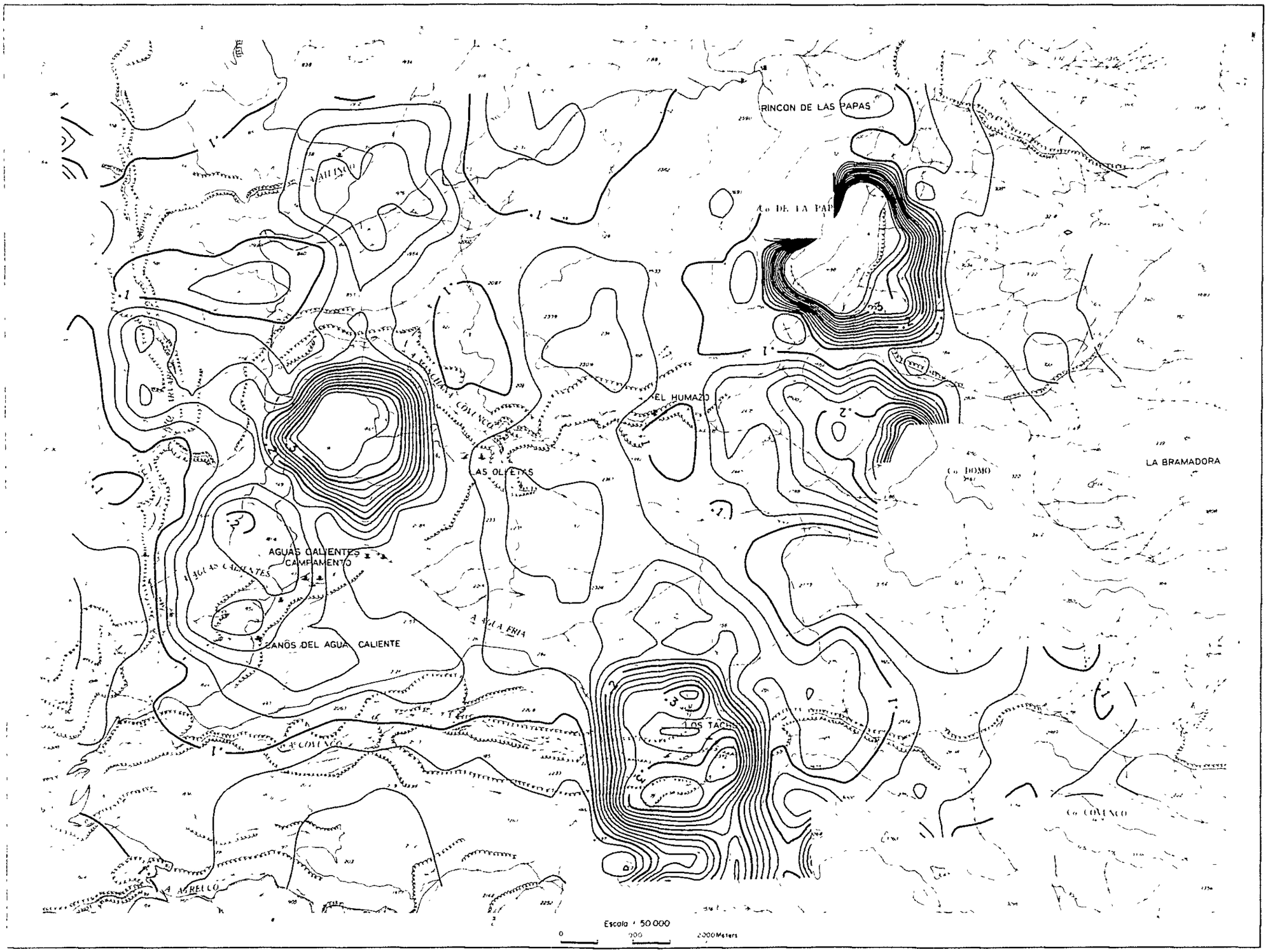

Fig.5-28 Distribution map of CO_2 - concentration in soil-air by running average method

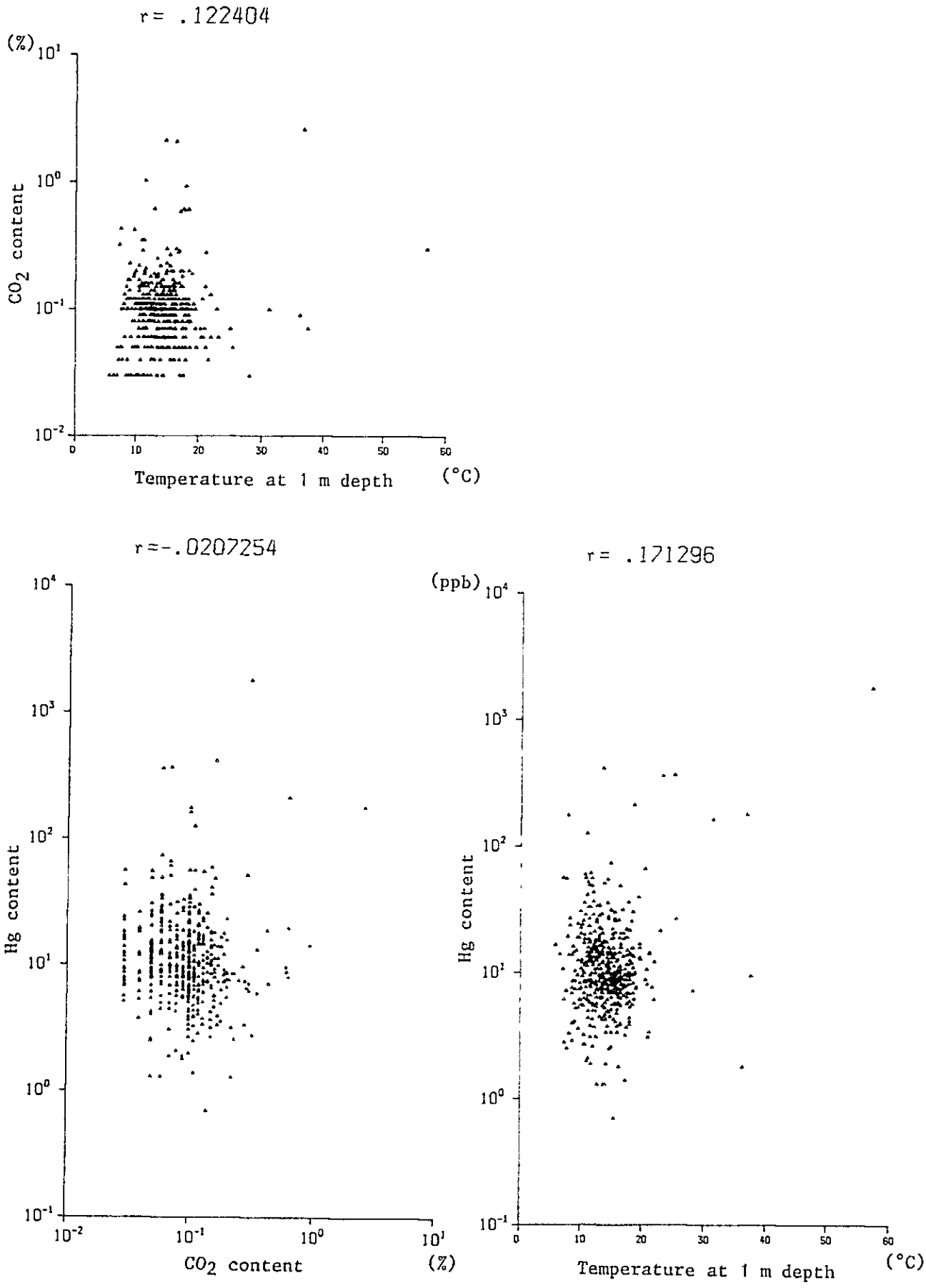

Fig.5-29 Correlations between ground temperature, and Hg and CO_2 - concentrations

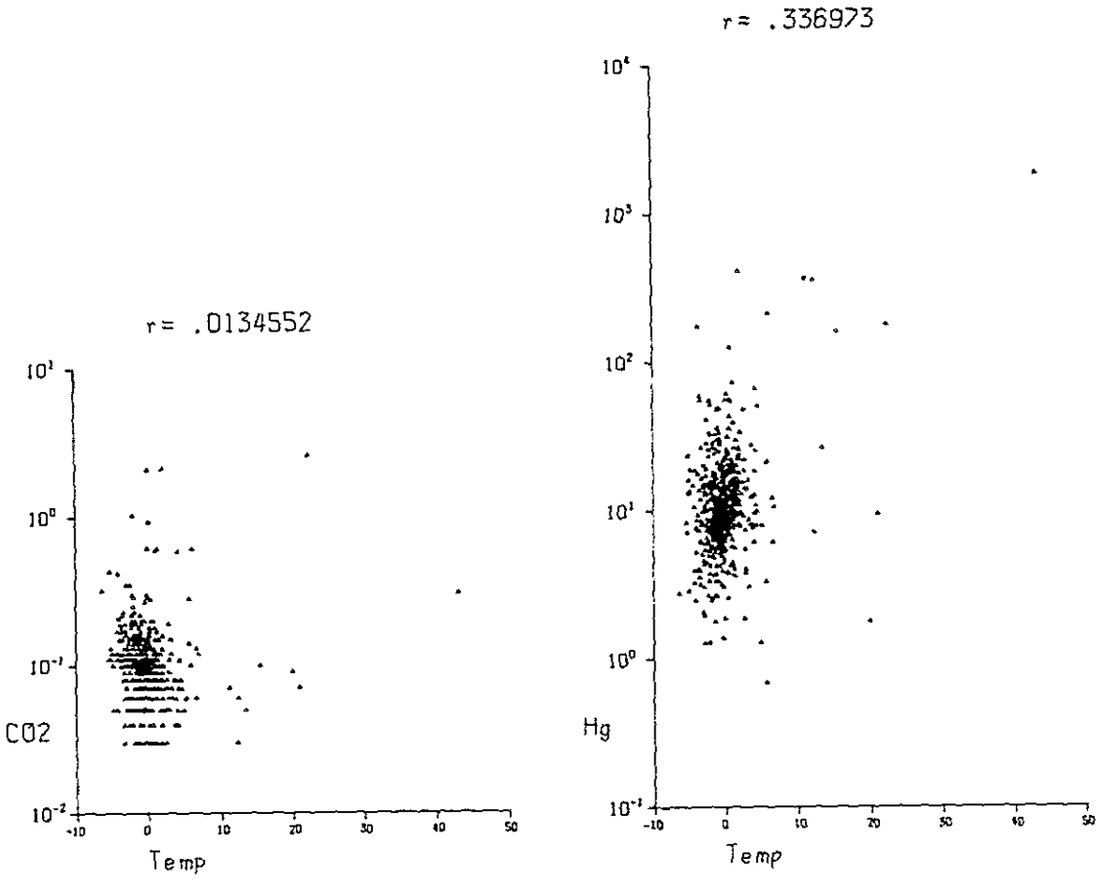

Fig.5-30 Correlations between residual ground temperature, and CO_2 - concentration(1) and Hg - concentration(2)

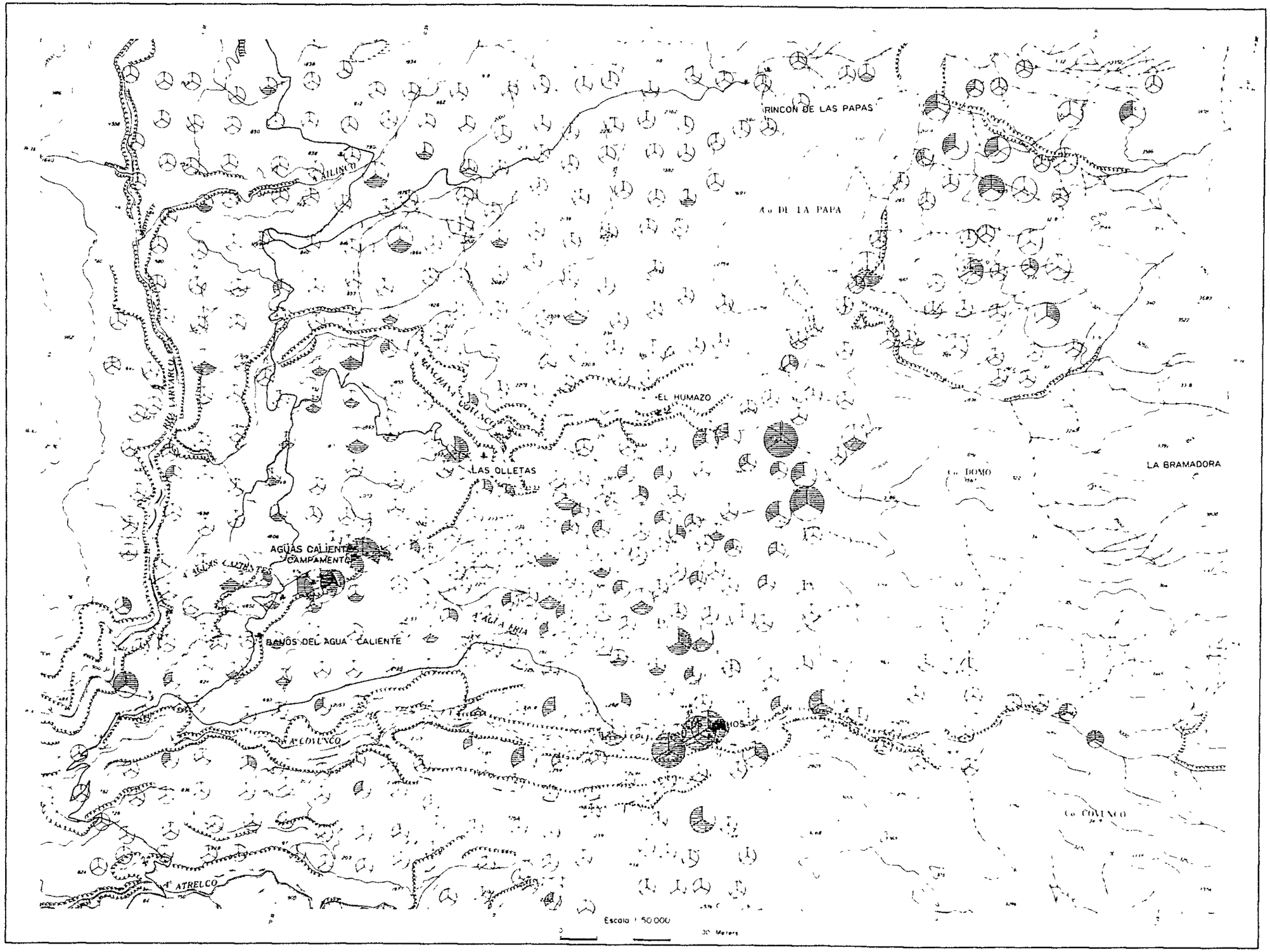

Fig.5-31 Relation map of anomalous values at 1 meter depth survey

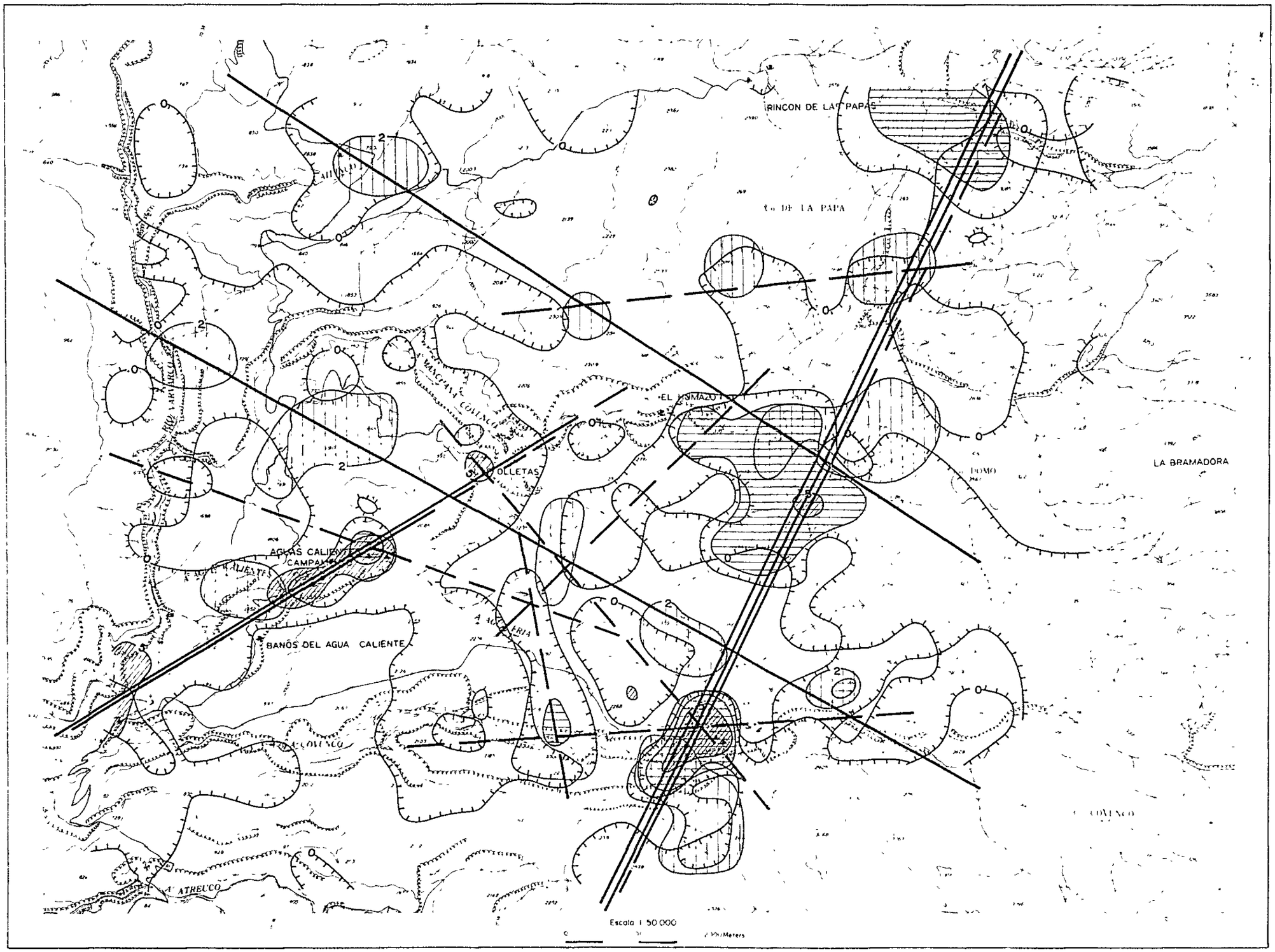

Fig.5-32 Composite map of anomalous areas of ground temperature and Hg - CO_2 geochemistry

6. Circulation Mechanism of Geothermal Fluid in the Investigation Area

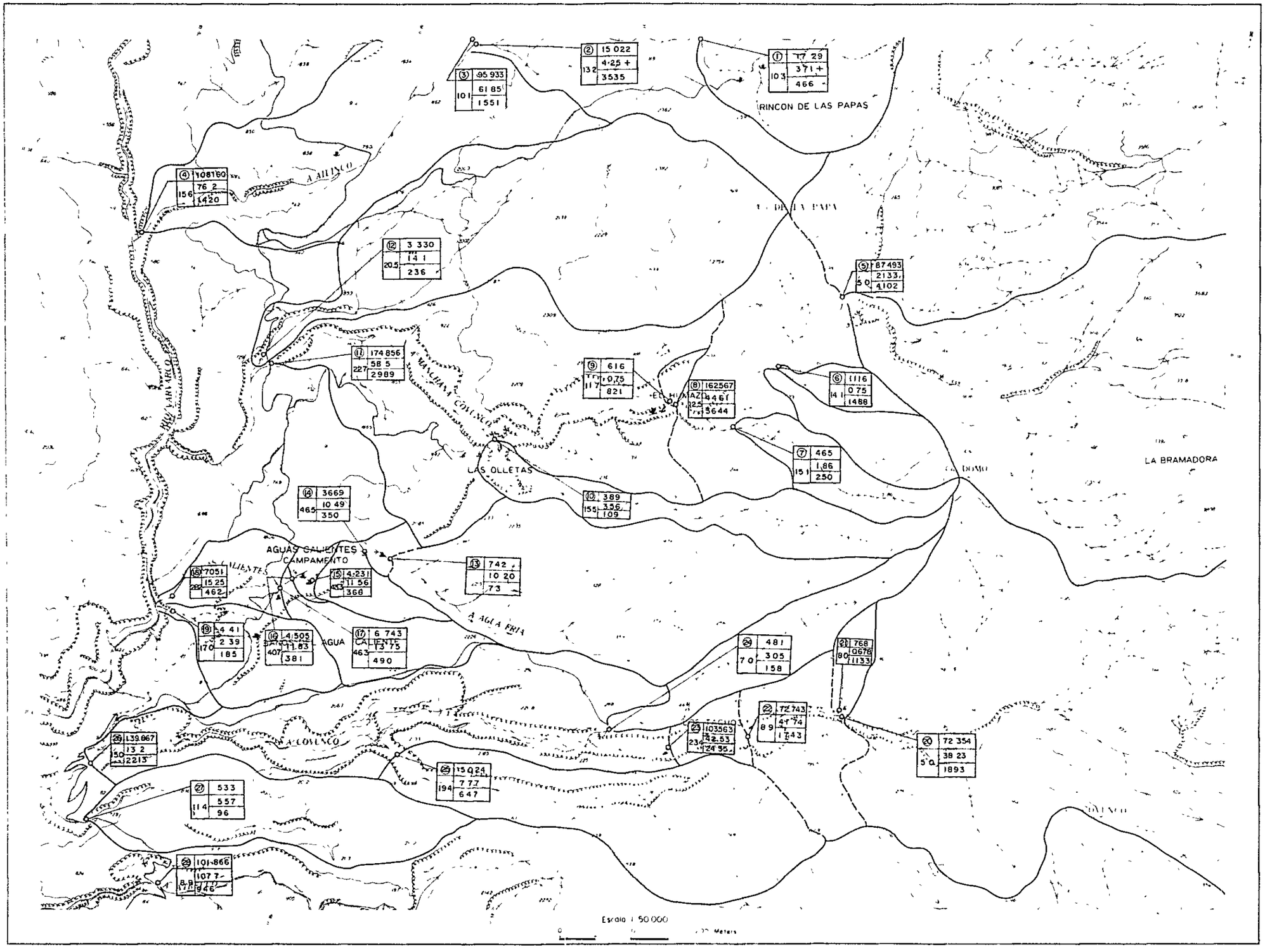

Fig.6-1 Location map of measurements of water discharge and calculations of specific rate of flow

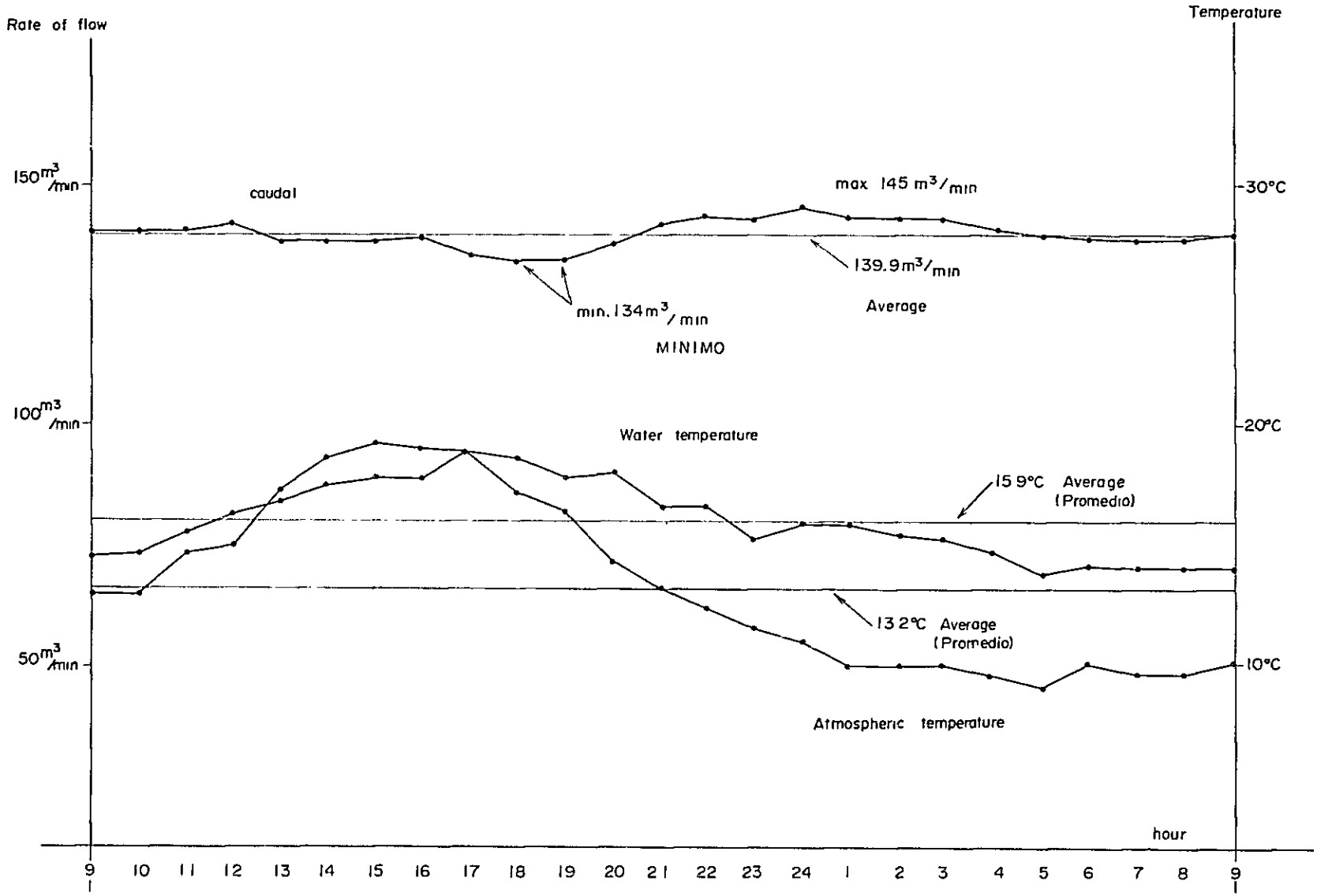

Fig.6-2 Daily variations of discharge, water temperature and atmospheric temperature

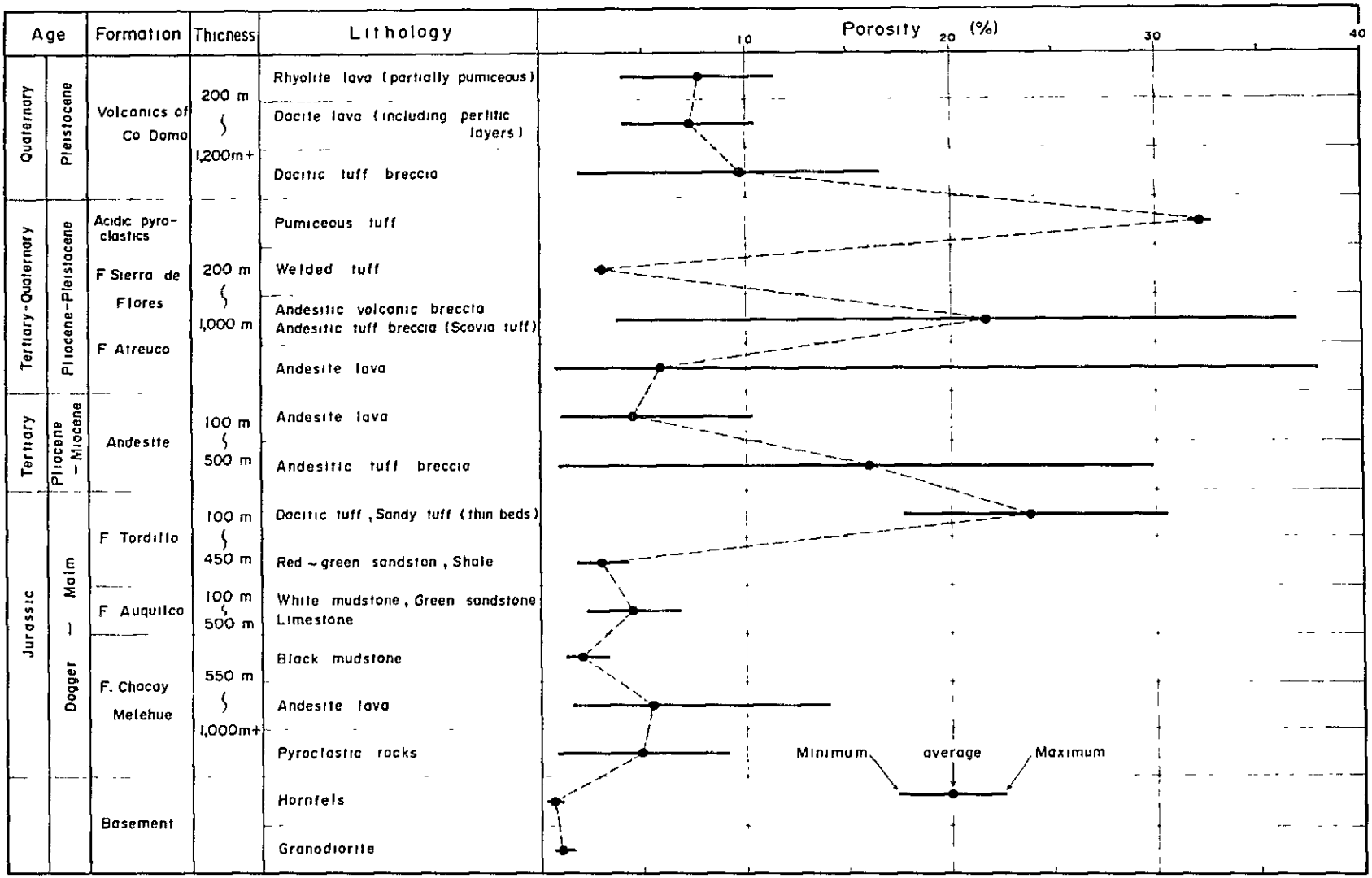

Fig.6-3 Schematic columnar section of effective porosity

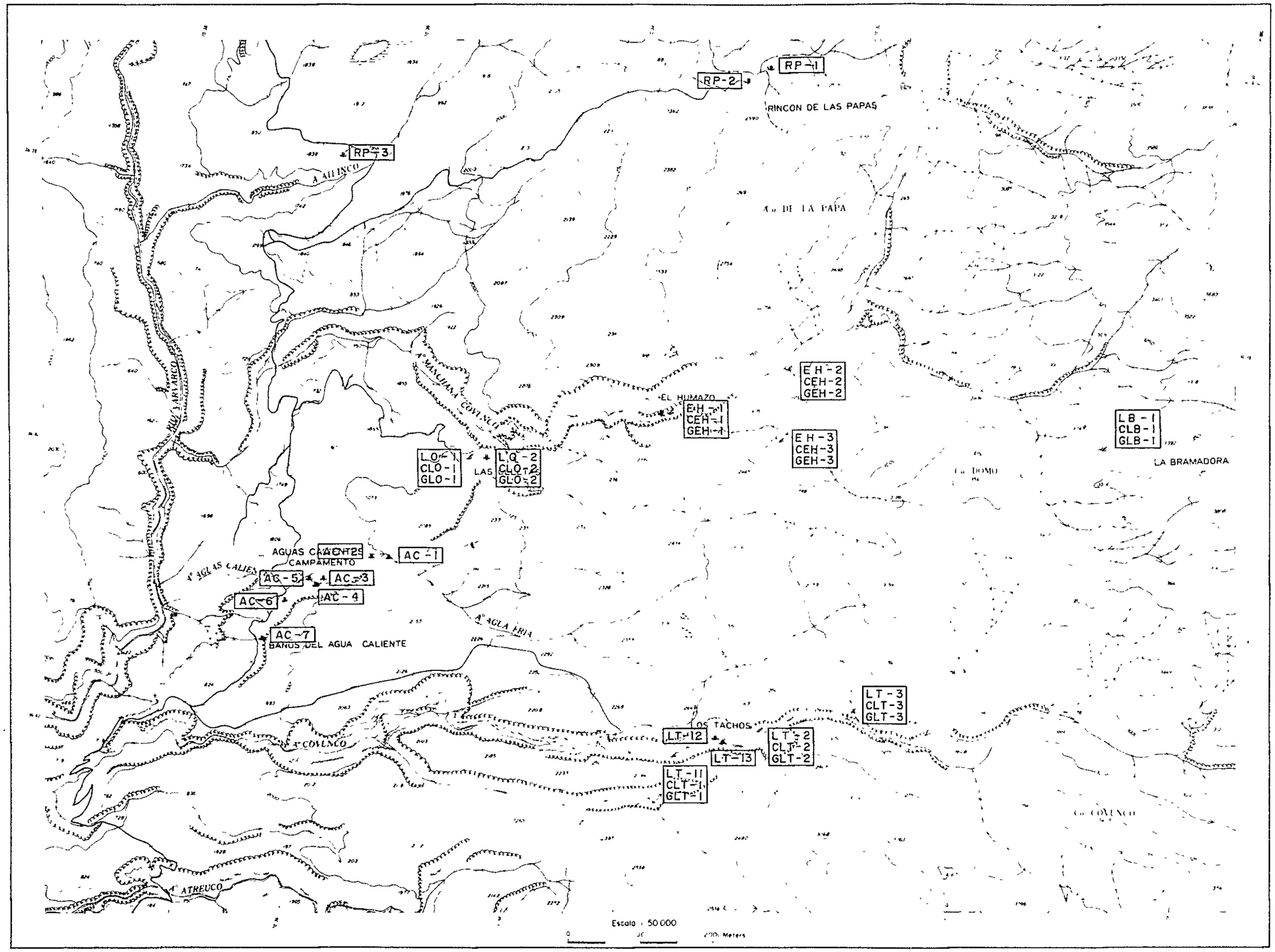

LEGEND

LO-1 Hot water
CLO-1 Condenced water
GLO-1 Fumaloic gas

Fig.6-4 Location map of hot water, fumaloic gas and condensed water samplings

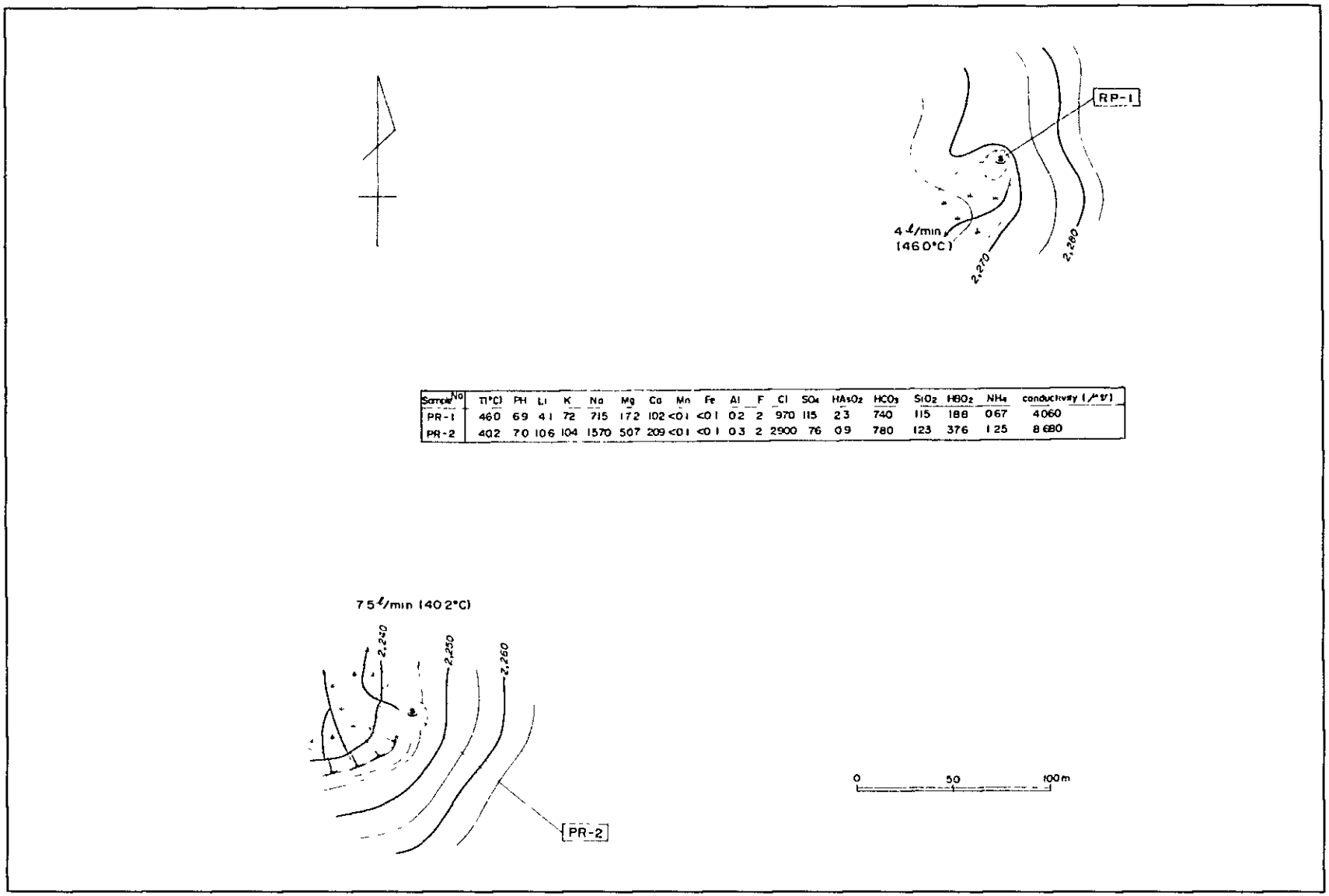

Sample No	T(°C)	PH	Li	K	Na	Mg	Ca	Mn	Fe	Al	F	Cl	SO_4	$HAsO_2$	HCO_3	SiO_2	HBO_2	NH_4	conductivity (μS)
PR-1	46.0	6.9	4.1	7.2	7.15	1.72	1.02	<0.1	<0.1	0.2	2	970	115	2.3	740	115	1.88	0.67	4060
PR-2	40.2	7.0	10.6	10.4	15.70	5.07	2.09	<0.1	<0.1	0.3	2	2900	76	0.9	780	123	3.76	1.25	8680

Fig.6-5 Detailed sketch of geothermal manifestation (1) Rincon de Las Papas

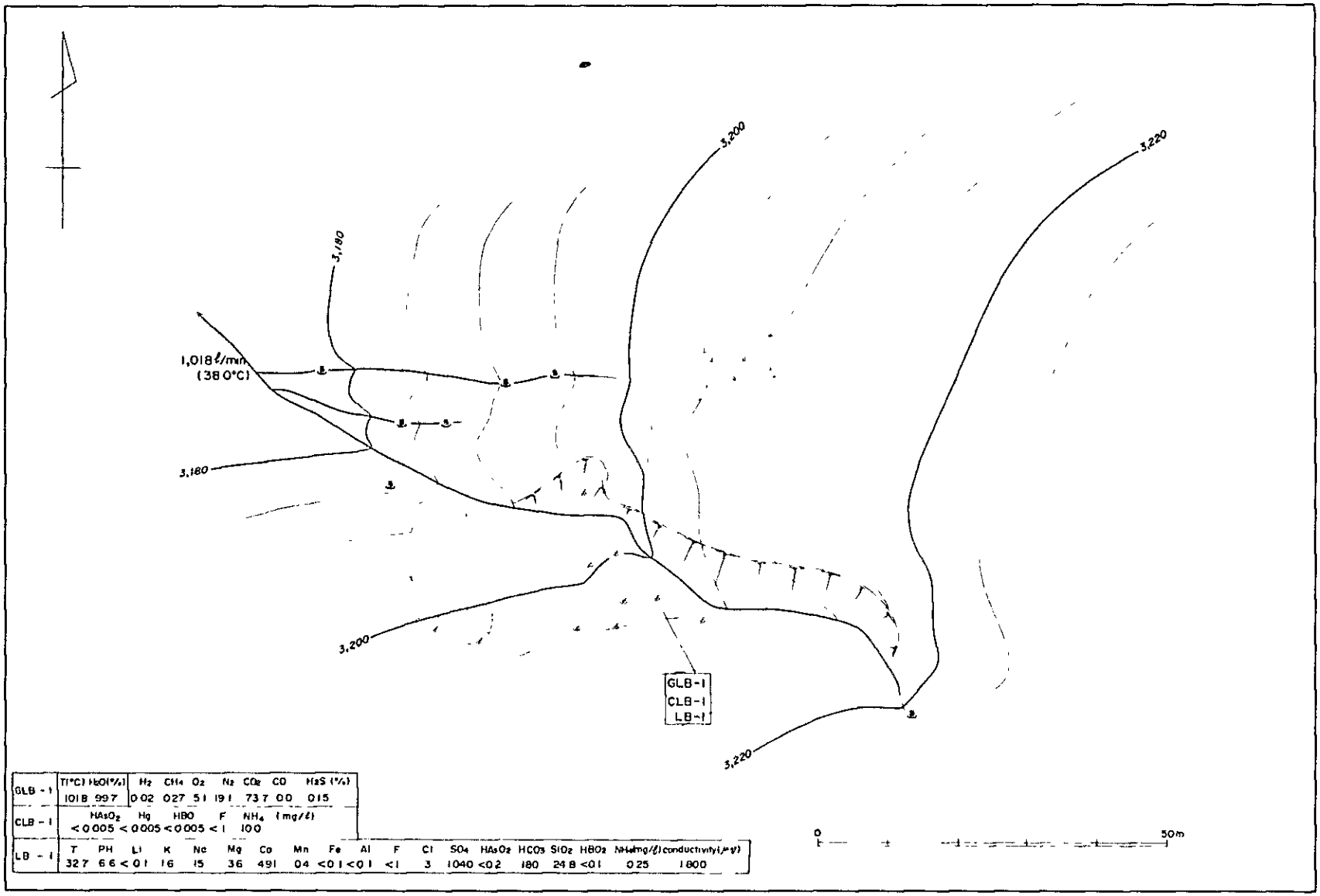

	T(°C)	H₂O(%)	H₂	CH₄	O₂	N₂	CO₂	CO	H₂S (%)
GLB-1	101.8	99.7	0.02	0.27	5.1	19.1	73.7	0.0	0.15

	$HAsO_2$	Hg	HBO	F	NH_4 (mg/ℓ)
CLB-1	< 0.005	< 0.005	< 0.005	< 1	10.0

	T	PH	Li	K	Na	Mg	Ca	Mn	Fe	Al	F	Cl	SO_4	$HAsO_2$	HCO_3	SiO_2	HBO_2	NH_4(mg/ℓ)	conductivity(μ℧)
LB-1	32.7	6.6	< 0.1	1.6	1.5	3.6	49.1	0.4	< 0.1	< 0.1	< 1	3	104.0	< 0.2	18.0	24.8	< 0.1	0.25	1800

Fig.6-6 Detailed sketch of geohtermal manifestation (2) La Bramadora

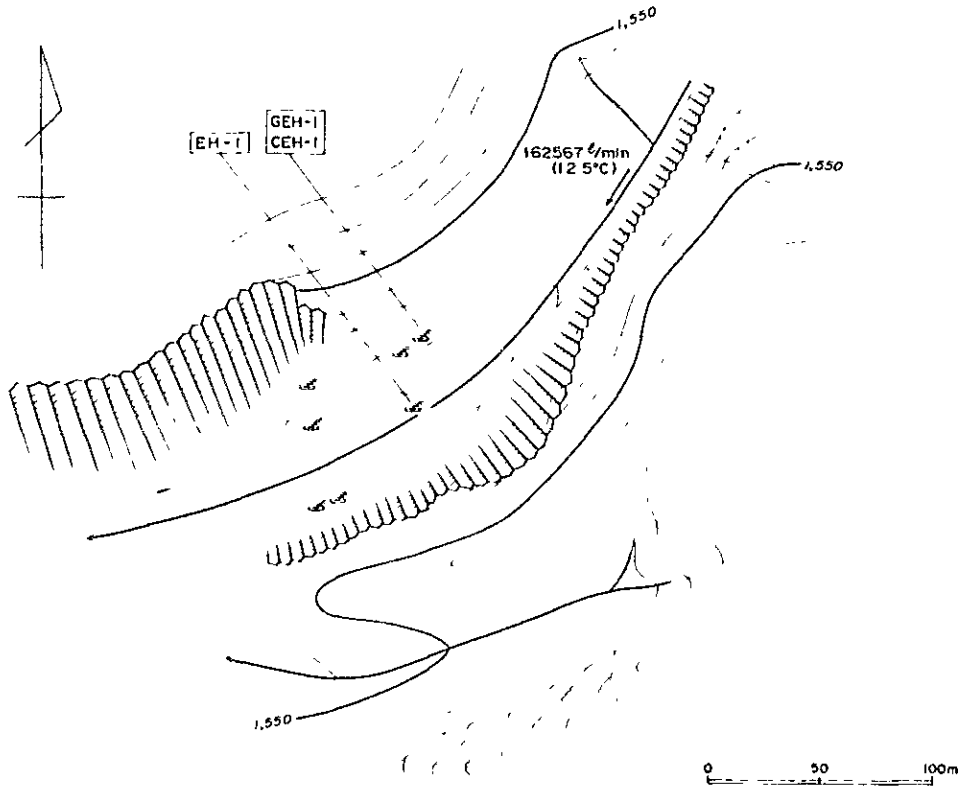

	T (°C)	H₂O (%)	H₂	CH₄	O₂	N₂	CO₂	H₂S	(%)
GEH-1	92.5	99.9	-	-	1.5	3.30	9.50	-	

	HAsO₂	Hg	HBO₂	F	NH₄	(mg/ℓ)
CEH-1	<0.005	<0.005	0.008	1	3.43	

	T(°C)	PH	Li	K	Na	Mg	Ca	Mn	Fe	Al	F	Cl	SO₄	HAsO₂	HCO₃	SiO₂	HBO₂	NH₄ (mg/ℓ)	conductivity
EH-1	97.5		12.1	152	1330	0.2	3.46	<0.1	<0.1	0.1	4	2000	230	32	100	240	454	0.52	6810

Fig.6-7 Detailed sketch of geothermal manifestation (3) El Humazo - 1

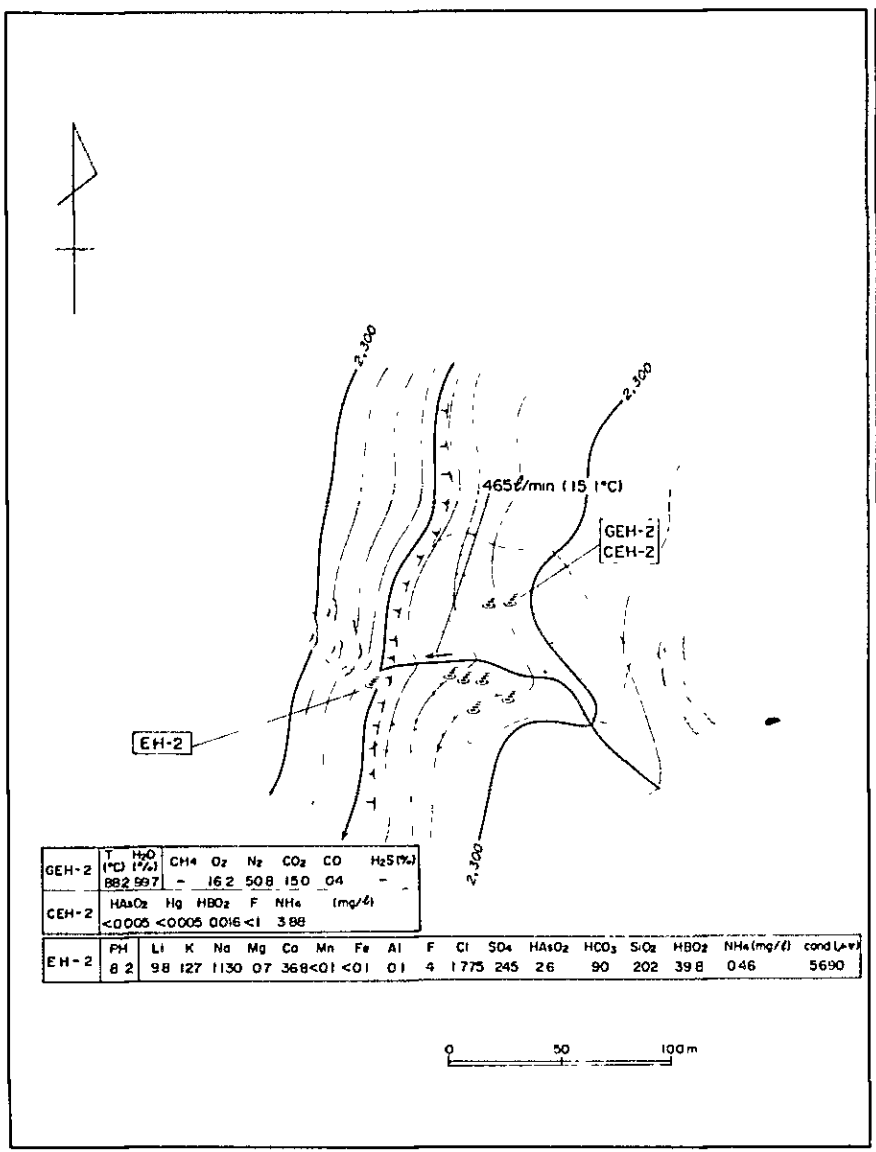

GEH-2	T (℃)	H_2O (%)	CH_4	O_2	N_2	CO_2	CO	H_2S (%)
	88.2	99.7	-	16.2	50.8	15.0	0.4	-

CEH-2	$HAsO_2$	Hg	HBO_2	F	NH_4	(mg/ℓ)
	<0.005	<0.0005	0.016	<1	3.88	

EH-2	PH	Li	K	Na	Mg	Ca	Mn	Fe	Al	F	Cl	SO_4	$HAsO_2$	HCO_3	SiO_2	HBO_2	NH_4 (mg/ℓ)	cond (μ·v)
	8.2	9.8	12.7	113.0	0.7	36.8	<0.1	<0.1	0.1	4	177.5	24.5	2.6		9.0	20.2	39.8	0.46	569.0

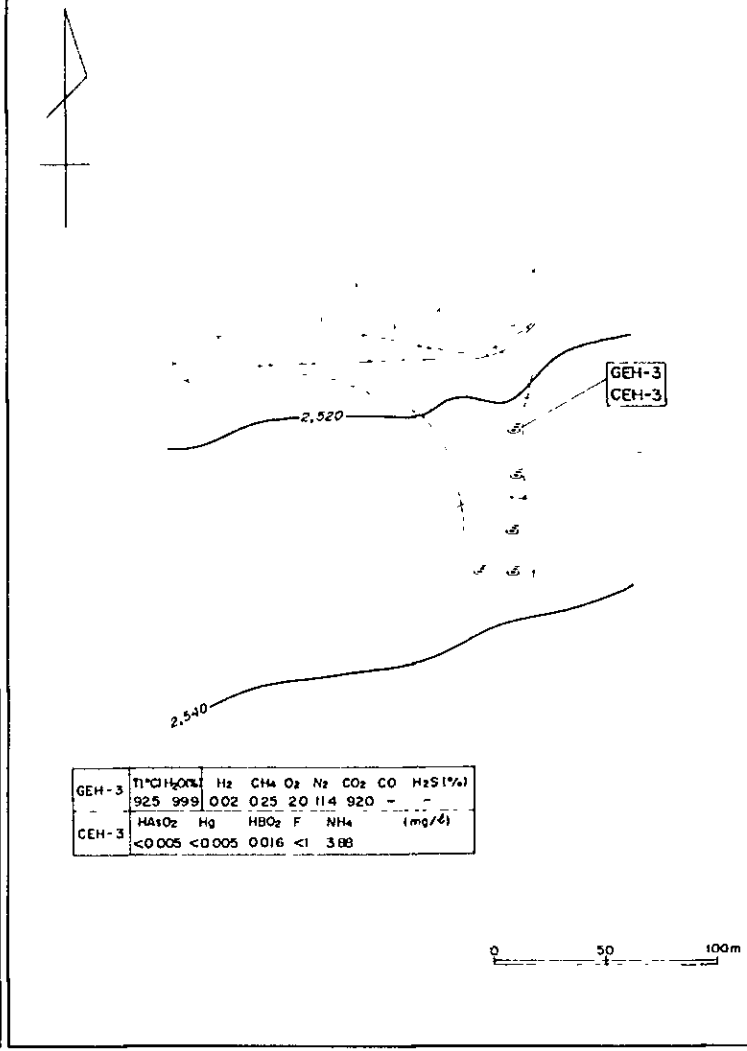

GEH-3	T(℃)	H_2O(%)	H_2	CH_4	O_2	N_2	CO_2	CO	H_2S (%)
	92.5	99.9	0.02	0.25	2.0	11.4	92.0	-	-

CEH-3	$HAsO_2$	Hg	HBO_2	F	NH_4	(mg/ℓ)
	<0.005	<0.005	0.016	<1	3.88	

Fig.6-8 Detailed sketch of geothermal manifestation (4) El Humazo - 2

Fig.6-9 Detailed sketch of geothermal manifestation (5) El Humazo - 3

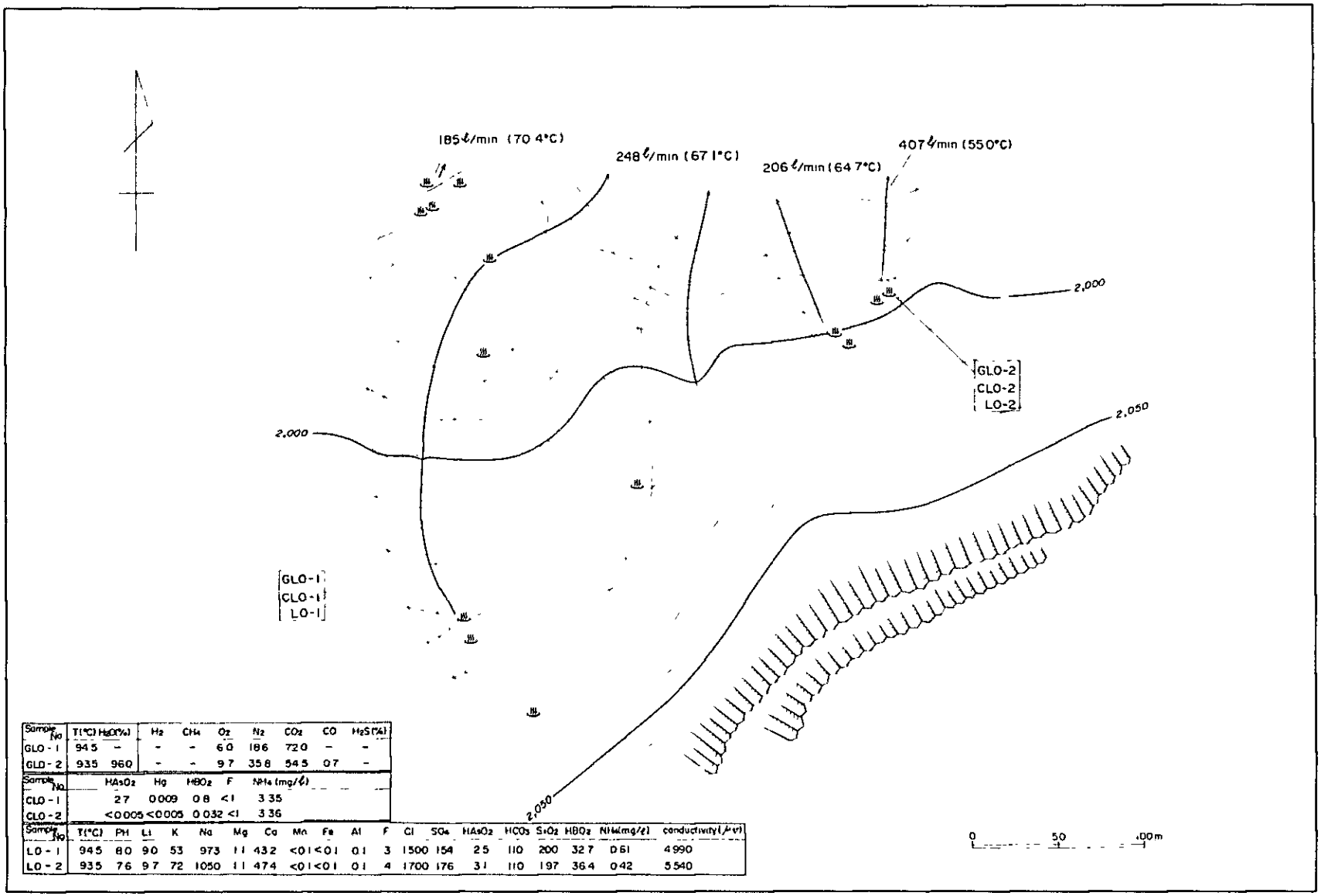

Sample No.	T(°C)	H₂O(%)	H₂	CH₄	O₂	N₂	CO₂	CO	H₂S(%)
GLO-1	94.5	–	–	–	6.0	18.6	72.0	–	–
GLO-2	93.5	96.0	–	–	9.7	35.8	54.5	0.7	–

Sample No.	HAsO₂	Hg	HBO₂	F	NH₄ (mg/ℓ)
CLO-1	2.7	0.009	0.8	<1	3.35
CLO-2	<0.005	<0.005	0.032	<1	3.36

Sample No.	T(°C)	PH	Li	K	Na	Mg	Ca	Mn	Fe	Al	F	Cl	SO₄	HAsO₂	HCO₃	SiO₂	HBO₂	NH₄(mg/ℓ)	conductivity(μ℧)
LO-1	94.5	8.0	9.0	5.3	97.3	1.1	43.2	<0.1	<0.1	0.1	3	1500	154	2.5	110	200	32.7	0.61	4990
LO-2	93.5	7.6	9.7	7.2	105.0	1.1	47.4	<0.1	<0.1	0.1	4	1700	176	3.1	110	197	36.4	0.42	5540

Fig.6-10 Detailed sketch of geothermal manifestation (6) Las Olletas

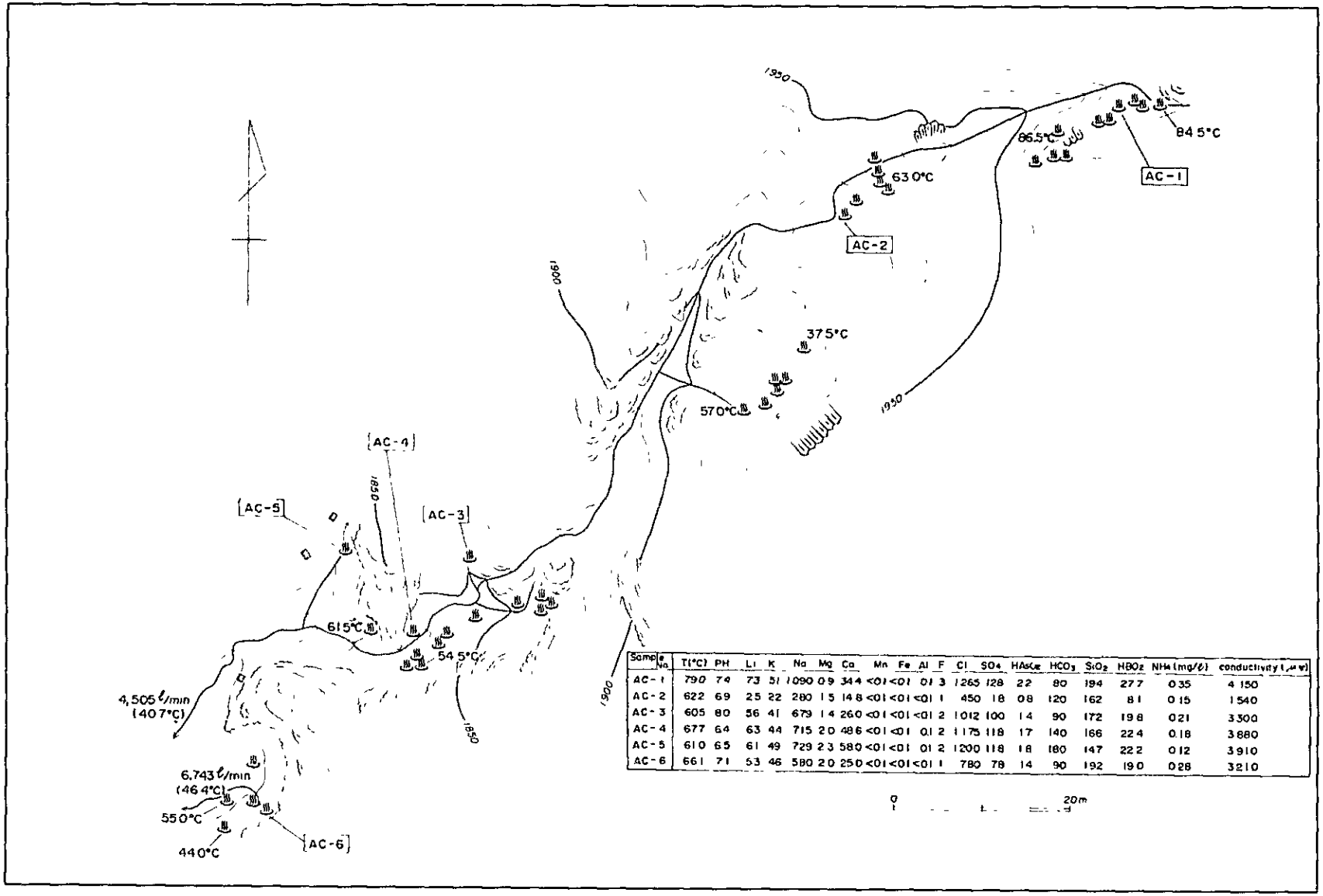

Samp. No.	T(°C)	PH	Li	K	Na	Mg	Ca	Mn	Fe	Al	F	Cl	SO4	HAsO2	HCO3	SiO2	HBO2	NH4 (mg/ℓ)	conductivity (μ mho)
AC-1	79.0	7.4	7.3	5.1	1090	0.9	3.44	<0.1	<0.1	0.13		1265	128	2.2	80	194	27.7	0.35	4 150
AC-2	62.2	6.9	2.5	2.2	280	1.5	14.8	<0.1	<0.1	<0.1	1	450	18	0.8	120	162	8.1	0.15	1540
AC-3	60.5	8.0	5.6	4.1	679	1.4	2.60	<0.1	<0.1	<0.1	2	1012	100	1.4	90	172	19.8	0.21	3300
AC-4	67.7	6.4	6.3	4.4	715	2.0	4.86	<0.1	<0.1	0.1	2	1175	118	1.7	140	166	22.4	0.18	3880
AC-5	61.0	6.5	6.1	4.9	729	2.3	5.80	<0.1	<0.1	0.1	2	1200	118	1.8	180	147	22.2	0.12	3910
AC-6	66.1	7.1	5.3	4.6	580	2.0	2.50	<0.1	<0.1	<0.1	1	780	78	1.4	90	192	19.0	0.28	3210

Fig.6-11 Detailed sketch of geothermal manifestation (7) Aguas Calientes

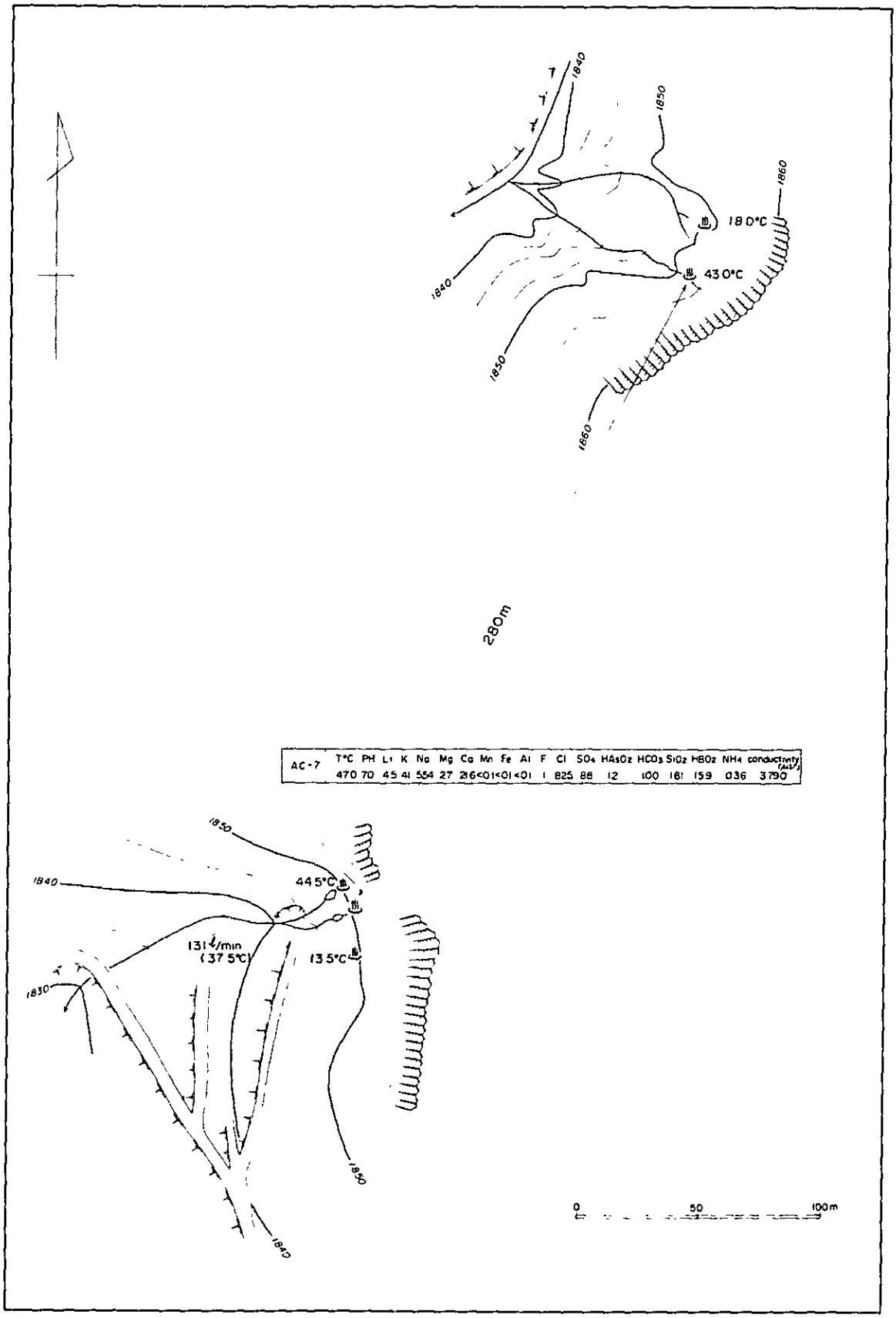

Fig.6-12 Detailed sketch of geothermal manifestation
(8) Banõs del Agua Caliente

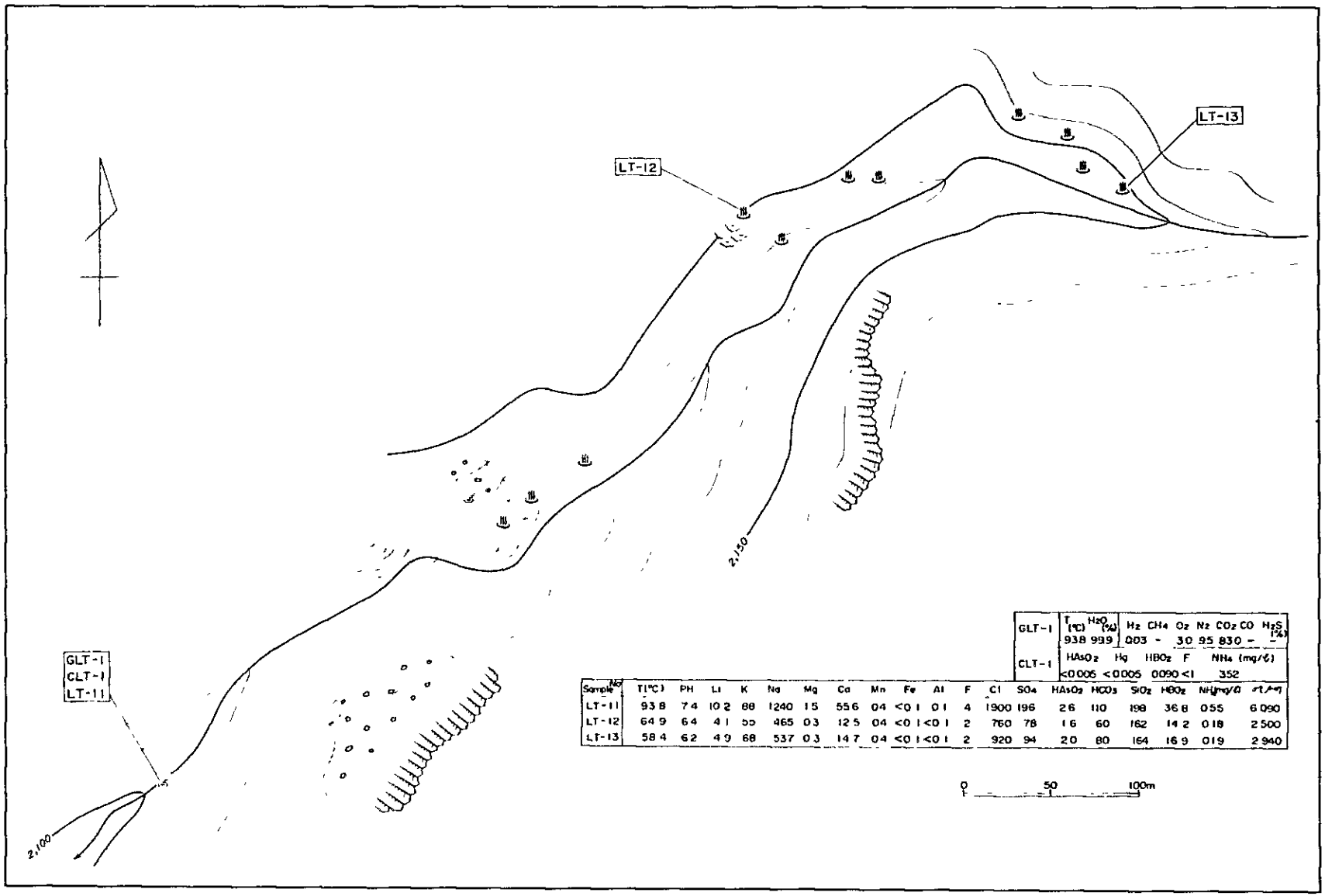

	T (°C)	H_2O (%)	H_2	CH_4	O_2	N_2	CO_2	CO	H_2S (%)
GLT-1	938	999	003	-	30	95	830	-	-
CLT-1	$HAsO_2$	Hg	HBO_2	F	NH_4 (mg/ℓ)				
	<0.005	<0.005	0090	<1	352				

Sample No.	T(°C)	PH	Li	K	Na	Mg	Ca	Mn	Fe	Al	F	Cl	SO_4	$HAsO_2$	HCO_3	SiO_2	HBO_2	NH_4(mg/ℓ)	ℓ/min
LT-11	93.8	7.4	10.2	88	1240	1.5	55.6	0.4	<0.1	0.1	4	1900	196	2.6	110	198	36.8	0.55	6 090
LT-12	64.9	6.4	4.1	5.5	465	0.3	12.5	0.4	<0.1	<0.1	2	760	7.8	1.6	60	162	14.2	0.18	2 500
LT-13	58.4	6.2	4.9	6.8	537	0.3	14.7	0.4	<0.1	<0.1	2	920	9.4	2.0	80	164	16.9	0.19	2 940

Fig.6-13 Detailed sketch of geothermal manifestation (9) Los Tachos - 1

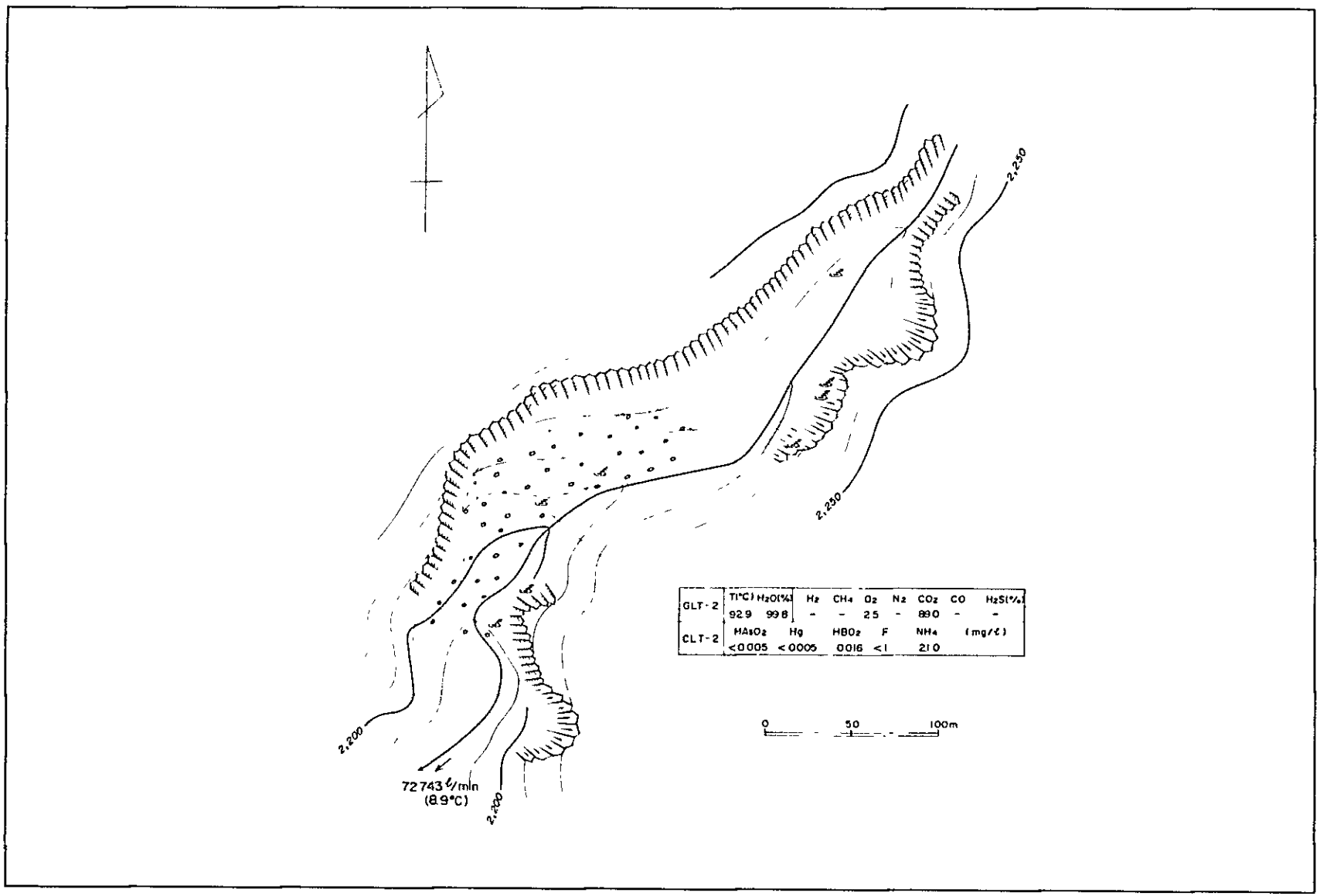

Fig.6-14 Detailed sketch of geothermal manifestation (10) Los Tachos - 2

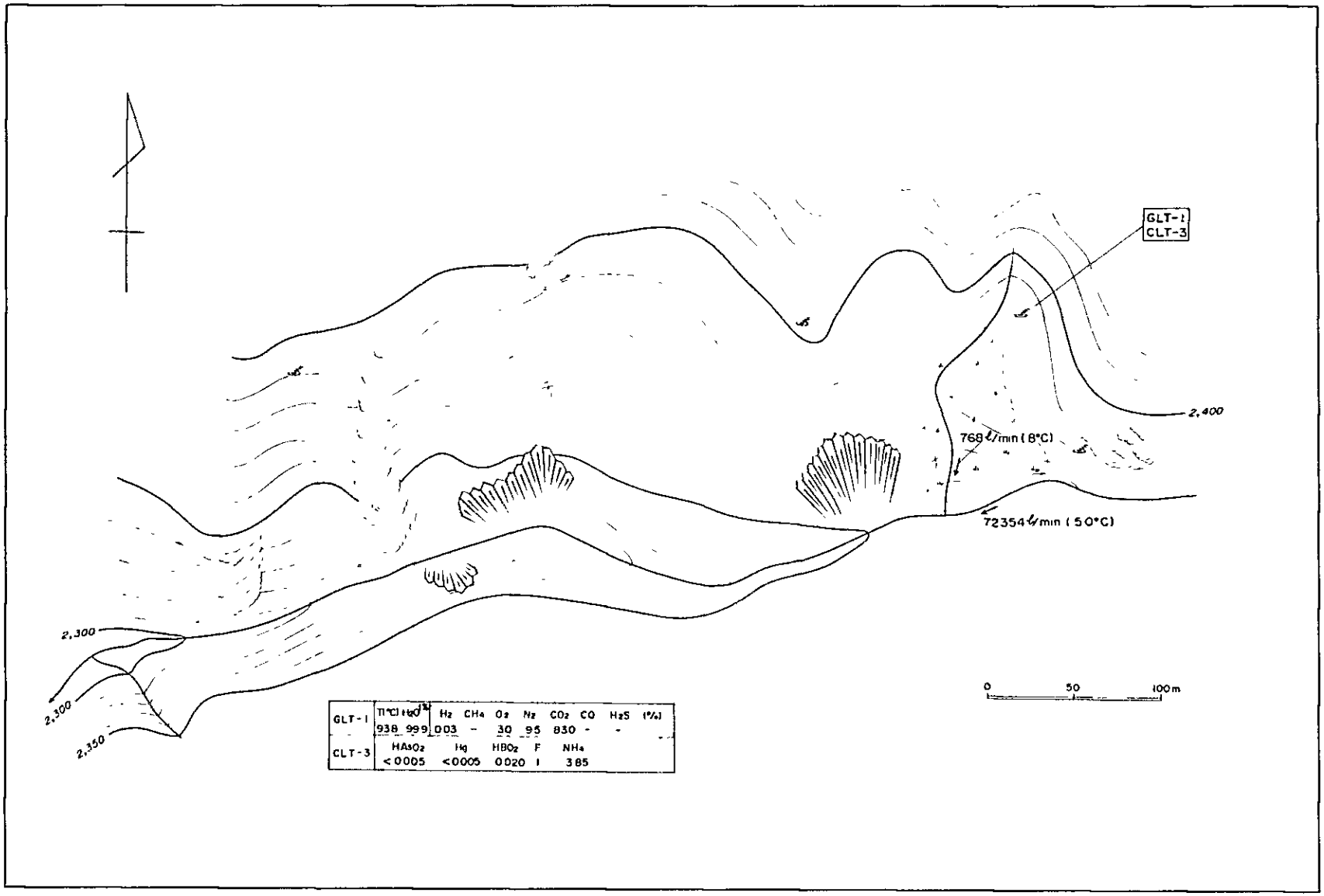

Fig.6-15 Detailed sketch of geothermal manifestation (11) Los Tachos - 3

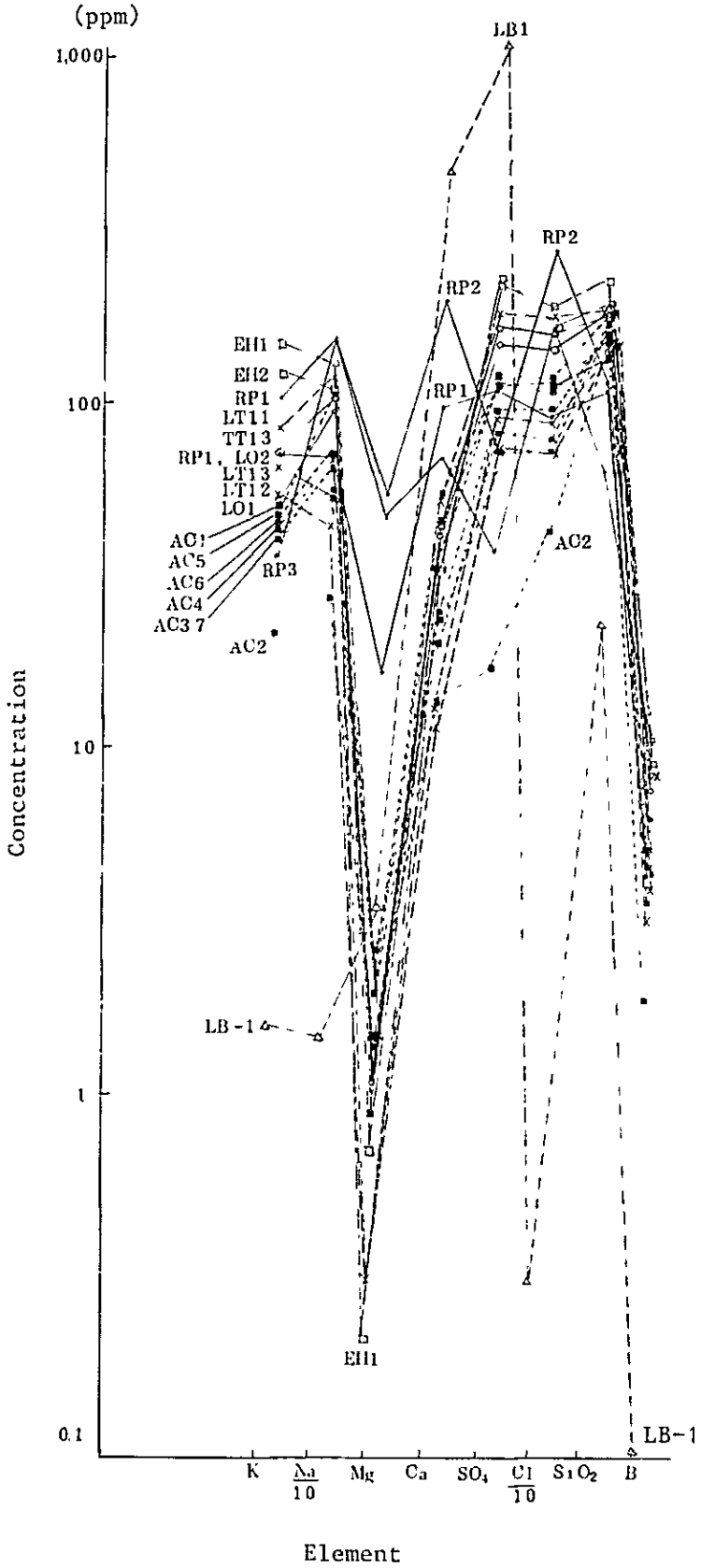

Fig.6-16 Main chemical compositions of hot water

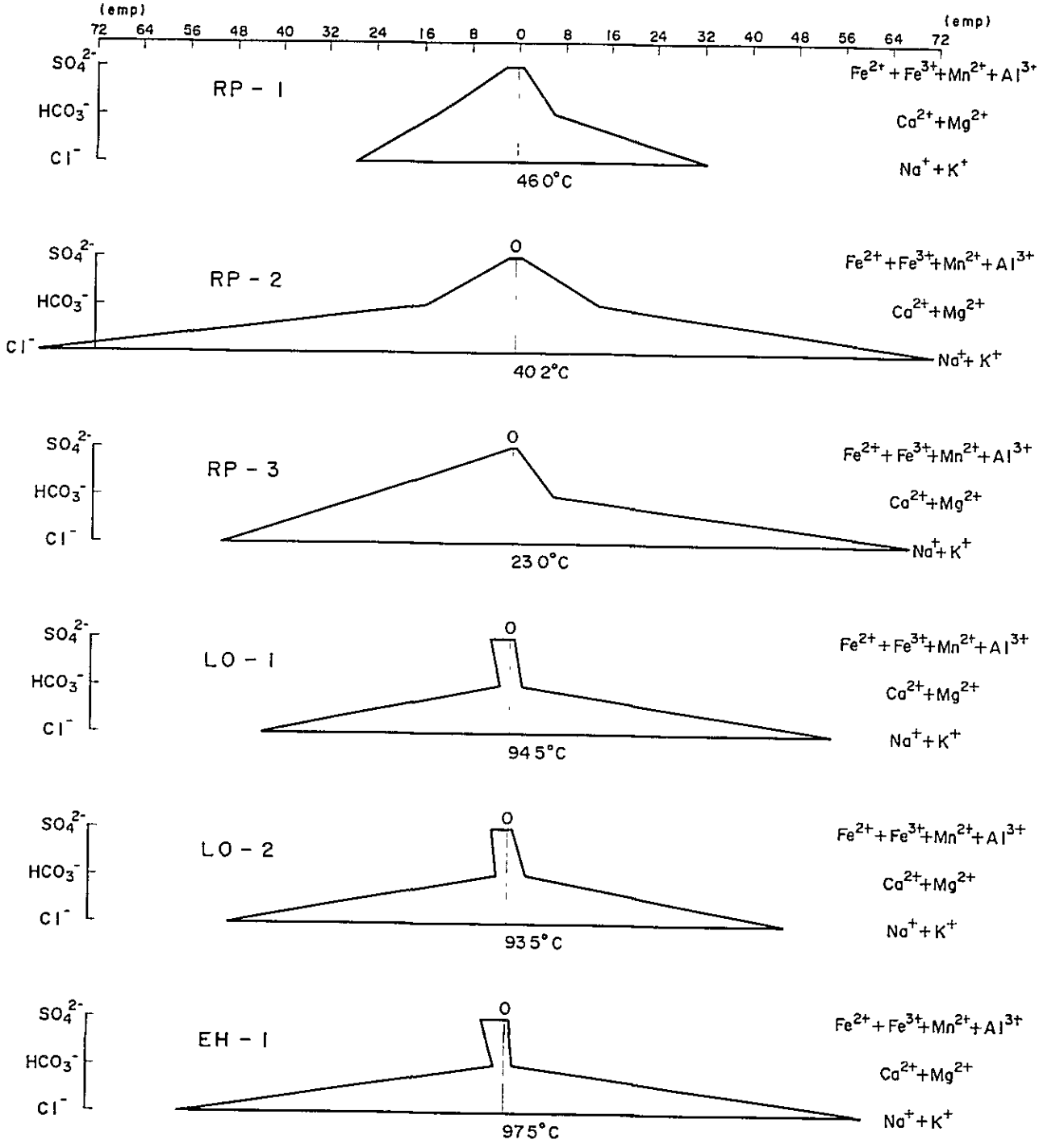

Fig.6-17(1) Hexadiagrams of main chemical compositions of hot water

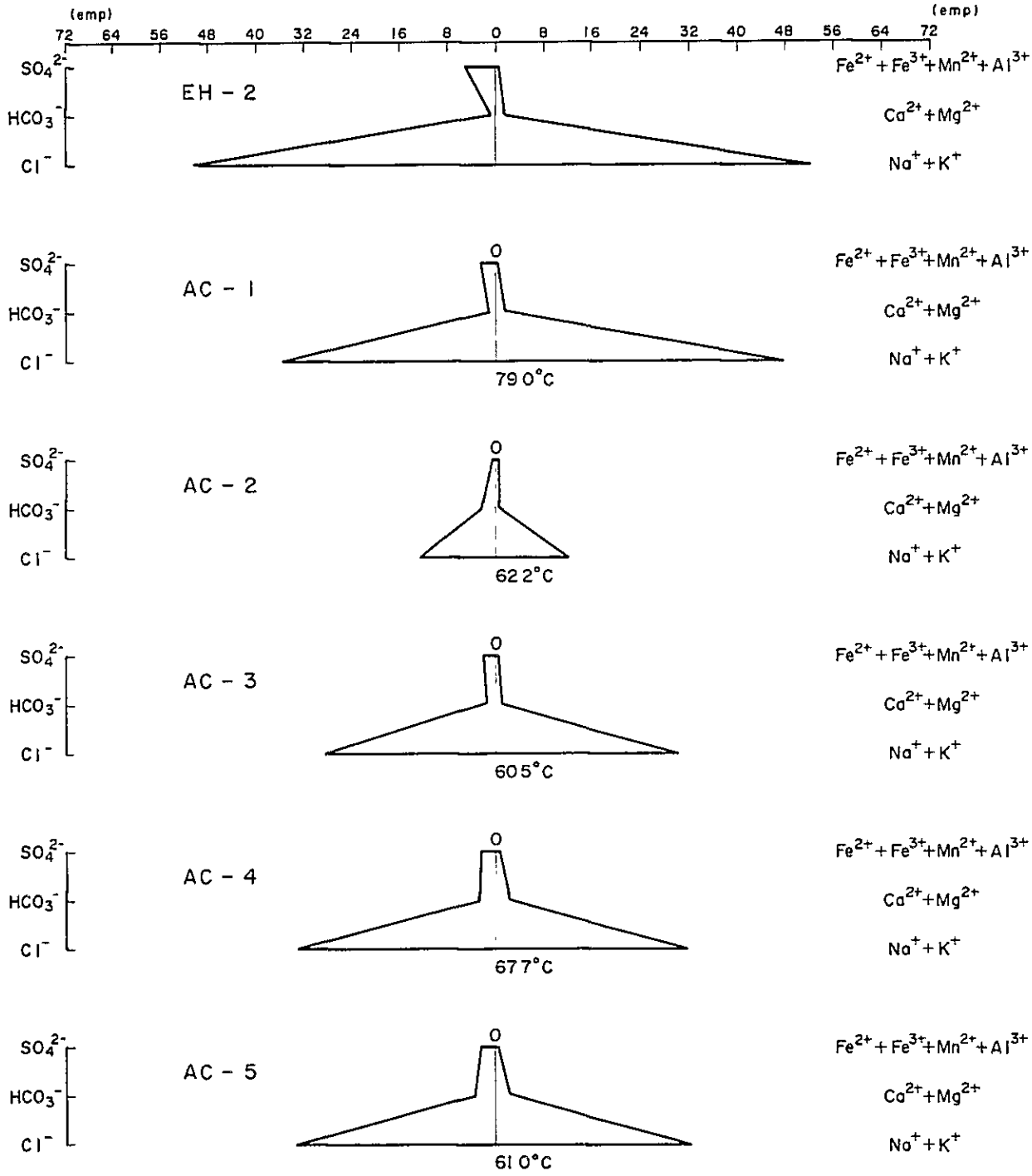

Fig.6-17(2) Hexadiagrams of main chemical compositions of hot water

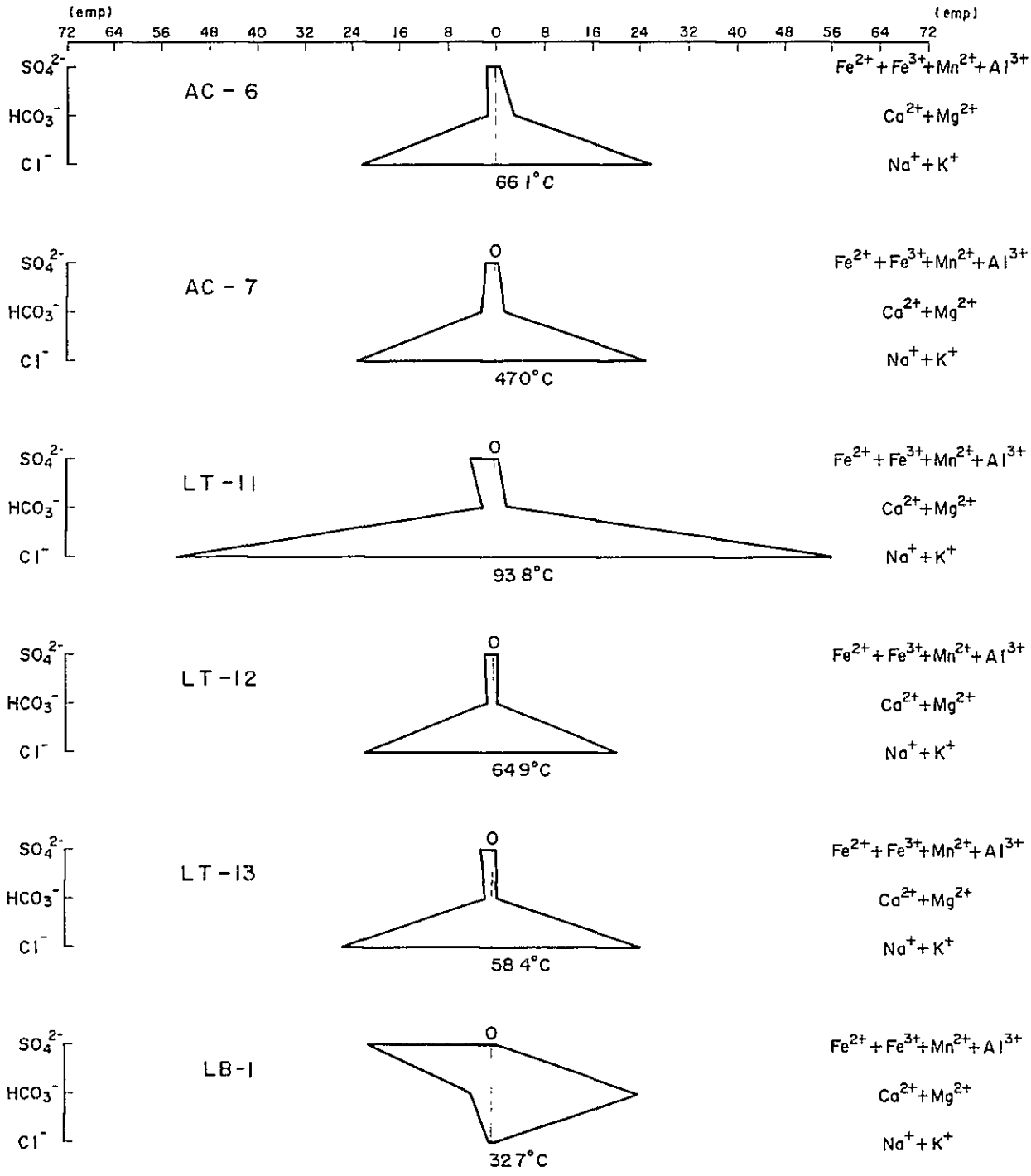

Fig.6-17(3) Hexadiagrams of main chemical compositions of hot water

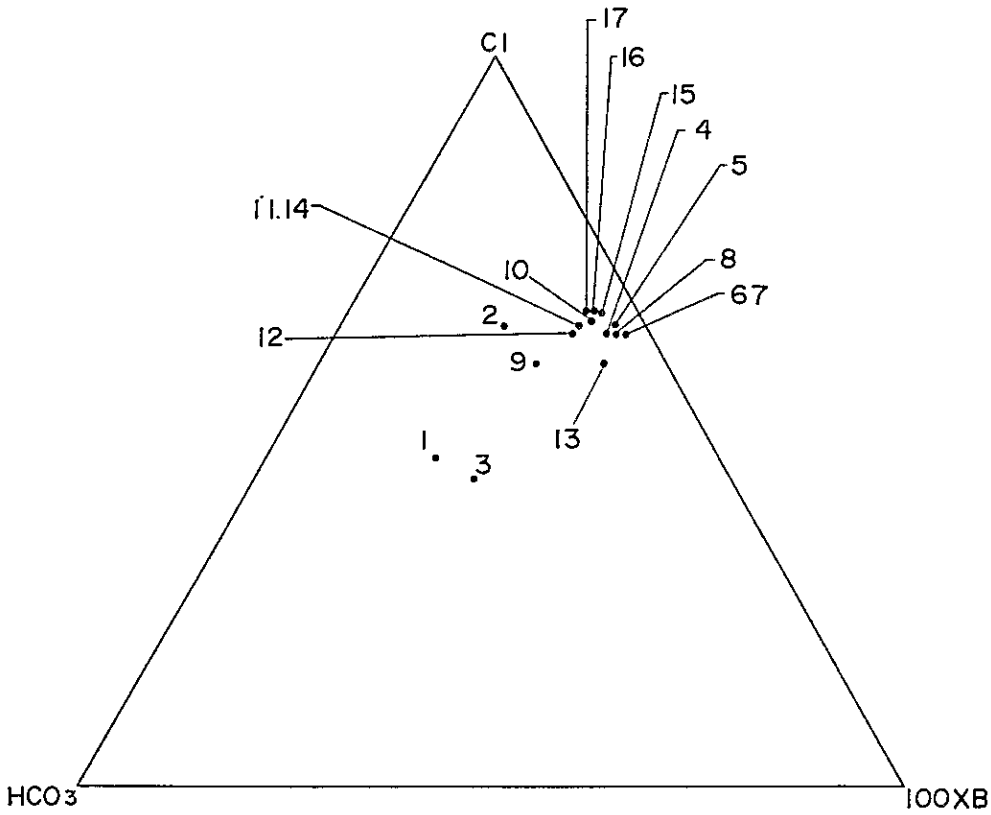

1	RP-1	7	EH-2	13	AC-6
2	RP-2	8	AC-1	14	AC-7
3	RP-3	9	AC-2	15	LT-11
4	LO-1	10	AC-3	16	LT-12
5	LO-2	11	AC-4	17	LT-13
6	EH-1	12	AC-5		

Fig.6-18 Diagram of Cl - HCO_3 - B contents of hot water

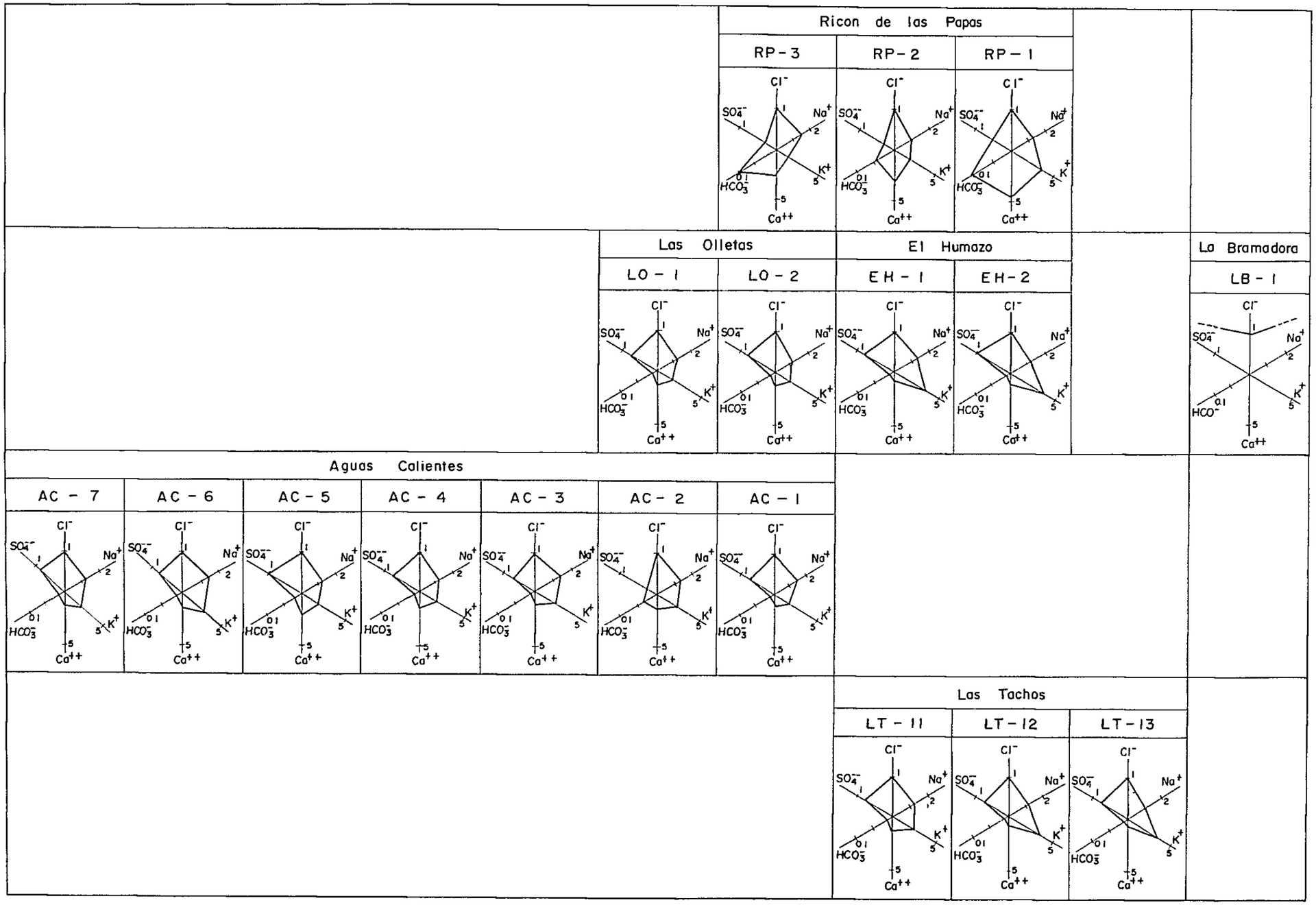

Fig.6-19 Comparative diagrams of ion - concentration index between sea water and hot water

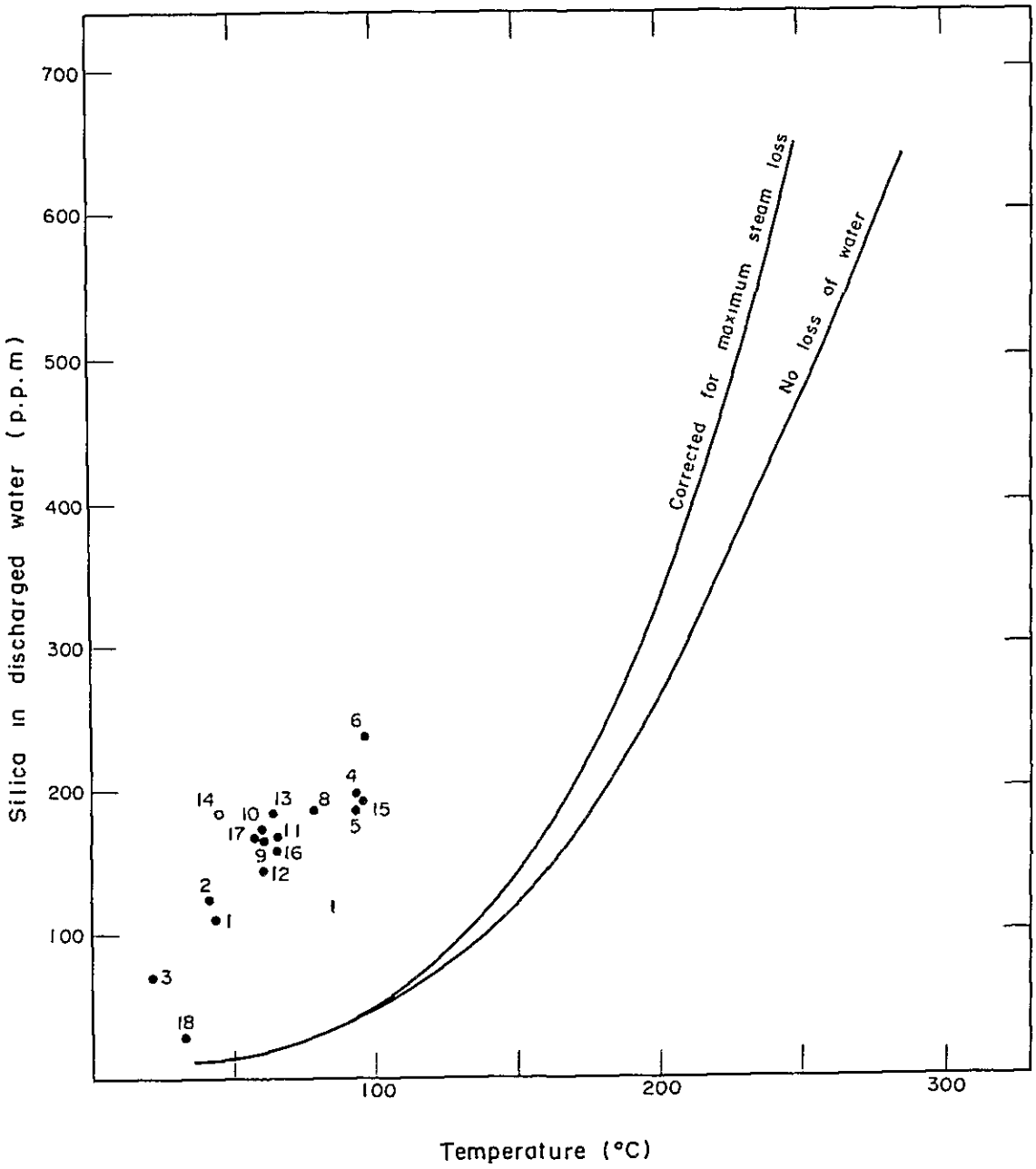

Rincón de las Papas		Las Olletas		El Humazo		Aguas Calientes		Los Tachos		La Bramadora	
No	Sample No	No	Sample No	No	Sample No	No	Sample No	No	Sample No	No	Sample No
1	RP - 1	4	LO - 1	6	EH - 1	8	AC - 1	15	LT - 11	18	LB
2	" - 2	5	" - 2		" - 2	9	" - 2	16	" - 12		
3	" - 3					10	" - 3	17	" - 13		
						11	" - 4				
						12	" - 5				
						13	" - 6				
						14	" - 7				

Fig.6-20 Silica - geochemical geothermometer

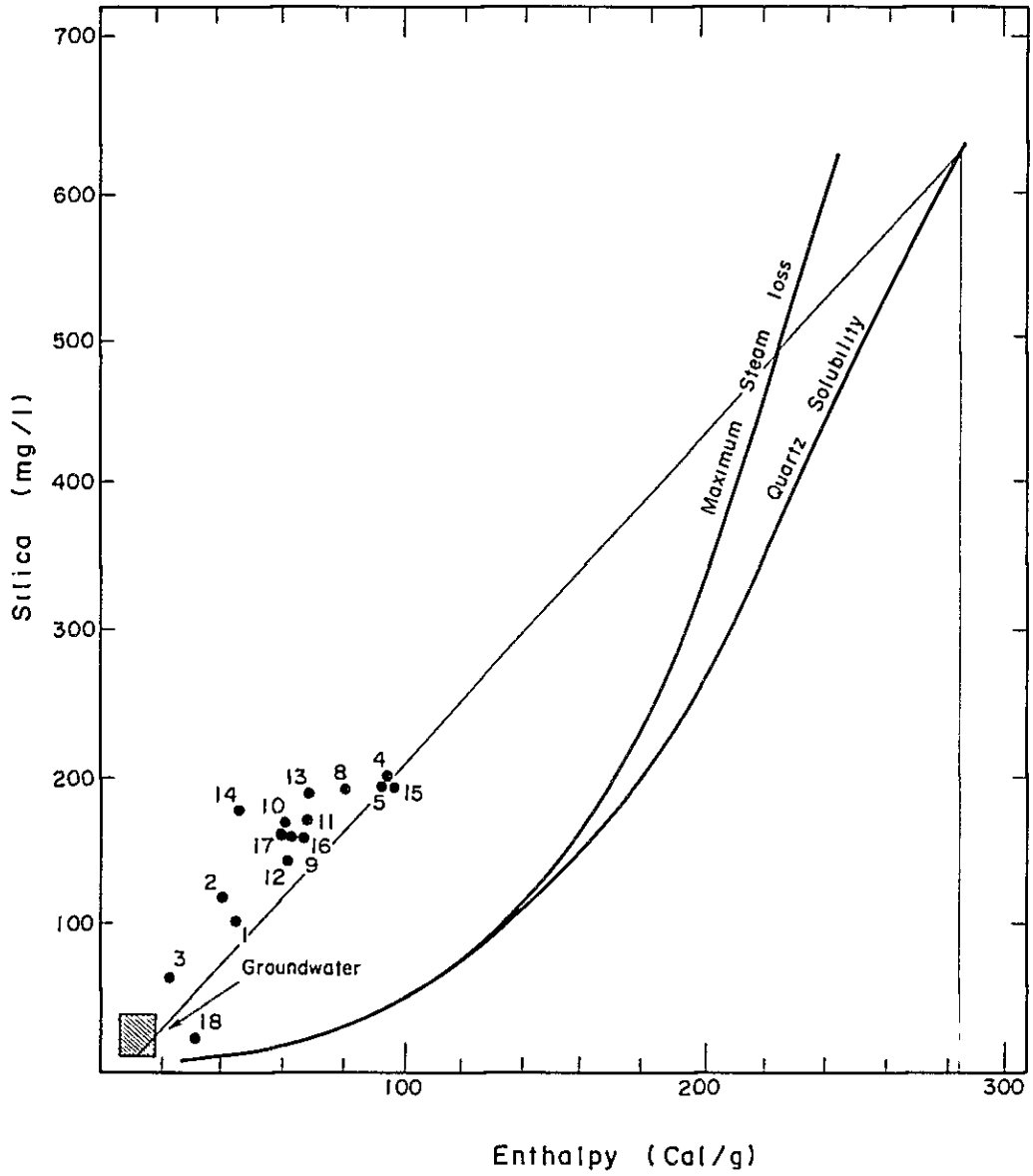

Rincón de las Papas		Las Olletas		El Humazo		Aguas Calientes		Los Tachos		La Bramadora	
No	Sample No	No	Sample No	No	Sample No	No	Sample No	No	Sample No	No	Sample No
1	RP - 1	4	LO - 1	6	EH - 1	8	AC - 1	15	LT - 11	18	LB
2	" - 2	5	" - 2		" - 2	9	" - 2	16	" - 12		
3	" - 3					10	" - 3	17	" - 13		
						11	" - 4				
						12	" - 5				
						13	" - 6				
						14	" - 7				

Fig.6-21 Silica - geochemical geothermometer (mixing model 1-1)

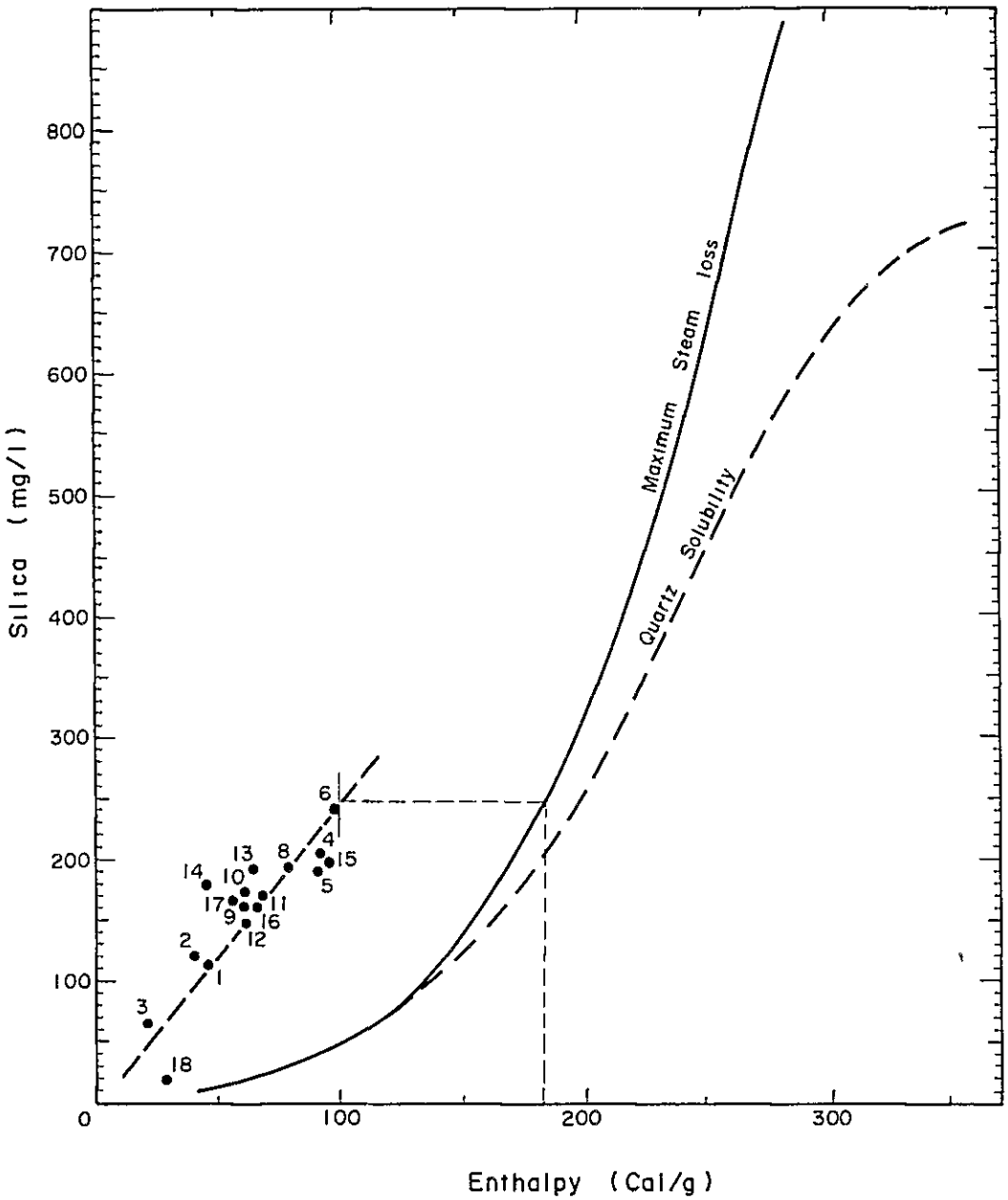

Rincón de las Papas		Las Olletas		El Humazo		Aguas Calientes		Los Tachos		La Bramadora	
No	Sample No	No	Sample No	No	Sample No	No	Sample No	No	Sample No	No	Sample No
1	RP - 1	4	LO - 1	6	EH - 1	8	AC - 1	15	LT - 11	18	LB
2	〃 - 2	5	〃 - 2		〃 - 2	9	〃 - 2	16	〃 - 12		
3	〃 - 3					10	〃 - 3	17	〃 - 13		
						11	〃 - 4				
						12	〃 - 5				
						13	〃 - 6				
						14	〃 - 7				

Fig.6-22 Silica - geochemical geothermometer
(mixing model 1 - 2)

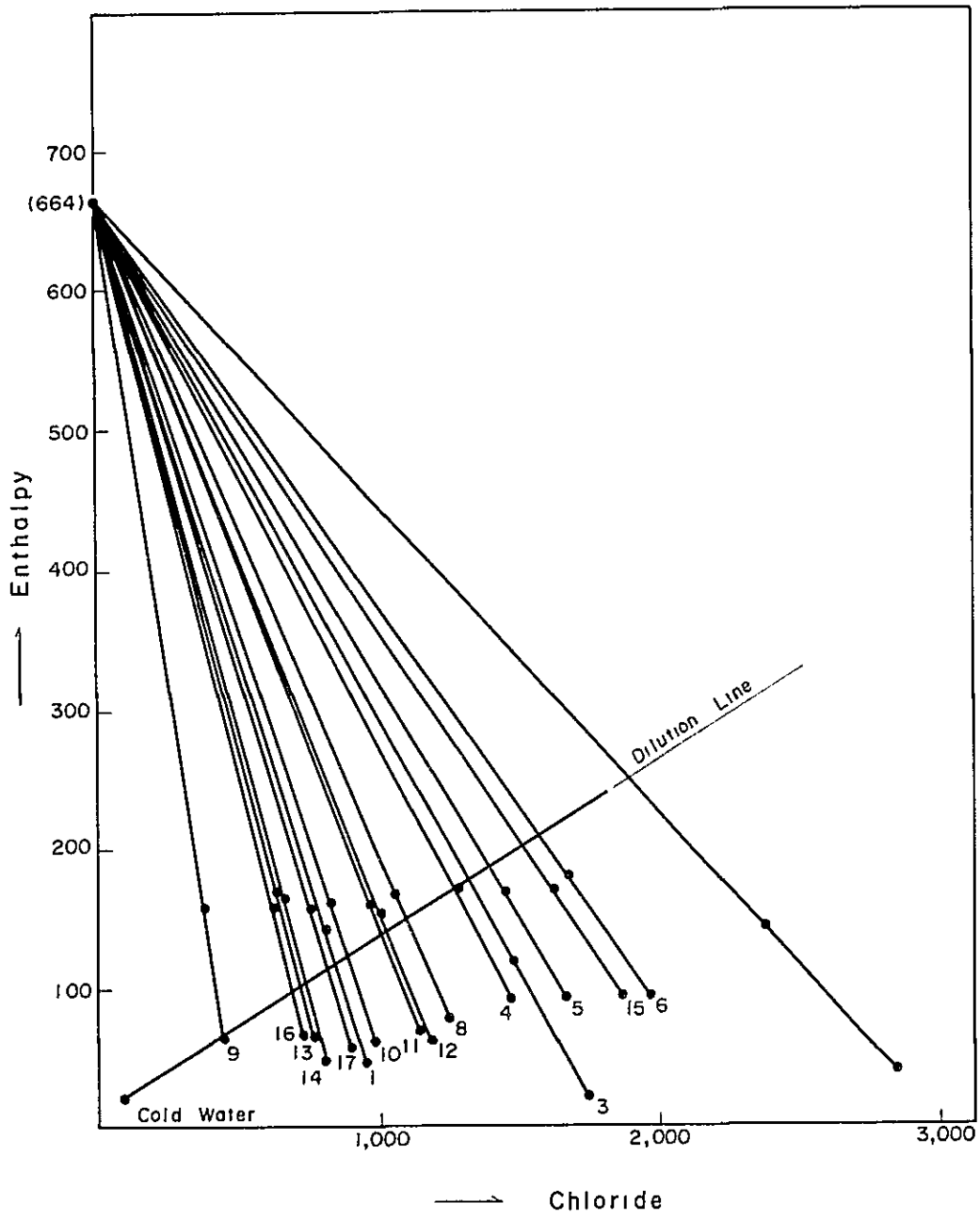

Rincón de los Papas		Las Olletas		El Humazo		Aguas Calientes		Los Tachos		La Bramadora	
No	Sample No	No	Sample No	No	Sample No	No	Sample No	No	Sample No	No	Sample No
1	RP - 1	4	LO - 1	6	EH - 1	8	AC - 1	15	LT - 11	18	LB
2	〃 - 2	5	〃 - 2		〃 - 2	9	〃 - 2	16	〃 - 12		
3	〃 - 3					10	〃 - 3	17	〃 - 13		
						11	〃 - 4				
						12	〃 - 5				
						13	〃 - 6				
						14	〃 - 7				

Fig.6-23 Silica - geochemical geothermometer (mixing model 2)

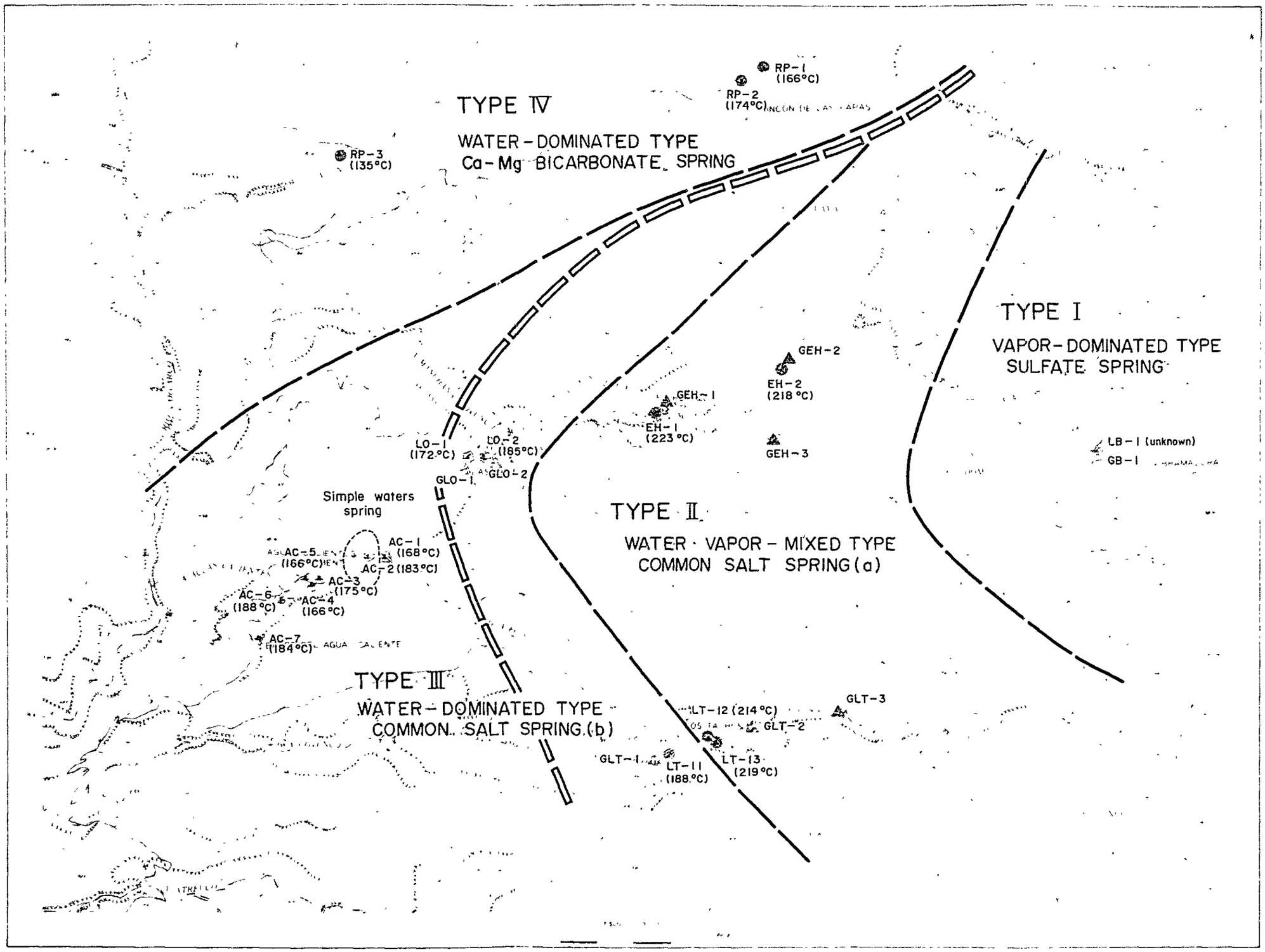

LEGEND

Type	hot water	(geochemical geothermo-temperature)	fumaloic gas	(detected gas)
Ⅰ vapor-dominated type sulfate spring		(unknown)		(H_2, CH_4 H_2S, SO_2)
Ⅱ water · vapor-mixed type common salt spring (a)	●	(> 200°C)	△	(SO_2)
Ⅲ water-dominated type common salt spring (b)	○	(< 200°C)		
simple spring	·	(< 200°C)		
Ⅳ water-dominated type Ca-Mg bicarbonate spring	◉	(< 200°C)		

boundary of classification of hot spring by chemical composition

boundary of existence of fumarole

Fig.6-24 Composite map of zoning of hot spring - fumarole and geochemical geothermo-temperature

7. Model of Geothermal System

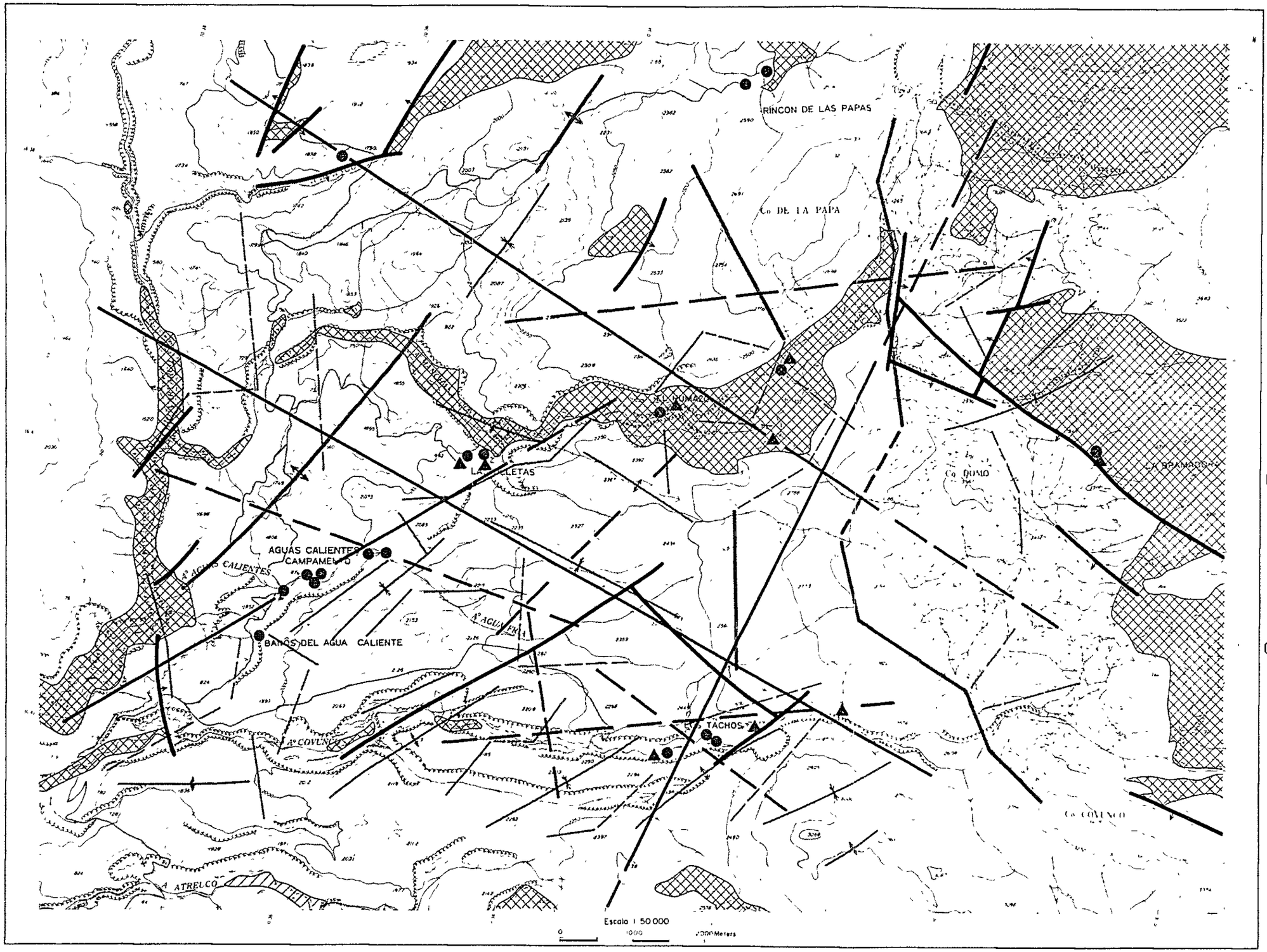

LEGEND

(Geology)

- basement & Mesozoic formation
- fault

(Gravity)

- high gravity area
- low gravity area
- gravimetric lineament (distinct)
- gravimetric lineament (indistinct)
- gravimetric anticline
- gravimetric syncline

(Ground temperature & Geochemistry)

- trend of anomalies (distinct)
- trend of anomalies (indistinct)

(Geothermal manifestation)

- hot spring
- fumarole

Fig.7-1 Synthetic interpretation map of geologic structure

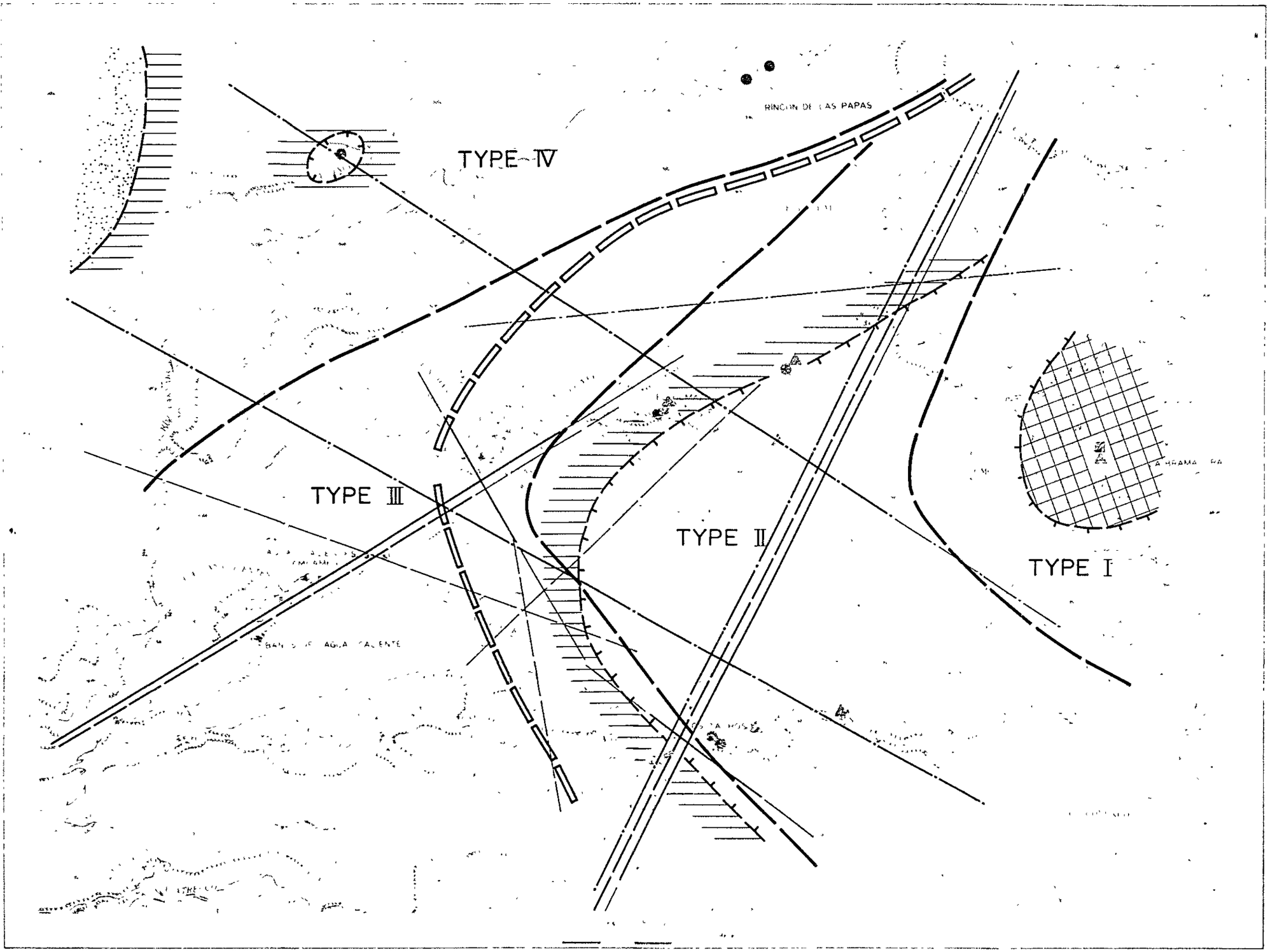

LEGEND

(Geothermal manifestation)

boundary of classification of hot spring by chemical composition

boundary of existence of fumarole

(hot water) (fumaloic gas) (geochemical geothermometer temperature)

I vapor-dominated type sulfate spring (unknown)

II water · vapor-mixed type common salt spring (a) (> 200°C)

III water-dominated common salt spring (b) (< 200°C)

IV water-dominated type Ca-Mg bicarbonate spring (< 200°C)

(Ground temperateue & Geochemistry)

trend of anomalous area

residual ground temperature

Hg-concentration

CO_2-concentration

(thick — — distinct
thin ——— indistinct)

(Alteration)

(temperature)
high
low

kaoline-alunite zone

kaoline zone

montmorillonite-crystobalite zone

opal zone

Fig.7-2 Synthetic interpretation map of heat flow structure

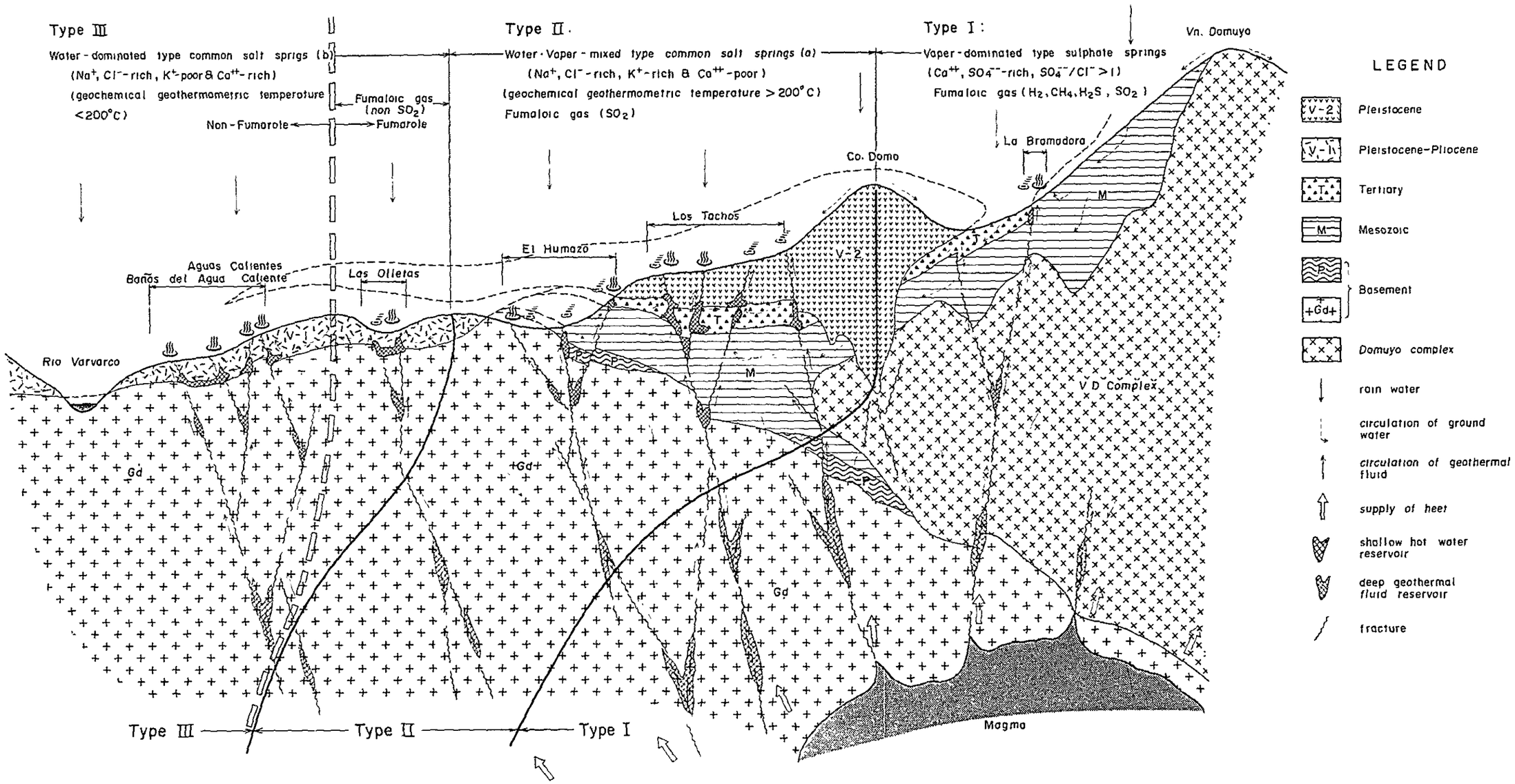

Fig.7-3 Model of circulation mechanism of geothermal fluid and geothermal reservoir structure (1)

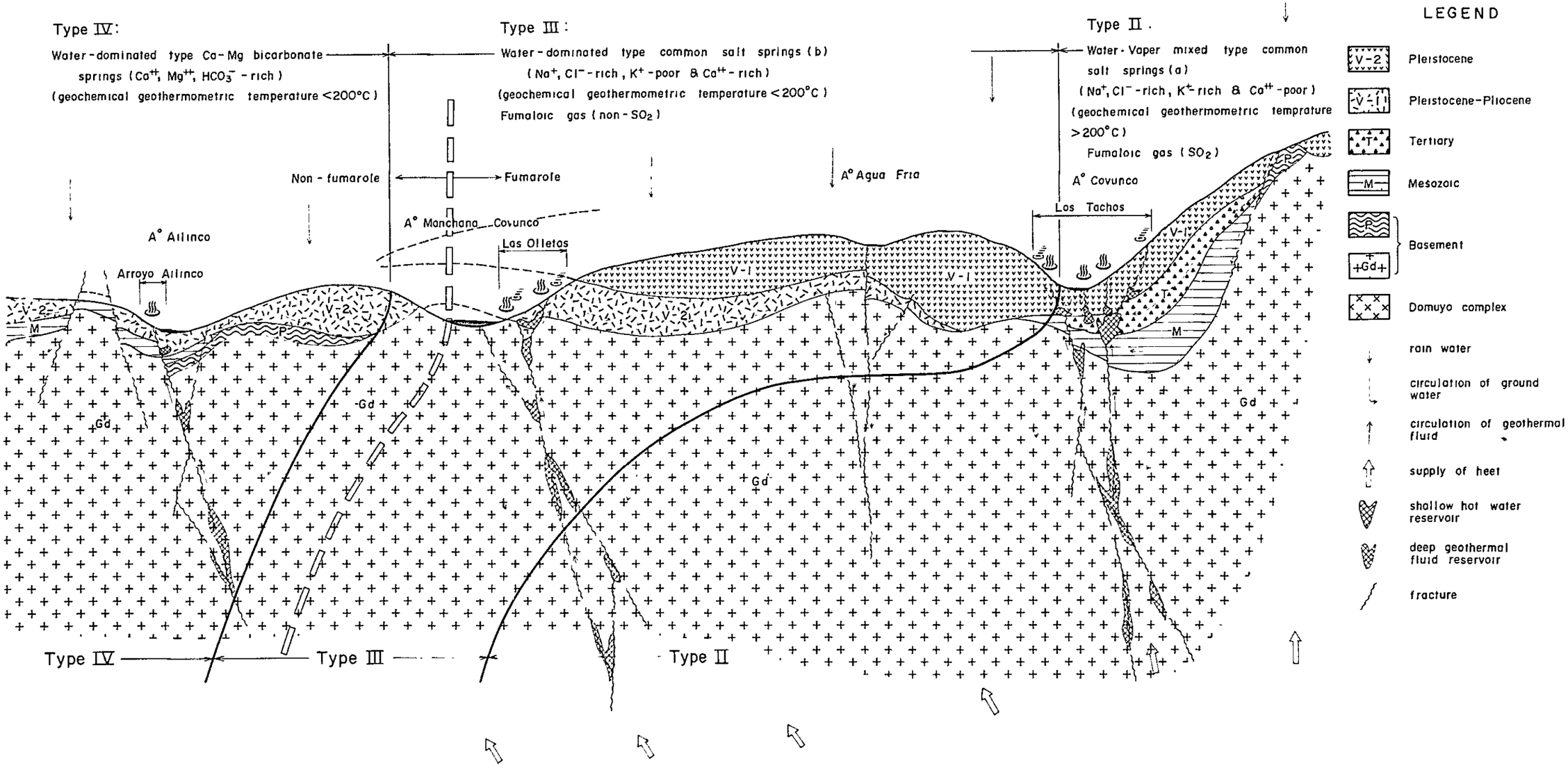

Fig.7-4 Model of circulation mechanism of geothermal fluid and geothermal reservoir structure (2)

8. Summary and Conclusion

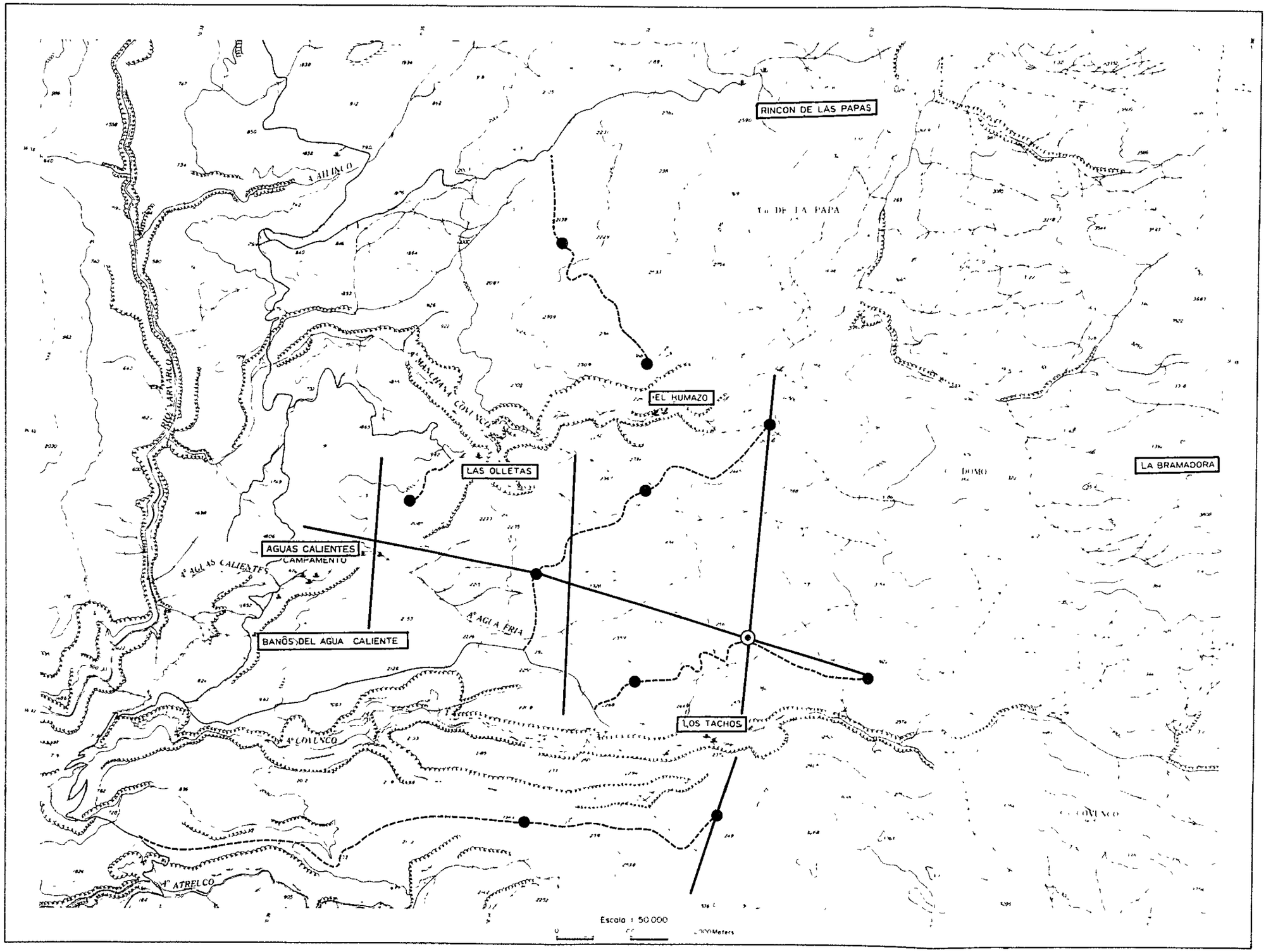

Fig.8-1 Proposed working plan of the third phase survey